

DISS. ETH NO. 17881

**Genetic and Biochemical Characterization
of the Singlet Oxygen-Induced Cell Death
in Arabidopsis**

A dissertation submitted to the
SWISS FEDERAL INSTITUTE OF TECHNOLOGY ZURICH
for the degree of
DOCTOR OF SCIENCES

presented by

JEAN-CHARLES ISNER

M.Sc in Biochemistry, University of Strasbourg
Born January 10th, 1976
in Mulhouse, France

Accepted on recommendation of
Professor Klaus Apel
Professor Nikolaus Amrhein

2009

Summary

The conditional *flu* mutant of *Arabidopsis* overaccumulates protochlorophyllide (Pchl) within the chloroplast when in the dark. Upon reillumination, Pchl acts as a photosensitizer giving rise to singlet oxygen, a nonradical reactive oxygen species (ROS). This ROS activates a genetically determined stress response program resulting in the death of seedlings and the inhibition of growth of mature *flu* plants. Different groups of second-site mutants were identified which are able to abrogate either one or both stress responses of the *flu* mutant. One of these groups contained the Singlet Oxygen-Linked Death Activator (*soldat*) mutants that are able to survive after a dark-to-light shift at the seedling stage, even though they accumulate similar levels of Pchl as the *flu* mutant. However, the growth inhibition of mature *flu* plants is only partially suppressed by the *soldat* mutations. In the present work the *soldat30/flu* double mutant was characterized. A map-based cloning approach revealed that the mutated locus in *soldat30* encodes the chloroplast polyribonucleotide nucleotidyltransferase (PNPase). Complementing *soldat30/flu* plants with a wild type copy of the PNPase gene restored the original *flu* phenotype.

PNPase activity determines the efficiency of mRNA 3'-end processing, the correct maturation of chloroplast rRNA, the degradation of tRNA and the extent of polyadenylation in chloroplasts which modifies the stability of chloroplastic mRNA. The mutation within an allelic gene of *soldat30* was shown to lead to an overaccumulation of Methyl Erythritol Phosphate (MEP) pathway enzymes. This could explain an increase in α -tocopherol, a well known singlet oxygen scavenger, observed in *soldat30*. The scavenging role of tocopherols was confirmed in *flu* by investigating cell death of the *flu/vte1* double mutant and *flu* protoplasts treated with tocopherol after a light dark shift. *soldat30* mutant seedlings showed an enhanced tolerance of photoinhibitory conditions (high light + cold) compared to the wild type, which can also be attributed to the increased accumulation of tocopherols. Taken together, these results suggest that PNPase might be a key component in the sensing of environmental cues which lead to an upregulation of tocopherols and to a higher resistance to photooxidative stress. The PNPase might also be a key component in the acclimation process. A biochemical approach was also undertaken to characterize *flu* cell death. Although carotenoid content decreased after a dark-light shift, the level of one pigment increased dramatically. MS and NMR analysis revealed that this pigment was an oxidation product of

chlorophyll a, the 13²-HO-Chl. a. Further characterization showed that it was located in all photosystem subcomplexes. Synthesis of 13²-HO-Chl. a could be reproduced *in vitro* using the photosensitizer Rose Bengal. Its accumulation *in vivo* was also observed following treatment with superoxide or H₂O₂. The 13²-HO-Chl. a might have some role in promoting the cell death during oxidative stress.

Zusammenfassung

Die konditionale fluoreszierende Arabidopsis-Mutante (*flu*) akkumuliert im Dunkeln freies Protochlorophyllid (Pchlid) in Plastiden. Pchlid kann als Photosensitizer Lichtenergie auf molekularen Sauerstoff übertragen, wobei Singulett Sauerstoff produziert wird, eine nichtradikalische, reaktive Sauerstoffspezies. Unmittelbar nach Belichtung der *flu* Mutante beginnt die Freisetzung von Singulett-Sauerstoff, durch den anschließend ein genetisch determiniertes Stress-Programm aktiviert wird, welches zum Zelltod bei Keimlingen und zur Wachstumshemmung bei vollentwickelten *flu* Pflanzen führt. „Second-site“-Mutanten wurden identifiziert, welche fähig sind, eine oder beide Stressreaktionen der *flu* Mutante zu unterdrücken. Diese Mutanten wurden in unterschiedliche Klassen eingeteilt. Der „*singlet oxygen-linked death activator*“ (*soldat*) bezeichnet eine dieser Klassen. Eine der *soldat* Mutanten, *soldat30*, wurde in der vorliegenden Arbeit einer detaillierten genetischen und physiologischen Analyse unterzogen. Keimlinge der *soldat30/flu* Mutante können einen Wechsel von Dunkelheit zu Licht überleben, obwohl sie ähnliche Mengen an Pchlid wie *flu* akkumulieren. Die Wachstumshemmung der adulten *flu* Pflanzen während eines Licht-Dunkel-Wechsels wird dagegen durch die *soldat30* Mutation nicht unterdrückt. Mittels kartierungsbasierter Klonierung konnte gezeigt werden, dass der mutierte Locus von *soldat30* die plastidäre Polyribonuclease Polynucleotide Phosphorylase (PNPase) kodiert. Die Wildtyp-Kopie des PNPase-Genes konnte, nachdem sie in die *soldat30/flu* Mutante eingeführt worden war, die Mutation komplementieren und den elterlichen *flu* Phänotyp wiederherstellen.

Die PNPase Aktivität beeinflusst die Effizienz der mRNA Prozessierung am 3'Ende, die korrekte Reifung der rRNA in Chloroplasten, den Abbau der tRNA und den Grad der Polyadenylierung in Chloroplasten, die die Stabilität der chloroplastidären RNA verändert. Die Mutation von *SOLDAT30* verursacht so eine Ueberakkumulation von Enzymen des Methyl Erythritol Phosphat (MEP) Weges, der zu einer erhöhten Akkumulation von α -Tocopherol führt, einem Scavenger von Singulett-Sauerstoff. Die Schutzfunktion von Tocopherol wurde in der *flu* Mutante durch die Untersuchung des Zelltods in der *flu/vte1* Doppelmutante und durch die Wirkung von exogenem Tocopherol in *flu* Protoplasten nach einem Dunkel/Licht Wechsel bestätigt. Keimlinge von *soldat30* zeigten gegenüber dem Wildtyp eine erhöhte Resistenz unter einer kombinierten Starklicht/Niedrigtemperatur Behandlung, die auf eine erhöhte Akkumulation von Tocopherol zurückgeführt werden kann. Insgesamt lassen diese Ergebnisse

vermuten, dass die PNPase eine Schlüsselaufgabe bei der Wahrnehmung von Umweltreizen spielt, durch die Tocopherole hochreguliert werden und eine erhöhte Resistenz gegenüber photooxidativem Stress ausgelöst wird. Die PNPase könnte auch eine wichtige Rolle bei der Akklimatisierung spielen.

Zusätzlich wurde in dieser Arbeit mit einem biochemischen Ansatz der Zelltod in der *flu* Mutante charakterisiert. Obwohl nach einem Dunkel/Licht Wechsel der Carotinoidgehalt allgemein abnimmt, steigt die Konzentration eines einzelnen Pigments drastisch an. MS- und NMR-Analysen identifizierten dieses Pigment als ein Oxidationsprodukt von Chlorophyll a, das 13²-HO-Chl a. Die weitere Charakterisierung ergab, dass dieses Pigment in allen Subkomplexen der Photosynthesemembran auftritt. Die Synthese von 13²-HO-Chl a konnte auch unter in vitro Bedingungen durch Zugabe des Photosensitizers Rose Bengal sowie nach Behandlung mit Superoxid oder H₂O₂ erreicht werden. 13²-HO-Chl a könnte bei der Auslösung des Zelltods während oxidativem Stress eine Rolle spielen.

Table of Contents

Summary	2
Zusammenfassung	4
Table of Contents	6
Abbreviations	11
1. Introduction	13
1.1. Stress in plants	13
1.2. The signalling of stress	13
1.2.1. Biotic stress	13
1.2.2. Abiotic stress	14
1.3. ROS in plants	15
1.3.1. Oxygen	15
1.3.2. The ROS and their generation	15
1.3.3. Singlet oxygen formation	18
1.3.4. Avoiding production of ROS	19
1.3.5. ROS scavenging mechanisms	20
1.4. Photooxidation and singlet oxygen	21
1.4.1. Modification of bio-molecules induced by singlet oxygen	21
1.4.2. Signalling by singlet oxygen	22
1.5. The <i>flu</i> system to study the singlet oxygen pathway	23
1.5.1. The <i>flu</i> mutant	23
1.5.2. Second-site mutagenesis of the <i>flu</i> mutant	25
1.5.2.1. Second-site mutagenesis	25
1.5.2.2. Identification of EXECUTER1	25
1.5.2.3. The soldat mutants	25
1.5.2.4. The <i>soldat30/flu</i> mutant	26
2. Materials and Methods	27
2.1. Material	27
2.1.1. Plant material	27
2.1.2. Microorganisms	27
2.1.3. Genomic clone	27

2.1.4. Plasmid vectors	28
2.1.5. Enzymes	28
2.1.6. Oligonucleotides	29
2.1.7. Genetic markers	30
2.1.8. Chemicals	31
2.1.9. Culture media	31
2.1.10. Antibiotics	31
2.2. Methods	32
2.2.1. Culture methods	32
2.2.1.1. Culture of <i>Arabidopsis</i> on MS plates	32
2.2.1.2. <i>Arabidopsis</i> culture on soil	32
2.2.2. DNA techniques	32
2.2.2.1. Genomic DNA isolation	32
2.2.2.2. PCR	33
2.2.2.3. BAC complementation	33
2.2.2.3.1 BAC isolation	33
2.2.2.3.2 Partial digestion	33
2.2.2.3.3 Ligation of BAC fragments with pBIC20 and transformation	33
2.2.2.3.4 <i>E.coli</i> plasmid isolation	34
2.2.3. RNA techniques	34
2.2.3.1. RNA extraction	34
2.2.3.2. Analysis of RNA	34
2.2.3.3. DNase treatment	35
2.2.3.4. cDNA synthesis	35
2.2.4. Transformation methods	35
2.2.4.1. Preparation of VCS257 competent cells	35
2.2.4.2. Transfection of <i>E.coli</i> VCS257 by the cosmid constructs	36
2.2.4.3. Preparation of electro-competent <i>Agrobacterium tumefaciens</i> C58 cell	36
2.2.4.4. Electroporation	36
2.2.4.5. Verification of the transformed <i>Agrobacterium</i>	37
2.2.5. Transformation of <i>Arabidopsis thaliana</i> with <i>Agrobacterium</i>	37

2.2.5.1. Plant growth	37
2.2.5.2. <i>Agrobacterium</i> growth	37
2.2.5.3. Transformation of <i>Arabidopsis</i> by the floral dip method	37
2.2.5.4. Selection of positive transformants	38
2.2.6. Pigment techniques	38
2.2.6.1. Extraction of the pigments for carotenoid and chlorophyll quantification	38
2.2.6.1.1 Extraction of the pigments	38
2.2.6.1.2 High Performance Liquid Chromatography	38
2.2.6.1.3 Determination of Pchl _a content	39
2.2.7. Green-gel	39
2.2.7.1. Isolation and solubilization of membrane sample	39
2.2.7.2. Electrophoresis conditions	40
2.2.7.3. Extractions of pigments from bands	40
2.2.7.4. MS and NMR spectra	40
2.2.8. Protoplast experiments	41
2.2.8.1. Preparation of protoplasts	41
2.2.8.2. Evans blue staining	41
3. Results	42
3.1. Genetic approach to study the effect of singlet oxygen in the <i>flu</i> mutant	42
3.1.1. Isolation of <i>soldat/flu</i> suppressor mutants	42
3.1.2. Phenotypic and physiological analysis of <i>soldat30/flu</i>	42
3.1.2.1. Phenotype of <i>soldat30/flu</i> at the rosette leaf stage	42
3.1.2.2. Phenotype of <i>soldat30/flu</i> at the seedling stage	44
3.1.3. Pchl _a accumulation	46
3.1.4. Map-based cloning	46
3.1.5. Creating the mapping population	47
3.1.6. Crude mapping	48
3.1.7. Isolation of <i>flu</i> KO mutant	49
3.1.8. Creating a second mapping population and fine mapping of <i>soldat30/flu</i>	50
3.1.9. The complementation of <i>soldat30</i> with a BAC clone	52

3.1.10. Complementation of the <i>soldat30/flu</i> phenotype	53
3.1.11. Determination of the <i>soldat30</i> gene	55
3.1.12. In silico analysis of the <i>soldat30</i> gene	56
3.1.12.1. Gene and protein sequence <i>soldat30</i>	56
3.1.12.2. The effect of the mutation on the maturation of 23S rRNA	57
3.1.13. Analysis of tocopherols in <i>soldat30/flu</i> and their role in the singlet oxygen signalling pathway	60
3.1.13.1. Measurement of the content of tocopherols in <i>soldat30/flu</i>	60
3.1.13.2. The <i>vte1</i> mutant	61
3.1.13.3. The induction of cell death in the double mutant <i>vte1/flu</i>	62
3.1.13.4. Tocopherols can attenuate the cell death in <i>flu</i> protoplast	65
3.1.14. <i>soldat30</i> has also an increased resistance to superoxide	66
3.1.15. The effect of <i>soldat30</i> in seedlings exposed to natural stress conditions	68
3.1.16. The effect of acclimatation on the tocopherol content of <i>soldat30</i> and WT seedlings	72
3.2. The biochemical characterization of the effect of singlet oxygen in the <i>flu</i> mutant	75
3.2.1. Pigment accumulation in <i>flu</i> after a dark-light shift	75
3.2.2. Spectrum of the unknown pigment in <i>flu</i>	77
3.2.3. The localization of the pigment in different photosystem sub-complexes	78
3.2.4. Accumulation of the Chl derivative under different stress conditions	80
3.2.5. <i>In vitro</i> oxidation of Chl a by Rose Bengal	81
3.2.6. Accumulation of the Chl a derivative in <i>soldat30/flu</i> double mutant	82
3.2.7. Structural analysis of the pigment	83
3.2.7.1. MS analysis	83
3.2.7.2. NMR analysis of the Chl a derivative	85
4. Discussion	86
4.1. Oxidative stress and mode of action of ROS	86
4.2. The <i>flu</i> system to study the singlet oxygen effects	87
4.3. Comparison between <i>soldat30</i>, <i>soldat8</i> and <i>soldat10</i> mutants	88
4.4. The mutation of SOLDAT30 suppresses the <i>flu</i> phenotype	

by increasing the tocopherol content	89
4.4.1. The mutation of the PNPase in <i>soldat30</i> reverts the <i>flu</i> phenotype ...	92
4.5. Scavenging effect of tocopherol in singlet oxygen-induced cell death	94
4.5.1. Tocopherols	94
4.5.2. The mutant <i>flu/vte1</i> is more sensitive to singlet oxygen than <i>flu</i>	95
4.5.3. The role of tocopherol in reversion of the <i>flu</i> phenotype in <i>soldat30/flu</i>	96
4.6. Biochemical characterization of singlet oxygen-induced cell death	97
4.6.1. The carotenoid content decreased after the release of singlet oxygen	97
4.6.2. A chlorophyll a derivative is produced after the dark-light shift in the <i>flu</i> mutant	98
4.6.3. The chlorophyll a derivative accumulates in all photosystem subcomplexes	98
4.6.4. The accumulation of the chlorophyll a derivative is induced by other ROS	98
4.6.5. In vivo significance of the 13 ² -HO-Chl a	99
4.7. Conclusion and future prospects	100
5. References	102
Acknowledgements	109
List of publications	110
Curriculum vitae	111

Abbreviations

AA	ascorbic acid
ABA	abscisic acid
ALA	aminolevulinic acid
BHT	2-butyl-6-hydroxy toluene
bp	base pair
CAPS	Cleaved Amplified Polymorphic Sequences
cDNA	complementary DNA
cGMP	cyclic guanosine monophosphate
Chl	chlorophyll
cpRNA	chloroplastic RNA
cM	centimorgan
Col	Columbia
DCMU	3-(3', 4' - dichlorophenyl) - 1,1 - dimethylurea
DES	divinyl ether synthase
DNA	deoxyribonucleic acid
<i>E.coli</i>	<i>Escherichia coli</i>
EDTA	ethylenediaminetetraacetic acid
HPLC	High Pressure Liquid Chromatography
hPNPase	human PNPase
HR	hypersensitive response
JA	jasmonic acid
LB	Luria-Bertrani
LD	long day
Ler	Landsberg
LHC	Light Harvesting Complex
LL	continuous light
LOX	lipoxygenase
MDHA	monodehydroascorbate;
MEP	methylerythritol phosphate
MW	molecular weight
MeJA	methyl jasmonate

NADP+,NADPH	nicotinamide adenine dinucleotide phosphate
mRNA	messenger RNA
MS	Murashige & Skoog
PAGE	polyacrylamide gel electrophoresis
PCD	programmed cell death
Pchl _{id}	protochlorophyllide
PCR	polymerase chain reaction
PNPase	polyribonucleotide nucleotidyltransferase
POR	NADPH-protochlorophyllide oxidoreductase
PR	pathogene related
PSI	photosystem I
PSII	photosystem II
PUFA	polyunsaturated fatty acid
RNA	ribonucleic acid
ROS	reactive oxygen species
rRNA	ribosomal RNA
RT	room temperature
R _t	retention time
RT-PCR	reverse transcription polymerase chain reaction
SA	salicylic acid
SDS	sodium dodecyl sulfate
SNP	single-nucleotide polymorphisms
SOLDAT	singlet oxygen-linked death activator
SSLP	simple sequence length polymorphism
TAIR	The <i>Arabidopsis</i> information resource
tRNA	transfer RNA
UV	ultra violet
v/v	volume/volume
w/v	weight/volume
WT	wild type

1. Introduction

1.1. Stress in plants

Just like humans and animals, plants are exposed to numerous stress factors. The crop yield can be reduced by up to 50 percent under stress conditions (Boyer, 1982). We can distinguish biotic such as fungi, bacteria, virus, insects and weeds and abiotic stress factors, respectively, such as high light, UV, water deficit, salinity, high temperature, cold, heavy metals or mechanical wounding. Biotic stress has been extensively studied and research has identified already many compounds to prevent and also to cure these stress effects. Even though abiotic stress can be the reason for dramatic yield loss in many regions of the world (Bray *et al.*, 2000), little progress has been made to mitigate abiotic stress effects. Therefore, we obviously need more information about how cues are perceived by plants and how they react in response to stress.

1.2. The signalling of stress

Because plants are sessile organisms, they had to evolve elaborated strategies to cope with their sometimes hostile environment. Indeed, plants cannot escape from excess temperature or toxic environment or move into a richer soil. Thus, plants had to set up an efficient internal signalling network to sense the cues from their environment in order to induce defence mechanisms which will allow them not only to survive but also to grow and to reproduce, sometimes conferring the acquired resistance to the offspring (Bird, 2007).

1.2.1. Biotic stress

In case of biotic stress, the signalling during a pathogen attack has been well documented. We can distinguish two kinds of interactions between a host and a pathogen: a compatible and a non-compatible interaction. In compatible interactions, the pathogen can multiply and infect the whole plant. An incompatible interaction involves the recognition of the pathogen by the host. The host indeed developed a way to recognize the pathogen in sensing specific molecules and to prevent its expansion. The visible symptoms are restricted and the pathogen does not multiply. The incompatible interaction involves elicitors produced by the pathogen or by the host itself which will lead to induction of a defense response in the host. The response consists of reinforcing the cell wall by a deposition of callose and lignin, a production of lytic enzymes (e.g. chitinase) and other like pathogenesis-related proteins (PR) and finally programmed cell

death. All these reactions are relatively late events because they occur after several hours or days. These late responses may be triggered by second messengers like plant hormones (e.g. salicylic acid, abscisic acid, jasmonic acid or ethylene). Nevertheless, the reaction has to be sensed directly by the cell itself. The early events which may trigger the stress and which were observed are changes in membrane potential, ion fluxes, production of active oxygen species, lipid peroxidation and protein phosphorylation which will induce eventually a local or systemic defence.

1.2.2. Abiotic stress

When plants experience abiotic stress, they alter their gene expression which may lead to a stress tolerance in the case of successful acclimation. But the change in gene expression can also fail to confer a successful acclimation to a new environment. In such a case, the plant is considered to be sensitive to the new conditions.

Cold stress is up to now one of the best understood abiotic stress response pathways in plants. Transcription factors involved in cold stress signalling have been identified. They are named dehydration-responsive element binding factors (DREB) and they bind to a dehydration responsive element (DRE). Constitutive expression of certain of DREB family members confers a freezing or a drought tolerance by inducing a cold acclimatized-like state. DREB transcription factors were thought to be specific to cold stress. However, recently DREBs were also found to be involved in biotic stresses (Agarwal *et al.*, 2006). Common pathways are thus found between biotic and abiotic stresses. An increase of cytoplasmic calcium concentration is observed during a cold stress as it is observed after pathogen attack. The involvement of phytohormones (ABA, SA, JA, ET), MAP kinases or transcriptions factors like MYC, MYB, ZF (Fujita *et al.*, 2006) have also been shown to be involved in both cases.

Moreover, recent studies mentioned that the response of plants induced by simultaneous abiotic and biotic stress is unique (Mittler, 2006), implying signalling pathways which are not activated during an single stress. It shows that stress signalling has a very high degree of complexity, and that we are only at the beginning of understanding this complexity.

1.3. ROS in plants

Molecular oxygen makes up 21% of our atmosphere. It is mainly produced by photoautotrophic organisms via photosynthesis from H₂O. Its level in the atmosphere has been stable for 400 million years since its production has been balanced by its consumption (Berman-Frank *et al.*, 2003). O₂ is necessary for aerobic organisms to live. It serves as an electron acceptor in mitochondria but it is also the byproduct of photosynthesis. Unfortunately, aerobic reactions which involve oxygen, produce highly reactive forms of oxygen as well. Depending on the molecular structure of the oxygen species, we can distinguish different ROS. They can be more or less stable in time and more or less reactive towards neighbor molecules.

1.3.1. Oxygen

The oxygen molecule (O₂) is a free radical. In fact it is a diradical, as it has two unpaired electrons. Molecules whose outermost pair of electrons have antiparallel spins are considered to be in "triplet" state. At standard temperature and pressure, oxygen exists as a diatomic molecule with the formula O₂, in which the two oxygen atoms are bonded to each other with the electron configuration of triplet oxygen. This bond has a bond order of two. The electron configuration of the molecule has two unpaired electrons occupying two degenerate molecular orbitals. These orbitals are classified as antibonding, so the diatomic oxygen bond is weaker than the diatomic nitrogen bond, where all bonding molecular orbitals are filled. Even though unpaired electrons are commonly associated with high reactivity in chemical compounds, triplet oxygen is relatively (and fortunately) non-reactive by comparison with most radicals.

1.3.2. The ROS and their generation

Reactive oxygen species were first considered to be by-products of biochemical reactions which have deleterious effects on many biomolecules within the cell. In bacteria, molecular oxygen is reduced by various cellular constituents, including reduced flavins, flavoproteins, quinones, thiols, and iron-sulfur proteins which lead to superoxide. In animals, the main source of ROS is the mitochondrion during respiration and the peroxisome mainly during inflammatory processes (Schrader and Fahimi, 2004). In plants, oxygen is continuously produced during photosynthesis in chloroplasts. Under ideal conditions, all electrons coming from the Photosystem II (PSII) will serve to reduce ultimately NADP⁺ to NADPH by the FNR

(Ferredoxin NADP⁺ reductase) complex. However, under natural conditions, electrons from FNR may also reduce molecular oxygen to superoxide (1 in Fig. 1.1). Superoxide is reduced to H₂O₂ either spontaneously or by the superoxide dismutase (SOD). H₂O₂ is also produced in plant peroxisomes during photorespiration by the glycolate oxidase (2 in Fig. 1.1).

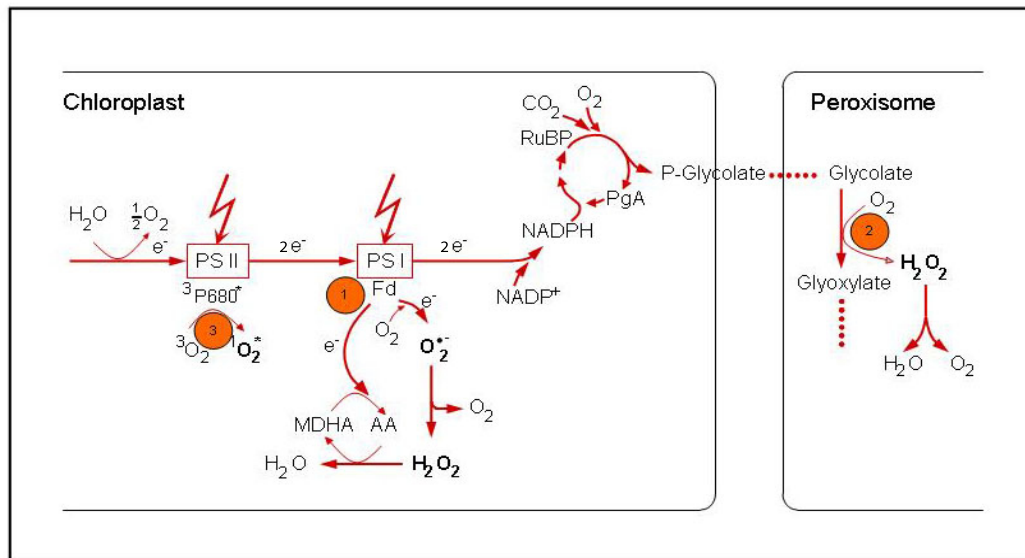


Figure 1.1: Main sources of ROS during photosynthesis

Adaptation from Apel and Hirt, 2004.

Interestingly, ROS can react with each other to produce other ROS. H₂O₂ can react with superoxide to produce the highly reactive hydroxyl radical by the reaction of Haber-Weiss (Figure 1.2). However, it has a negligible rate constant, but this reaction is enhanced drastically in the presence of iron (Fe²⁺)(Fenton reaction, Figure 1.3).

Peroxide can be converted to H₂O₂ in the presence of water. In the Haber-Weiss cycle, peroxide can react with the hydroxyl radical to produce superoxide or with superoxide to produce hydroxyl radical and hydroxyl ion (Figure. 1.4).

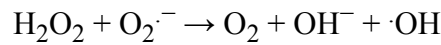
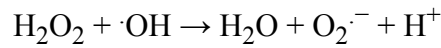


Figure 1.2: Haber-Weiss cycle

H_2O_2 can be very harmful in the presence of metal ions. The Fenton reaction (Figure 1.3) shows that H_2O_2 is converted to the hydroxyl radical. This reaction occurs mainly at low pH (pH 3-6). If the pH is too high the iron precipitates as $\text{Fe}(\text{OH})_3$ and decomposes H_2O_2 to oxygen.

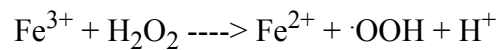
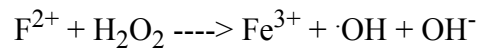


Figure 1.3: The Fenton reaction, reaction between iron and hydrogen peroxide

Iron and hydrogen peroxide react to generate hydroxyl radicals as shown in the equations. The typical range for the iron dose is 1 part of Fe per 5-25 parts of H_2O_2 .

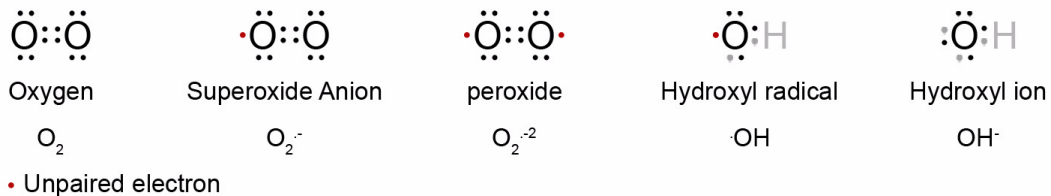


Figure 1.4: The main Reactive Oxygen Species present in a cell

Sequential reduction of molecular oxygen (equivalent to sequential addition of electrons) leads to the formation of a group of reactive oxygen species. The main forms of ROS present in cells are superoxide anion, peroxide (hydrogen peroxide), and hydroxyl radical. The structure of these radicals is shown along with the corresponding notation. Note the difference between hydroxyl radical and hydroxyl ion, which is not a radical.

1.3.3. Singlet oxygen formation

In addition to the formation of ROS by the reduction of molecular oxygen, singlet oxygen ($^1\text{O}_2$), a non radical molecule, can be formed by energy transfer.

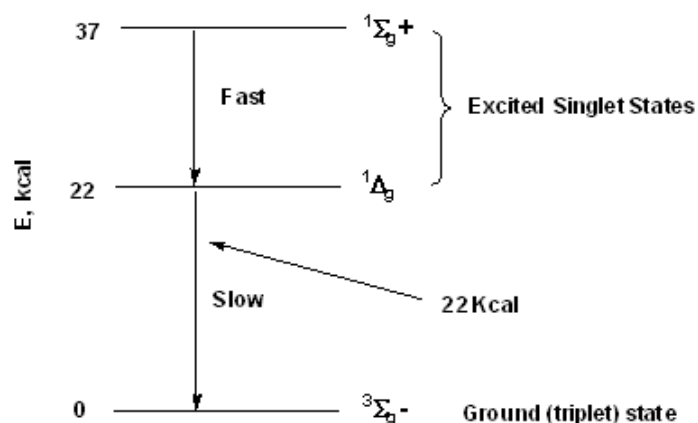


Figure 1.5: Singlet oxygen states

Singlet oxygen is the name of two metastable states of oxygen. The highly excited state $^1\Sigma_g^+$ has a very short life and quickly relaxes to the lower state $^1\Delta_g$.

Singlet oxygen is a molecular state in which all electrons are spin-paired. These electronic states differ only in spin difference and in the occupancy of the two degenerated antibonding π_g^- orbitals. Two forms of singlet oxygen exist, a highly excited state ($^1\Sigma_g^+$) and a lower excited state ($^1\Delta_g$). The highly excited state is very short lived and relaxes quickly to the lower excited state. Due to the spin, the symmetry and the parity selection rules, singlet oxygen is able to react with all molecules which have a double bond in a triplet state. These molecules are represented by the majority of biological compounds including lipids, proteins, nucleic acids, and sugars. Because singlet oxygen is very reactive towards biological molecules, it has *in vivo* a very short half life (in the nanosecond range) compared to the half life of H_2O_2 (1ms). The half life is higher in aprotic solvents or in membranes.

In plants, it is continuously produced in the reaction center of PS II (3 in Figure 1.1). Under ideal conditions, the excitation of the reaction center results in charge separation between P680 and pheophytin and the subsequent sequential reduction of the quinone electron acceptors Q_A and Q_B . When the redox state of the quinone pool is over-reduced because of excess light energy for example, charge separation cannot be completed and the oxidized P680 chlorophyll recombines

with the reduced pheophytin. Under these conditions, the formation of the triplet state of P680 is favored, leading to the generation of $^1\text{O}_2$ by energy transfer (Apel and Hirt, 2004).

1.3.4. Avoiding production of ROS

Since ROS can be very toxic, plants had to set up strategies to avoid their production.

One way to reduce the cell damage induced by ROS is to compensate their over-production. The mitochondria have several strategies to limit it (Moller, 2001). The stimulation of proton leakage in potato mitochondria by $\text{O}_2^{\cdot-}$, probably via the stimulation of an uncoupling protein, is an interesting mechanism for lowering the reduction level of the electron transport chain, and thus to lower the production of further $\text{O}_2^{\cdot-}$.

In plants exposed to light, the major site of ROS production is the chloroplast. To lower the production of ROS within the chloroplast, plants have evolved several strategies to lower the energy reaching the reaction centre of photosystems. When stress for example limits CO_2 fixation, which results in the absorption of more light energy than can be utilized productively by photosynthesis, we can observe plant defence mechanisms already at a macroscopic level. For example, the leaves are turning down to limit light absorption (Koller, 1990). Chloroplast movement can also be observed to avoid that an excess of light energy reaches and damages the photosystems (Jarillo *et al.*, 2001). Chloroplast localization near the upper surface of the cells is changing when exposed to strong light. They move towards the lateral wall, where they shade each other, thus minimizing the absorption of light.

At the cellular level, plants have also evolved strategies to reduce damage caused by an excess of light. The xanthophyll cycle is a well characterized system which converts light energy to heat. Because it does not induce any photochemical reaction, it is called non-photochemical quenching. Under high light, violaxanthin is converted to zeaxanthin, and PsbS, a subunit of PSII, is protonated due to the low pH of the lumen (Li *et al.*, 2000). The energy of $^1\text{Chl}^*$ is transferred to a Chl-zeaxanthin heterodimer. The Chl-Zea* is split in $\text{Chl}^{\cdot-}$ and $\text{Zea}^{\cdot+}$ by a charge separation. A charge recombination forms back the heterodimer Chl-Zea (Holt *et al.*, 2005). Also, lutein was shown to have the property to quench harmful $^3\text{Chl}^*$ by binding at a specific site (the site L1) of the major LHCII complex of plants, thus preventing ROS formation (Dall'Osto *et al.*, 2006).

Under high light, plants decrease the ratio between the amounts of photosystem II (PS II) and photosystem I (PS I) (Niyogi, 2000; Krieger-Liszkay and Trebst, 2006). Under these conditions, there is enough PSI to accept electrons from PSII and prevent the chlorophyll of the reaction

centre of the PS II to be excited to the triplet state.

Another pathway is thought to be essential for protecting the chloroplast from photooxidative stress: the cyclic electron flow (Shikanai, 2007). In cyclic electron flow, the electron originates in PS I, passes from the primary acceptor to ferredoxin, then to a complex of two cytochromes, and then to plastocyanin before returning to chlorophyll. This transport chain produces a proton-motive force, pumping H^+ ions across the membrane; this produces a concentration gradient which can be used to power ATP synthase during chemiosmosis. This pathway is known as cyclic photophosphorylation, and it produces neither O_2 nor NADPH.

Another electron safety valve in C3 plants is the photorespiration (Reumann and Weber, 2006). A low cellular concentration of CO_2 induces an increase of photorespiration. The Rubisco, instead of carboxylating ribulose-1,5-biphosphate, catalyzes its oxygenation which leads to the production of 2-phosphoglycolate and 3-phosphoglycerate. The glycolate has to be converted is converted to 3-phosphoglycerate using ATP and NADPH in peroxisomes and mitochondria. The generation of ADP and $NADP^+$ serves as an electron sink and allows the oxidation of the reduced forms of the two photosystems. Thus, under a low concentration of CO_2 , NADPH and ATP cannot be used by the Calvin cycle and instead will be utilized by photorespiration. The importance of the glycolate pathway has been shown by using photorespiratory mutants. Photorespiratory mutants are lethal in the presence of low CO_2 but grow under high CO_2 concentrations (Reumann and Weber, 2006).

1.3.5. ROS scavenging mechanisms

Even though plants have developed strategies to limit ROS production, ROS are inevitably produced. In consequence, plants had to develop additional strategies to limit the deleterious effects of ROS on cell components. They synthesize molecules which are able to quench or to deactivate ROS. In chloroplasts, glutathione (GSH) or ascorbate play an important role as cellular redox buffers. Electrons coming from the water splitting by PS II are taken up by PS I to reduce oxygen; O_2^- is produced. A membrane-attached copper/zinc superoxide dismutase (SOD) reduces O_2^- to H_2O_2 which is converted to water by a membrane-associated ascorbate peroxidase. The ascorbate is regenerated by electrons coming from PS I via glutathione. This water-water cycle is an efficient electron sink to avoid an over-reduction state of the photosystems. It was shown that knocking out the thylakoid-membrane associated SOD has severe deleterious effects on growth (Rizhsky *et al.*, 2003).

In peroxisomes, catalase enzymatically detoxifies H_2O_2 either during photorespiration or

during the β -oxidation of fatty acids (Fig. 1.1).

In chloroplasts, during high light stress $^1\text{O}_2$ is formed in the reaction center of PSII. The $^1\text{O}_2$ is quenched by the D1 protein which forms the reaction center. During this process, D1 is damaged and has to be replaced by a newly synthesized D1 protein via a highly controlled processes involving the metalloprotease FtsH1. Additionally, β -carotene located in the vicinity of the reaction center may also scavenge $^1\text{O}_2$.

In vitro but also *in vivo* studies have shown that tocopherols can efficiently quench singlet oxygen and scavenge various radicals, especially lipid peroxy radicals derived from polyunsaturated fatty acids (PUFAs), thereby terminating lipid peroxidation chain reactions (Kamal-Eldin and Appelqvist, 1996). Moreover, all isoprenoids can have such properties (Penuelas and Munne-Bosch, 2005). But these molecules are not ubiquitous. Thus, for instance, carotenoids (e.g. xanthophylls, β -carotene) and tocopherols are present in membranes because of their hydrophobicity and act more at the membrane level whereas ascorbate, glutathione, flavonoids (Matsufuji *et al.*, 2006) are hydrophilic molecules and act preferentially in the stroma (Penuelas and Munne-Bosch, 2005; Dall'Osto *et al.*, 2006).

1.4. Photooxidation and singlet oxygen

1.4.1. Modification of bio-molecules induced by singlet oxygen

Singlet oxygen reacts with a wide range of biological targets, including DNA, RNA, proteins, lipids, and sterols.

Because of the abundance of proteins and the high rate of the reaction of singlet oxygen with amino acid side chains, it is thought that proteins may be one of the principal targets of singlet oxygen (Davies, 2004). Mainly Trp, His, Tyr, Cys and Met are modified to peroxide derivatives (Wilkinson *et al.*, 1995). It was proposed that the decomposition of the Trp side chain could give molecules such as kynurenine which may act as photosensitizer and contribute to an escalating cycle of damage. Peroxide derivatives can also undergo a cross-linking reaction via peroxy radical formation. The peroxide derivatives also readily undergo reactions with low molecular weight molecules such as GSH (Davies, 2004) which may act as scavengers.

Lipids are very abundant in cells as well and undergo peroxidation by ROS. Besides oxidation triggered by oxygen radicals (hydroxyl radicals and peroxyradicals), non-radical species like singlet oxygen, ozone, or peroxynitrite are also known to oxidize unsaturated lipids (such as phospholipids, glycolipids, cholesterol, lipoprotein). Singlet oxygen is able to oxidize lipids to

lipid hydroperoxides (LOOHs) by the “ene” reaction (Ohloff, 1975). Because LOOHs are more polar than their respective precursors, they may perturb the structure/function of membranes leading to deleterious effects. Another aspect which is under intense investigation nowadays is that LOOH derivatives can act as signaling molecules and induce different stress-related pathways ranging from the synthesis of antioxidants to the induction of programmed cell death. Indeed, oxidation of unsaturated fatty acids leads to the production of hydroperoxides, which can be the substrate for jasmonic acid (JA) synthesis. JA was shown to promote cell death in the presence of singlet oxygen (Danon *et al.*, 2005). The LOOHs can be detoxified by glutathione reductases to alcohol derivatives. Otherwise, LOOHs may be converted to a wide range of reactive aldehyde, epoxide, keto or hydroxy compounds (aldehydes like 4-hydroxynonenal, 4-hydroxyhexenal, and malonaldehyde) which are believed to be involved in carcinogenesis and cell death (Esterbauer *et al.*, 1991).

Besides proteins and lipids, another class of molecules oxidized by singlet oxygen are nucleic acids (oligonucleotides, nucleosides, DNA and probably RNA). *In vitro*, in aqueous solution, guanine is oxidized to 8-oxo-7,8-dihydroguanine via the reduction of 8-hydroxyguanine. This product was also found *in vivo* in bacterial and human cells upon exposure to UVA (Cadet *et al.*, 2006). Few studies showed an accumulation of 8-oxo-7,8-dihydro-2'-deoxyguanosine after infiltration of a water-soluble endoperoxide whose thermal decomposition leads to singlet oxygen formation (Ravanat *et al.*, 2000, 2004).

1.4.2. Signalling by singlet oxygen

Singlet oxygen is known to induce apoptosis in animal cells. Indeed, photodynamic therapy (PDT) strategies use that property to induce cell death in cancerous cells. PDT consists of exciting a photosensitizer infiltrated into the tumor. The accumulation of the photosensitizer within the cells could also be achieved by infiltrating cells with δ -aminolevulinic acid (ALA), the specific precursor of tetrapyrroles. In that case, cells accumulate protoporphyrin IX. The tumor is then illuminated by a laser beam that has the wavelength corresponding to the maximum excitation wavelength of the photosensitizer. The excited photosensitizer reacts with oxygen to produce singlet oxygen. Singlet oxygen induces then a programmed cell death (apoptosis) which leads to the eradication of the tumor (Oleinick and Evans, 1998).

In plants, little is known about the signalling of singlet oxygen. Singlet oxygen may react directly with proteins which may be involved in signalling ((1) Figure 1.6). It may induce cell responses more indirectly, too, by changing the redox state of the cell or via lipid peroxidation.

The more oxidized cell status may be sensed by proteins like thioredoxines which could lead to a specific cell response.

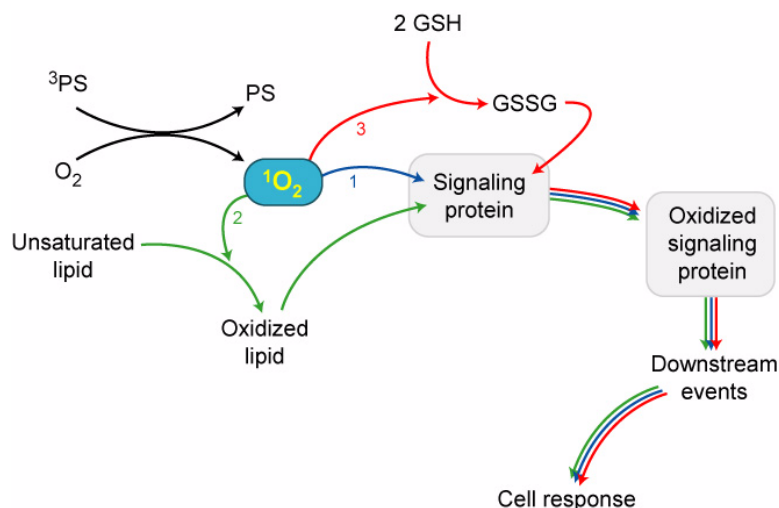


Figure 1.6: Singlet oxygen signaling (from Kochevar, 2004)

Singlet oxygen produced under stress can react with unsaturated lipids (2), with proteins (1) or with glutathione (GSH) (3). Oxidized lipids themselves can oxidize proteins as well as GSH. Their modification lead to Cell response, for instance cell death. Abbreviations: 3PS : photosystem at triplet stage

1.5. The *flu* system to study the singlet oxygen pathway

Because in cells under stress, different ROS are produced simultaneously, it is difficult to study the biological activity and mode of action of one particular ROS in a wild type background. We took advantage of the *flu* mutant isolated in our group (Meskauskiene *et al.*, 2001) which is deficient in the regulation of the chlorophyll biosynthesis pathway, to study singlet oxygen signalling. It is possible with this mutant to produce singlet oxygen in chloroplasts in a controlled and non-invasive manner.

1.5.1. The *flu* mutant

In higher plants, chlorophyll biosynthesis stops in the dark. Protochlorophyllide (Pchl_{id}), the immediate precursor of chlorophyllide accumulates, because the subsequent reaction leading to chlorophyllide requires light (Figure 1.7). When Pchl_{id} reaches a threshold level, its own biosynthesis stops via a negative feedback inhibition of the first specific step of the tetrapyrrole

pathway which requires the FLU protein (Meskauskiene *et al.*, 2001; Meskauskiene and Apel, 2002).

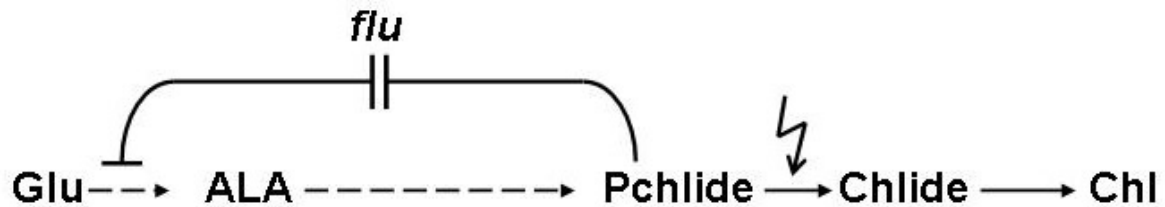


Figure 1.7: Regulation of the tetrapyrrole pathway in angiosperms by the FLU protein

The pchlido, once its content reaches a certain threshold in the dark, mediates a feedback control on the first step of tetrapyrrole biosynthesis via its interaction with the Glu-tRNA reductase. Abbreviations: Glu: Glutamic acid; ALA: δ -aminolevulinic acid; Pchlido: Protochlorophyllide, Chl; Chlorophyllide; Chl: Chlorophyll

In the *flu* mutant, this feedback inhibition is impaired and Pchlido overaccumulates. When the *flu* mutant is transferred to light, the pchlido accumulated during the dark in chloroplasts acts as a photosensitizer. Pchlido excited by light reacts with molecular oxygen and produces singlet oxygen. Immediately after the release of singlet oxygen, mature *flu* plants stop growing, whereas seedlings bleach and die. Because the synthesis of the chlorophyll is restricted to chloroplasts, it is possible to induce the release of singlet oxygen specifically within this organelle which is not possible by infiltrating an artificial photosensitizer.

1.5.2. Second-site mutagenesis of the *flu* mutant

1.5.2.1. Second-site mutagenesis

A forward genetic approach has been used to unravel the complexity of the $^1\text{O}_2$ signaling. For that purpose, an extensive second-site mutant screen was undertaken and allowed the identification of a large number of ethylmethanesulfonate (EMS)-induced suppressor mutants which revert the singlet oxygen-induced stress responses in *flu*. One group of mutants had a significantly reduced amount of protochlorophyllide after a dark period. These mutants are either impaired in chlorophyll biosynthesis or its regulation. Another group of mutants isolated has similar concentrations of Pchlde after the dark period and revert the stress responses of *flu* at the seedling stage or at rosette leaf stage.

1.5.2.2. Identification of EXECUTER1

A first subgroup is formed by 19 second-site mutants that still overaccumulate the same amount of pchlde and are able to abrogate the cell death response as well as the growth inhibition response of *flu* under non-permissive conditions. The mutants were shown to be allelic and to represent a single locus dubbed *EXECUTER1* (Wagner *et al.*, 2004). *executer1* mutants were shown to be also more resistant to treatment with DCMU (3-(3,4-dichlorophenyl)-1,1-dimethylurea), a herbicide which induces a release of singlet oxygen. EXECUTER1 is a nuclear-encoded protein targeted to the chloroplast. So far little is known about its role during singlet oxygen signalling.

1.5.2.3. The *soldat* mutants

Another subgroup of isolated mutants that still overaccumulate Pchlde was formed by 15 second-site mutants that are able to revert the stress response of *flu* grown under non-permissive conditions at the seedling stage, but not at the rosette leaf stage. These mutants were dubbed *Singlet-Oxygen-Linked-Death-Activator* mutant (*soldat*). Two of them have already been characterized (Sánchez-Coll, 2006; Würsch, 2006). *soldat8*, allelic to the chloroplastic transcription factor *SIGMA6*, and *soldat10*, a termination factor (cTERF) involved in the chloroplastic protein translation termination were found to be able to revert the *flu* phenotype at the seedling stage. In contrast to *flu*, *soldat10/flu* seedlings do not bleach when grown under non-permissive dark/light conditions, despite of their continuous overaccumulation of Pchlde

in the dark. The inactivation of cTERF results in the downregulation of plastid-specific rRNA levels and leads to a drastically reduced steady state concentration of the D1 protein of photosystem II. Even under low light intensities that have no apparent negative impact on wild-type seedlings, *soldat10* seedlings suffer from photooxidative stress to which they respond by activating an acclimatory response. Constitutive acclimation to light stress conferred by *soldat10* suppresses singlet oxygen-mediated responses in seedlings of the *soldat10/flu* double mutant (Sánchez-Coll, 2006; Würsch, 2006). However, the reduced amount of pchl_{ide} by 40% in both mutants after the dark period compared to *flu*, could also contribute to the reversion of the stress response in *soldat10/flu* or *soldat8/flu* double mutant.

1.5.2.4. The *soldat30/flu* mutant

The present work was aimed at characterizing another *soldat* mutant, *soldat30*.

While *soldat10/flu* and *soldat8/flu* were shown to have about 60% of pchl_{ide} compared to *flu*, *soldat30/flu* has about 90% of pchl_{ide}. *soldat30* was found to be allelic to a gene encoding a polyribonucleotide nucleotidyltransferase (PNPase) targeted to the chloroplast. The PNPase is involved in rRNA and tRNA processing, mRNA stability and probably other functions in signaling pathways. Its inactivation was shown to induce an accumulation of the key enzyme of the methylerythritol phosphate (MEP) pathway, involved in chloroplast isoprenoid biosynthesis. This leads to an overaccumulation of an end product of isoprenoids, tocopherol, that is known to scavenge singlet oxygen. The overaccumulation of tocopherols seems to be the main reason why *soldat30/flu* can revert the *flu* phenotype under non-permissive growth conditions.

2. Materials and Methods

2.1. Material

2.1.1. Plant material

Arabidopsis thaliana, ecotype Landsberg *erecta* (Ler) and Columbia (Col)

Mutants:

flu 5L: Ler EMS mutant crossed 5 times back into Ler

flu T-DNA: T-DNA insertion mutant

soldat30: second site mutant of *flu* mutant 2 times backcrossed in Ler

rif1: T-DNA insertion line isolated from SALK collection provided by Dr. Manuel Rodríguez-Concepción

vte1 : EMS mutant of Col-2 provided by Dr. Peter Dörmann (Porfirova et al., 2002)

2.1.2. Microorganisms

Escherichia coli strain DH5 α (Hanahan, 1983); Genotype F⁻, endA1, hsdR17(rk⁻, mk⁺), supE44, thi-1, rec⁻, gyrA96, relA1, ϕ 80, lacZM15

Escherichia coli strain NM544

Agrobacterium tumefaciens strain C58C1 with the helper plasmid pTIC58 (Zambryski et al., 1983)

2.1.3. Genomic clone

The Bac clones T11I18 (AC011698) and F20H23 (AC009540) were ordered at the ABRC (Arabidopsis Biological Resource Centre)

2.1.4. Plasmid vectors

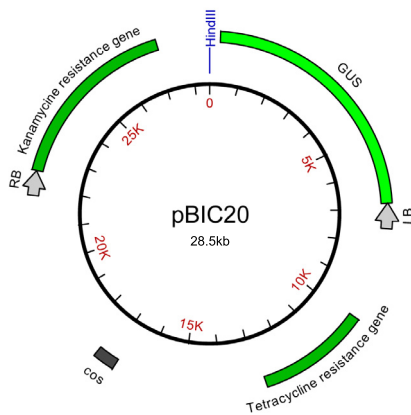


Figure 2.1: pBIC20 vector.

LB: Left Border, RB: Right Border, GUS: β -Glucuronidase, cos: bacteriophage λ cos site

The pBIC20 cosmid vector was obtained from Dr. Rasa Meskauskiene (Meskauskiene and Apel, 2002). The cosmid encodes a neomycin phosphotransferase conferring kanamycin resistance to *Agrobacterium tumefaciens* and plants, a tetracycline resistance gene for bacterial selection, a Hind III restriction site to integrate fragment from 9 to 25 kb, a cos site to allow transfection (Meyer et al., 1994).

2.1.5. Enzymes

All enzymes were purchased from New England Biolabs Ltd.

2.1.6. Oligonucleotides

Oligonucleotides were purchased from Microsynth (Balgach, Switzerland).

The following primer sequences were used in this work:

Crude mapping

F4P13	CAAGCCAAAAGGTCTTCACC	TAATCCAGGCCTCGCAAC
T1F15	CTTGGGAGGAAGCTCTATCG	TGCGCCATCAAATAATGTGT
ATHBIO2B	TGACCTCCTCTTCCATGGAG	TTAACAGAAACCCAAA
F19B11	TTCAAAGTTTCCACCTCATGC	TATGTGTGAGGCCAAGAACC
T21L14	TTCAAAGTTTCCACCTCATGC	TATGTGTGAGGCCAAGAACC
NGA 63	ACCCAAGTGATCGCCACC	CAACCAAGGCACAGAAGCG
NGA 139	GGTTTCGTTTCACTATCCAGG	AGAGCTACCAGATCCGATGG
K20J1	TGGGAAGACGATGATGGA	CCGCATGATGCATAGCAA
AP22	CACATCAATGAATTTGGGAAA	ATGACGACATATTGCACATTTT
T10P11	TCATGATAACACAGGGCGTAA	TTCGCATATCTCATGCCATC

Fine mapping

F13E7	CGCGTGTTCCTTAC	TCGACTCCAGTCCAAATGTTC
T17B22	TGCTTGACCAAAGATACCA	TTGGAACCAAAGACTAGAAATTGA
T12J13B	GCAAAACAGAACCCAGAGAGA	CTCCAATCGCCTTCAAGGTA
T12J13C	GGCAAGGAACCAACAACAAC	TCAACAAATCCATCCATCTTC
T12J13D	TTCCTTCGTTGTGCAGATTG	TCCGTATTGGTGGAATGTG
F20H23A	GTGAGGCACACGTGCAAA	CGCAATGTACGCATTTCC
F20H23B	CGAGTTTTGGATTTAACATTGC	ACGTTGACTGAGCATTTGTTT
T11I18B	GCAATCAACGTCAAATTTTCAG	CCCAAAAAGATAAGGCTCCTC
T11I18C	CAAAAGTAACACATTCTGTTTGAG	TCATCATCATCATCATCACAG
T11I18D	CGAAATGTAAGGCTTTTCTGG	TGACCCATTCAATTTCTCCATT
T6K12A	CATATATAATGGGTTGGTTACAATGG	AGATCGACCCGTAACCAGA
T6K12B	TTACCGGAGCATGTGCAATA	CGATCCGTTTTGGTTCAAAT
T27C4	GATCGCCGTTTTTGT	AAAGACACATCAATGCATCAGC
F7O18	TGCGCTCTTGAGAACAGG	GCGATCGAAGCCAGAAGA
F22F7	CAATGCCAGCTGCAAAGTT	TCATCGTTTTCTGGGCAA
F24P17	CAGTGCACATTGGACGAAC	GCCATTGGATGGCAACTT
F21O3	TGACGCTGTGTCGTTTGG	GAGGTGGGCAATGTGAGAA

Complementation

F20H23_1	GGTAGGATGTCTCCAAACATG	ACAGATACTCACCTAGACCAAG
F20H23_10	GAACTCTAGCATCCTTTGTTGG	CGAGCTCTGAGAGACTTAGC
F20H23_20	ATTCGCCTCAAGACGAAAC	ATCAAGACAACACGAAGATACC
F20H23_30	TATGCCAAACTCGGTCGTC	AACATAGAAAGAGAGGGAGAGG
F20H23_40	CCTCGTCGCAGGAAAAATC	GCTGCCTTTACCCAAATCAAGG
F20H23_50	TCCTTCTAGCGGTAAAGCTG	AGAACTCGTGACAGCCATG
F20H23_60	TGTTTCCGTTTCAATCTTTTCG	TGCAAATCTCCCATCGTAAAG
F20H23_70	TGAGAACCTTCACCCATGAAAG	ACAGTGACGAAATCTTCCCC
F20H23_80	CATAGACATCTCGAAACCACAG	CAAATTGTTGATTAGGTCGCTG
F20H23_90	ACAGCAAGTTGAAAAGTGCTTC	AATTGCTGCCTGGAGTATAGC
F20H23_100	AAGAGAAGCTGGGTCTTGG	GGAACACTCCTGGCAAATAC
T11118_1	TTGGTTCAAGGCAGAGGCG	GGGATATGAGGCTGGCAATA
T11118_10	TCTTCTTGGTTGCTCGGTCT	TTGGATCATCATCGTCATCG
T11118_20	GGGGAGAATTTCCGTGAATC	ATGCCACTTCACAGGGAAAC
T11118_30	ATTGTGGTTCAGGCCAATGT	ATTGAGCGGGAAGACAAGAA
T11118_40	CGATCATGGGACTCTGGAAA	GGATACGGATGGTGGGCAATAGA
T11118_50	TCGCTCTTTGCTTTGTTTCGT	TCTTTTCAATCGGAATCT

Sequencing

AT3G03710A	CCCTTTATGTTCACTATCAGG	CTAGCTGTGATTCTTCCATCTC
AT3G03710B	CAAACCTAGTCATTTCCCTTTGC	GAATGGTCTCCAATGCTCG
AT3G03710C	ACGCTAAGCCTCTCAAATATG	GCGAACTCTTGTCTTTGGTAG
AT3G03710D	GTTCGGGTTGGTCTTATTGG	AGCTTCGACGATACTTCTTTG
AT3G03710A	TGGGAAATTTAAAACCCGGTTC	CAAGAGACTCCAAAATTGCAAG
AT3G03710A	TTCGACTTAGTGTACGGGC	TTGGGAACTTTGACAAGCTG
AT3G03710A	TCCTCCATCGTCTGTTGG	GGCATTAGACTGGGCAATC

2.1.7. Genetic markers

SSLP PCR markers were created by identifying small insertions/deletions that are polymorphic between Ler and Col (Jander et al., 2002), designing primers flanking each insertion/deletion, and testing for polymorphisms between Ler and Col.

2.1.8. Chemicals

Most chemicals were purchased from Fluka and Sigma (Buchs, Switzerland)

2.1.9. Culture media

LB (Luria-Bertani)-medium: 25g/l Luria Broth Base (Invitrogen Life Technologies, UK)

Solid LB Medium: 1 x LB-medium, 0.8%(w/v) Bacto-Agar

Yeast extract pepton-medium (YEP):

20g/l Yeast extract

10g/l Bacto-peptone

2.1.10. Antibiotics

Table 1: Antibiotics

Antibiotics	Solvent	Stock solution	Final concentration
Kanamycin sulfate	Water	5 mg/ml	50 µg/ml
Tetracycline	Ethanol	5 mg/ml	10 µg/ml
Chloramphenicol	Methanol	5 mg/ml	12.5 µg/ml
Rifampicine	DMSO	25 mg/ml	100 µg/ml

2.2. Methods

2.2.1. Culture methods

2.2.1.1. Culture of Arabidopsis on MS plates

Seeds were surface-sterilized by incubating them in bleach solution (50% (v/v) sodium hypochlorite, 0.01%(v/v) triton X-100). After 10 min the seeds were washed 4 times in sterile water. Sterilized seeds were plated on MS-agar plates. MS medium was prepared as described in Danon et al. (2005). Briefly, the medium is composed of 3.06 g/l of Gamborg medium including vitamin B5, MES 0.5g/l, sucrose 0.5% (w/v), 8.5 g/l of plant agar, adjusted to pH 5.7 with KOH. Sown seeds were vernalized at 4°C for 4 days in the dark and then transferred to continuous light at 80-100 $\mu\text{mol photons m}^{-2}\text{s}^{-1}$, 21°C and 65% humidity. In case the settings of the experiment required other conditions, the specific treatment is mentioned.

2.2.1.2. Arabidopsis culture on soil

Seeds were sown on common rich soil (85% peat, 10% sand and 5% perlite) with low soluble fertilizer and after 10 days singled out in separate pots containing Klasmann Substrate No.2 (Klasmann-Deilmann GmbH, Geeste-Gross Hesepe, Germany), which contains 100% peat and soluble compound fertilizer. The plants were grown under continuous light until the rosette leaf stage and after bolting they were transferred to long day condition (16 h light/8 h dark) to test growth inhibition or kept under continuous light for transformation or seed collection.

2.2.2. DNA techniques

2.2.2.1. Genomic DNA isolation

One cauline leaf was frozen in liquid nitrogen and 500 μl of Shorty buffer were added (0.2 M Tris-HCl pH 9.0; 0.4 M LiCl; 25 mM EDTA pH 8; 1% (w/v) SDS) and ground with an electric micropestle. After 5 min of centrifugation at top speed and room temperature (RT), the supernatant was transferred to a fresh Eppendorf tube containing 350 μl of isopropanol. After centrifugation for 10 min at top speed and RT, the supernatant was discarded. The pellet was air-dried and dissolved in 400 μl of TE buffer (0.01 M Tris-HCl pH 8; 1 mM EDTA) by shaking at RT for 30 min. DNA was stored at -20°C.

2.2.2.2. PCR

This *in vitro* technique allows a fast amplification of a specific DNA fragment. The PCR mix was prepared by adding to an Eppendorf tube 2 µl of DNA solution, 2 µl of BioTherm™ Mix Buffer, 1.5 units of BioTherm™ DNA Polymerase (Genecraft GmbH, Lüdinghausen, Germany), 25 pmol dNTP (Fermentas GmbH, St. Leon-Rot, Germany), 20 pmol of the specific forward and reverse primers and water to a final volume of 20 µl.

The reaction was performed in an iCycler Thermocycler (Bio-Rad AG, Reinach, Switzerland) using the following program: 5 min initial denaturation at 94°C; 45 cycles including: 15s denaturation at 94°C, 30s annealing at 55-60°C (temperature depending on the melting temperature of the primers) and elongation at 72°C (time depending on length of the DNA fragment, 1Kb/min); 10 min final elongation at 72°C. The samples were run on an agarose gel.

2.2.2.3. BAC complementation

2.2.2.3.1. BAC isolation

The BAC DNA was isolated using the midiprep kit (Qiagen) as described in the manual except that the water was preheated to 65°C before the elution of the adsorbed DNA from the column.

2.2.2.3.2. Partial digestion

The BAC clones were purchased from the Arabidopsis Biological Resource Center (Columbus, OH, USA). The isolated DNA was partially digested with the Hind III restriction enzyme. For this purpose, 1 µg of the DNA was digested during 10-30 min at 37°C. The fragments larger than 9 kb were cut out of the gel and extracted with the gel extraction kit (Macherey-Nagel)

2.2.2.3.3. Ligation of BAC fragments with pBIC20 and transformation

The pBIC20 was cut with Hind III. The extracted fragments were ligated by the ligase with the cut pBIC20.

2.2.2.3.4. *E. coli* plasmid isolation

A miniprep kit was used to isolate cosmid from *E. coli* with minor modification. During the elution step, the temperature of the elution buffer was increased to 65°C that allows a better elution efficiency. A PCR combined with restriction analysis was used to determine the BAC portion inserted in the cosmid.

2.2.3. RNA techniques

2.2.3.1. RNA extraction

Seedlings grown on agar plates were frozen in liquid nitrogen and ground to a fine powder with mortar and pestle. Fifty to 100 mg of powder were transferred to a 2 ml Eppendorf tube and 1 ml of TRIZOL[®] Reagent (Invitrogen AG, Basel, Switzerland) was added. The tubes were centrifuged at 11,400 rpm for 15 min at 4°C (Eppendorf 5402) and the supernatants were transferred to a new tube. Chloroform was added (300 µl) and vortex was applied for 15 s. The samples were centrifuged again at 11,400 rpm for 15 min at 4°C and the aqueous phase was transferred to a new tube. After the addition of 750 µl of isopropanol the samples were incubated 10 min at RT and centrifuged at 11,400 rpm for 10 min at 4°C. After washing the pellet with 1 ml of 75% ethanol, the samples were centrifuged at 9,000 rpm for 5 min at 4°C. The pellet was air-dried and dissolved in 150 µl of RNase-free water with a pipette tip. To increase the solubility, the samples were incubated for 5 min at 55°C. For quantification, 100 µl of a 1:100 dilution from each sample were placed in a quartz cuvette and OD₂₆₀ and OD₂₈₀ were measured in a spectrophotometer (DU640 Beckman Coulter, USA). RNA concentration was calculated according to Sambrook *et al.* (1989). To assess the quality of RNA, an aliquot containing 2 µg was loaded on a 2% agarose gel. The RNA was stored at -80°C.

2.2.3.2. Analysis of RNA

Three µg of total RNA was loaded on normal TBE agarose gel and electrophoresis carried out for 1 hour at 60V.

2.2.3.3. DNase treatment

DNase treatment was performed in order to eliminate the remaining genomic DNA. For each 3 µg of RNA 1 unit of RQ1 RNase-Free DNase and 1 µl of RQ1 RNase-Free DNase 10x Reaction Buffer (Promega, Madison, USA) were mixed and water was added to a final volume of 10 µl. The reaction was incubated for 1h at 37°C and afterwards the enzyme was inactivated by adding 1 µl of a stop solution and incubating it at 65°C for 10 min.

2.2.3.4. cDNA synthesis

To synthesize the cDNA from the RNA samples, the SuperScript™ II Reverse Transcriptase system (Invitrogen AG, Basel, Switzerland) was used. Five hundred ng of Random Primers (Invitrogen AG, Basel, Switzerland) and 1 µl of 10 mM dNTP Mix were added to the RNA samples. After incubation at 65°C for 5 min, the samples were allowed to cool down at RT for 10 min. To perform the synthesis, 4 µl of 5 x First-Strand Buffer, 2 µl of 0.1 M DTT, 40 units of RNaseOUT™ Recombinant Ribonuclease Inhibitor and 200 units of SuperScript™ II Reverse Transcriptase were added to the tubes. The contents were mixed gently and the samples were incubated at 42°C for 50 min. The reaction was stopped by heating at 70°C for 15 min. After dilution with 80 µl of water the samples were used for PCR.

2.2.4. Transformation methods

2.2.4.1. Preparation of VCS257 competent cells

The *E. coli* VCS257 were prepared for the transfection by cosmid. Five ml pre-culture were incubated overnight at 37°C. The next day, 100 µl of this pre-culture was transferred to 50 ml of LB (+10mM MgSO₄ and 0.2% (w/v) Maltose) until the OD₆₀₀ reached 0.9. The bacteria were pelleted down at 500 for 10min. The cells were resuspend in an appropriate volume of 10 mM MgSO₄ to have an OD₆₀₀ of 0.5.

2.2.4.2. Transfection of *E. coli* VCS257 by the cosmid constructs

The ligation mixture was added to the packaging extract and incubated during 2 h at RT. Five hundred μl of the SM buffer (100mM NaCl, 50 mM Tris-HCl pH 7.5, 10 mM MgSO_4) were added to the tube and subsequently 20 μl of chloroform. After a brief centrifugation, the supernatant was stored until the transfection.

Twenty five μl of three dilutions (1, 1/10, and 1/50) of the cosmid packaging reaction mixture in the SM buffer and 25 μl of the appropriate bacterial cells were incubated 30 min at RT. Each sample was then incubated in 200 μl of LB medium for 3 hours, shaken once every 15 min. They were then spun down and spread on LB-tetracycline plates.

2.2.4.3. Preparation of electro-competent *Agrobacterium tumefaciens* C58 cell

A stock culture of *Agrobacterium* C58C1 was defrosted on ice and 10 μl were used to inoculate 2 ml of LB medium containing 100 $\mu\text{g}/\text{ml}$ ampicillin and 100 $\mu\text{g}/\text{ml}$ rifampicin. After overnight culture in a shaker (200 rpm) at 28°C, the cells were transferred to 500 ml of fresh LB medium containing the antibiotics and grown to an OD_{600} of 0.5. The culture was centrifuged for 15 min at 4°C and 5,000 rpm (Sorvall RC-5B) and the pellet was resuspended in 500 ml of 1 mM HEPES buffer, pH 7.4. The cells were again centrifuged as mentioned above, and the pellet was resuspended in 500 ml of the same buffer. After one more centrifugation step the pelleted cells were resuspended in 10 ml of 1 mM HEPES buffer, pH 7.4, and centrifuged again. The pellet was finally resuspended in 2 ml ice-cold 10% glycerol and aliquoted. This bacterial stock was immediately frozen on liquid nitrogen and stored at -80°C.

2.2.4.4. Electroporation

An 80 μl aliquot of the electro-competent *Agrobacterium* stock was thawed on ice and approx. 1 μg of the construct was added. After incubation for 3 min on ice, the mix was transferred to a precooled electroporation cuvette (0.2 cm electrode gap) and the following electroporation conditions were set on the Gene Pulser (Bio-Rad, AG, Reinach, Switzerland): 2.4 kV, 400 Ω and 30 μF . After electroporation the cuvette was immediately removed from the chamber and 1 ml of LB medium was added. The suspension was transferred to an Eppendorf tube and incubated 2 h in a shaker at 28°C. The culture was spread on selective kanamycin LB-agar plates and after 48 h at 28°C colonies started to appear.

2.2.4.5. Verification of the transformed *Agrobacterium*

Two ml of a 4 ml LB culture of the different colonies obtained after electroporation were spun down. A bacto-PCR with the corresponding primers used during the identification of the contig was used to confirm the presence of the insert. The other 2 ml were mixed with sterile glycerol (w/w) to prepare the glycerol stock.

2.2.5. Transformation of *Arabidopsis thaliana* with *Agrobacterium*

2.2.5.1. Plant growth

Arabidopsis was grown on soil under continuous light for five weeks or until bolting. The first emerging bolt was cut back to allow the proliferation of many secondary bolts. Four to 6 days after clipping, the plants were ready for transformation.

2.2.5.2. *Agrobacterium* growth

After 24 h growing in the shaker (200 rpm) at 28°C, the liquid pre-culture was transferred to 50 ml of the LB-medium containing antibiotics and was incubated for 12 h under the same conditions. For the last subculture step, the 50 ml bacterial culture was poured into 1 l of the selective LB medium and grown until an OD600 of 2. After 10 min of centrifugation at 5,000 rpm and 4°C, the supernatant was discarded. The pellet was resuspended in the infiltration medium (4.9 g of MS-salt (Murashige and Skoog 1962) with vitamins; 10% sucrose; 4 µl of 6-benzylaminopurine (10 mg/ml) and adjusted to an OD600 of 0.8 (approx. 2 l of medium).

2.2.5.3. Transformation of *Arabidopsis* by the floral dip method

The *Agrobacterium* infiltration solution was supplemented with 500 µl of the detergent Silwet L-77 and the above-ground parts of *Arabidopsis* were dipped for 2-3 seconds with gentle agitation. The plants (T0 plants) were then placed under a transparent plastic wrap film for 24 h to maintain high humidity. The T1 seeds were collected after approx. 10 weeks.

2.2.5.4. Selection of positive transformants

T1 seeds (seeds from T0 plants) were vernalized and sown on MS plates supplemented with 25 µg/ml of Basta. The seedlings were grown for 10 days under continuous light and resistant seedlings were selected and transferred to soil for the seed collection. Vernalized T2 seeds were sown as described above and the percentage of resistance on MS-Basta medium per transgenic line was calculated (lines with 75% of resistant plants correspond to 1 copy of the transgene inserted). In the T3 generation, homozygous lines with 100% resistance in MS-Basta were selected.

2.2.6. Pigment techniques

2.2.6.1. Extraction of the pigments for carotenoid and chlorophyll quantification

2.2.6.1.1. Extraction of the pigments

The pigments contained in 100 mg of leaves frozen in liquid nitrogen were extracted with acetone using a polytron. The extract was centrifuged at 10,000g during 1 min to precipitate the debris. The supernatant was conserved at -20°C until analysis.

2.2.6.1.2. High Performance Liquid Chromatography

The pigments extracted by acetone were separated using a reverse phase HPLC. A column Zorbax C18 ODS (250mm x 4.5mm) was used. Pigments were eluted by 100% of solvent A (methanol/acetone/water/triethylamine, 90 : 17 : 11 : 0.1, v/v) during 15 min followed by a linear gradient to 100% of solvent B (methanol/acetone, 60 : 40, v/v), which was maintained isocratically during 30 min. The peaks were detected at 420 nm, or by a diode array detector between 350 nm and 550 nm. The spectra allowed to determine the identity of the different carotenoids. In addition, their identity was confirmed using standards under the same conditions.

2.2.6.1.3. Determination of Pchl_a content

WT, *flu* and *soldat30/flu* seedlings were grown for 5 days under continuous light. After a 15-hour dark period, thirty seedlings per sample were mechanically homogenized with a polytron (Ultra-Turrax T25, IKA Labortechnik, Staufen i. Br., Germany) in 700 µl of 90% acetone (Spectralanal; Riedel-de Haën, Seelze, Germany) containing 0.1% NH₃ (32% stock solution). After 10 min of centrifugation at maximum speed (~13,000 rpm) and 4°C, the supernatant was transferred to a fresh tube and kept at 4°C. To detect Pchl_a, a gradient high performance liquid chromatography (HPLC) system was used, equipped with a fluorescence detector (Spectra System FL3000), a degaser (Spectra System SCM400) and a quaternary gradient pump (Spectra System P4000) from Thermo Separation Products (Allschwil, Switzerland) and a reverse phase column 25C18-25QK (Interchrom, Montluçon, France). Eighty µl of sample were injected into the 50 µl-loop of the HPLC system. The following gradient was applied: 5 min 60% acetone, 20 min gradient from 60 to 100% acetone, 5 min gradient from 100 to 60% acetone. Running solutions (60% and 100% acetone) were supplemented with 50 µg/l of acetic acid. The fluorescence was measured at 630 nm using an excitation wavelength of 430 nm and chl_a was quantified based on peak heights and areas calculated by a ChromJet computing integrator (Spectra-Physics, Fremont, USA).

2.2.7. Green-gel

The green gel was carried out according to Peter et al. (1991) with some modifications.

2.2.7.1. Isolation and solubilization of membrane sample

Fifty 5 day old seedlings were mixed in chilled grinding buffer (0.4 M sorbitol, 10 mM Tricine-NaOH, pH 7.6, 10 mM MgCl₂) and homogenized 3 times for 5 s at full power in a Waring Blender. The homogenate was poured through 4 layers of Miracloth and the filtrate was centrifuged at 3020 g for 2-5 min at 4°C. The chloroplast pellet was resuspended in 40 ml of lysis buffer (10 mM Tricine-KOH, pH 7.6, 2 mM Na₂EDTA) with a glass-glass homogenizer and repelleted at 20,000g for 5 min at 4°C. The green thylakoid membranes were resuspended to 1.1 mg of chlorophyll/ml in gel buffer (12.4 mM Tris, 48 mM glycine, pH 8.6) plus 10% glycerol and stored at -70°C. The concentration of the chlorophyll was determined spectrophotometrically at 652 nm. When ready for use, the membranes were thawed quickly at

20°C, but were not allowed to reach room temperature, before being chilled on ice. These membranes were solubilised by combining 9 vol of membranes with 1 vol of surfactant stock (decyl maltoside 10% (w/v)), to yield a final 10:1 weight ratio of surfactant to chl. The surfactant extracts were spun 2 min in a microfuge to remove starch, and the green supernatant was applied to gels for PAGE.

2.2.7.2. Electrophoresis conditions

Twenty five µg of chlorophyll were loaded per lane. The reservoir buffer consisted of 124 mM Tris-base, Glycine 960 mM, pH 8.3, and 0.2% (v/v) Deriphat 160. The gels were run at 100V for 60 min.

2.2.7.3. Extractions of pigments from bands

Bands were cut with a scalpel and were ground with a pestle in 3 equivalent volumes of reservoir buffer in a mortar. Three equivalent volumes of water were added and mixed. An equivalent volume of chloroform was added, mixed vigorously and centrifuged for 2 min. The organic fraction was concentrated in a rotary evaporator to a volume of less than 1 ml. The remaining fraction was then completed to 2 ml with methanol and was filtered through a 20 µm sieve before injection into the HPLC.

2.2.7.4. MS and NMR spectra

Mass spectra and NMR spectra analysis were done at the laboratory of Prof. Bernard Kräutler (Innsbruck, Austria) by Dr. Thomas Müller.

2.2.8. Protoplast experiments

2.2.8.1. Preparation of protoplasts

Five-day old seedlings grown in continuous light on MS-Agar petri dishes were digested during 16 hours, in the dark or in the light depending on the experiment, in 0.5 M mannitol, 1 x MS, 1.2% cellulase, 0.8% mazerozym, pH 5.8. The protoplasts were obtained by filtering the digested seedlings through a 100 µm sieve. The filtrate was poured gently on 10 ml of 21% (w/v) sucrose and centrifuged 10 min at 600 rpm (Heraeus Minifuge RF). The protoplasts were pipetted out and were washed 2 times in 15 ml W5A medium (0.6 M mannitol, 1 mM MgCl₂, 5 mM glucose, 154 mM NaCl, 1.2 mM CaCl₂, 5 mM KCl, 0.1% MES/KOH (w/v), pH 5.8). The purified protoplasts were eventually placed in the culture medium (1x MS, 0.4 M mannitol, 0.4 M glucose, 0.1% MES, pH 5.8).

2.2.8.2. Evans blue staining

To measure the extent of cell death, the ratio of dead to living protoplasts was determined. To detect dead protoplasts, 2 µl of 0.5% Evans Blue were added to 20 µl of aliquot of protoplasts. The dead blue protoplasts were counted under the microscope.

3. Results

3.1. Genetic approach to study the effect of singlet oxygen in the *flu* mutant

3.1.1. Isolation of *soldat/flu* suppressor mutants

Second site mutations of *flu* were characterized that selectively suppress the singlet oxygen-mediated cell death response of seedlings. For that purpose, seeds of the *flu* mutant were chemically mutagenized with ethylmethanesulfonate (EMS). Approximately 200 seeds from each of 60 different M2 seed batches were germinated separately on MS agar plates and kept for 7 days under 16h light/8h dark long day conditions. All of the original *flu* seedlings bleached and died under these growth conditions, whereas some of the M2 seedlings started to green and survived. One group of suppressor mutants which showed a similar high intensity of red fluorescence in etiolated seedlings under blue light as the *flu* mutant was selected for this study. This similar red fluorescence shows that the suppressor mutants might have a higher Pchl_a accumulation after the dark period compared to the wild type (WT). The selected suppressor mutants were backcrossed 2 times with the original *flu* mutant. The segregation analysis of the F2 generations of these crosses showed that in each case the second site mutant phenotype was caused by a single recessive mutation. These mutants were dubbed Singlet Oxygen Linked Death Activator (*soldat*). One of these mutants, *soldat30/flu*, was chosen for a more detailed analysis based on the clear suppression of cell death at the seedling stage under non-permissive light/dark conditions. However, *soldat30/flu* does not revert the singlet oxygen-induced growth inhibition at the rosette stage.

3.1.2. Phenotypic and physiological analysis of *soldat30/flu*

3.1.2.1. Phenotype of *soldat30/flu* at the rosette leaf stage

WT, *flu* and *soldat30/flu* were grown under continuous light until they reached the rosette leaf stage. They were then transferred to long day conditions (16h light/8h dark). Although WT continued to grow, *soldat30/flu* stopped growing and developed necrotic lesions ((A) Figure 3.1) as *flu* does. However, under continuous light *soldat30/flu* was less affected than the parental *flu*. If the plants were not transferred to long day conditions, *flu* plants grew normally. Even though the size of the *soldat30/flu* mutant is the same as WT, green areas can be seen mainly at the cauline leaves, probably due to the effect of the *soldat30* mutation.

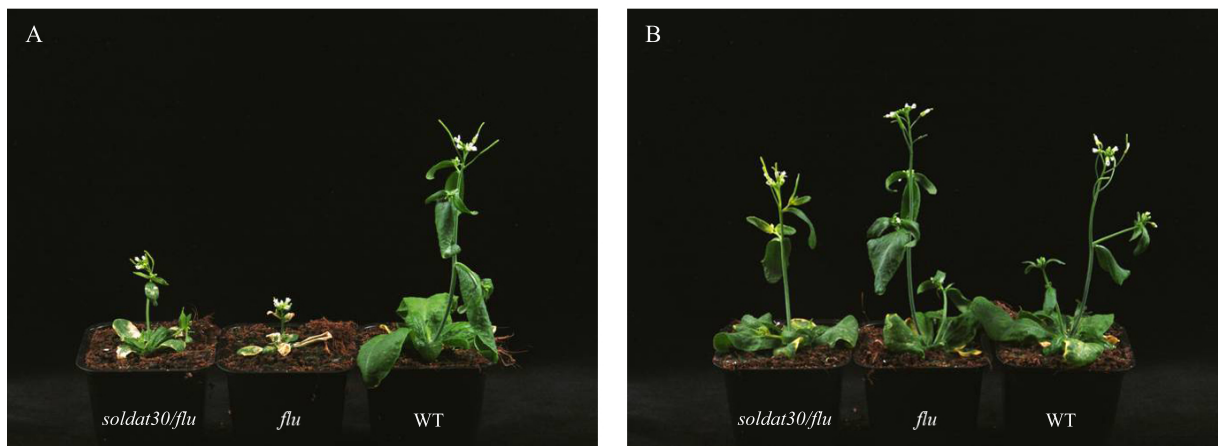


Figure 3.1: Phenotype at rosette leaf stage

Plants were grown under continuous light until the rosette leaf stage was reached. They were then transferred to long day conditions for one week (A). *flu* and *soldat30/flu* developed necrotic lesions due to the singlet oxygen release during reillumination after the dark period and stopped growing. *soldat30/flu* seems to be a bit less susceptible to singlet oxygen than *flu*. If plants were kept under continuous light, *flu* grew as WT.

3.1.2.2. Phenotype of *soldat30/flu* at the seedling stage

Originally, *soldat30/flu* was isolated in the suppressor mutant screen by growing seeds on agar plates under long day conditions. However, for a better physiological characterization, a 5 day-old seedling stage was chosen. The seeds were stratified for one week and seedlings were grown under continuous light for 5 days. They were subsequently kept for 8h in the dark, to allow Pchl_a accumulation to occur, and were then reexposed to light. *flu* seedlings bleached and died after 24 hours, whereas *soldat30/flu* seedlings remained green and continued growing (Figure 3.2).

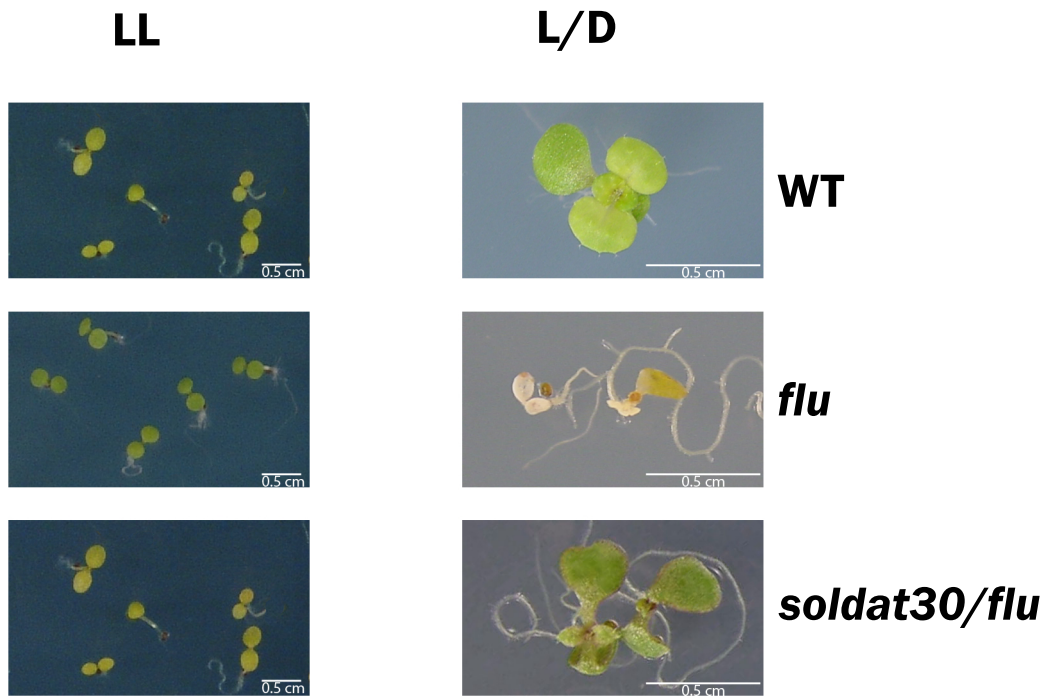


Figure 3.2: Phenotype of *soldat30/flu* at the seedling stage

Phenotype of the WT, *flu*, *soldat30/flu*. LL: the seedlings were grown under continuous light conditions for 5 days. L/D: the seedlings were grown under continuous light for 5 days before being transferred to non permissive light conditions during 5 additional days.

3.1.3. Pchlride accumulation

Preliminary fluorescence measurements after the dark period suggested a similar Pchlride level in both *flu* and *soldat30/flu*. To confirm this result, a more accurate procedure was used. The relative content of Pchlride in *soldat30/flu* seedlings compared to *flu* was determined by using a high performance liquid chromatography approach (HPLC). In 5 day-old seedlings, Pchlride accumulated in *flu* after 8h dark is 8 times higher than in the wild type.

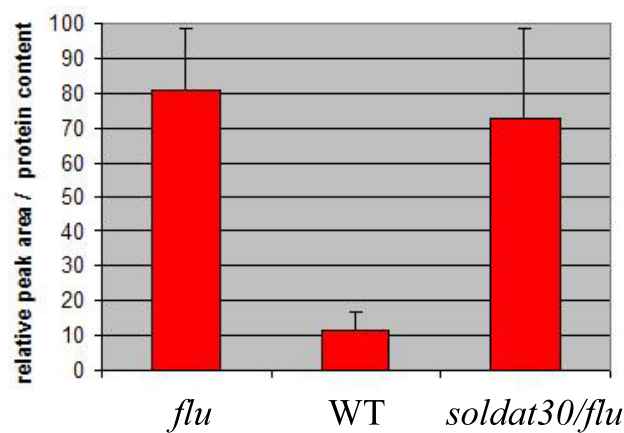


Figure 3.3: Pchlride content in seedlings grown for 5 days under continuous light followed by an 8 hour-dark period. Data are the average of five independent biological experiments

3.1.4. Map-based cloning

A map based cloning approach was used to identify the *soldat30* gene responsible for the reversion of the *flu* mutant. This method exploits the genetic variations between two ecotypes within the same species. It consists of locating (mapping) the gene on the plant's chromosome by crossbreeding with another ecotype, and looking for traits (markers) that cosegregate in the offspring. Markers usually used with Arabidopsis are Simple Sequence Length Polymorphism (SSLP), Cleaved Amplified Polymorphic Sequence (CAPS), or Single Nucleotide Polymorphisms. After narrowing down the region of interest to a suitable size, the genes residing in this region have to be complemented to check whether or not the introduction of a wild type copy of the gene can restore the original phenotype.

3.1.5. Creating the mapping population

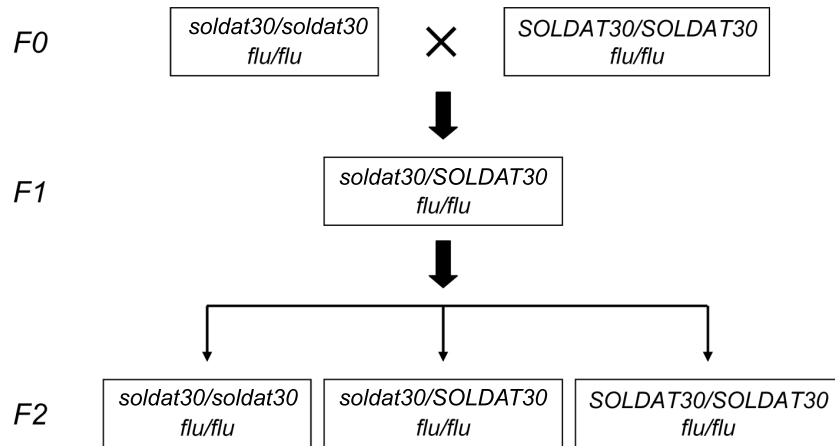


Figure 3.4: Scheme of a cross of *soldat30* and *flu*

The *soldat30/flu* was crossed with *flu*-Columbia (*flu*-Col). *flu*-Col had been obtained by backcrossing 2 times *flu*-Ler in WT-Col. The genomes of Ler and Col ecotypes have been fully sequenced (<http://www.arabidopsis.org/browse/Cereon/>), and polymorphic markers are known that could be used for the map based cloning of the mutated gene. Thanks to these sequences, it is relatively easy to create markers close to *SOLDAT30*. The F2 generation of these crosses consists of a plant population which can have 2 different phenotypes under the non-permissive light/dark conditions, either the *flu* phenotype (plants die) or the *soldat30* phenotype (plants survive). The segregation observed was 1:3 for the mutation in the *SOLDAT30* gene. The *soldat30* mutation is therefore recessive since both *soldat30* gene copies have to be mutated to confer resistance to singlet oxygen. *soldat30* F2 seedlings were selected as mentioned in paragraph 3.1.2.2. A mapping population of 500 F2 plants which had the *soldat30* phenotype were selected for the map-based cloning.

3.1.6. Crude mapping

For the crude mapping, DNA was extracted from the plants and analyzed with SSLP markers along the whole genome. SSLP markers exploit the difference in lengths of repeat regions between the two ecotypes. Typically, two SSLP markers per chromosome are designed and the genetic distance between each marker and the *SOLDAT30* locus is calculated with the following formula:

$$\text{Genetic distance} = \frac{2 \times (\text{number of non linked signals}) + (\text{number of heterozygous signals})}{2 \times \text{total number of selected plants}} \times 100$$

The first crude mapping indicated that the gene responsible for the *soldat30* phenotype was localized at the top of chromosome III (Figure 3.5), close to the location of the *flu* gene. Because the WT-Col line used for this mapping population was obtained by backcrossing *flu*-Ler with WT-Col, the selected *soldat30/flu* line still retained Ler chromosomal material in the vicinity of the *FLU* locus. To overcome this problem, another mapping population had to be used which was made by crossing the *soldat30/flu*-Ler with a *flu*-TDNA line with a pure Columbia background.

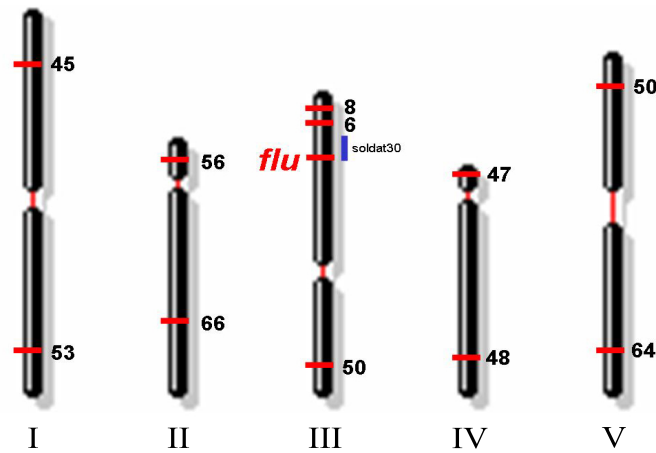


Figure 3.5: Crude mapping

Crude mapping localized the *SODLAT30* gene close to the *FLU* gene. Numbers indicate the calculated distance to the *soldat30* locus in Centimorgan.

3.1.7. Isolation of *flu* KO mutant

The putative *flu* T-DNA KO line (*flu*-KO) mutant was found in the Syngenta collection of T-DNA which is in *Arabidopsis Columbia*. The predicted insertion of the T-DNA in the putative *flu*-KO mutant was detected by using a PCR approach. We found that the T-DNA was inserted within the last exon of the *flu* gene at position 1034 after the ATG of the spliced RNA.

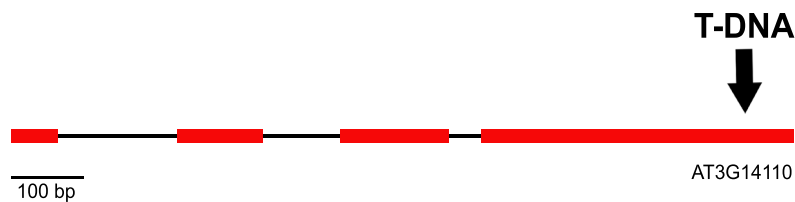


Figure 3.6: Location of the T-DNA insertion in the *flu*-KO line

The insertion of the T-DNA normally leads to an inactivation of the gene. By PCR, homozygous plants were selected and their seeds were collected. Seeds were germinated under dark conditions. Seven day-old etiolated seedlings were then transferred to the light and the

phenotype was observed. The homozygous *flu*-KO seedlings died after the dark/light shift like *flu*-5C (*flu*-Ler 5 times backcrossed in WT-Col) whereas WT-Col started to green.

3.1.8. Creating a second mapping population and fine mapping of *soldat30/flu*

The *soldat30/flu* mutant was crossed with the *flu*-KO mutant. Roughly 1000 F2 plants were selected from the new population to finalize the mapping. The region surrounding the *flu* locus could be narrowed down to about 150kb between the markers F20H23 and T11I18, which was still too big to identify the gene. No further polymorphisms were found within this region, probably due to the low recombination rate in this area of the chromosome.

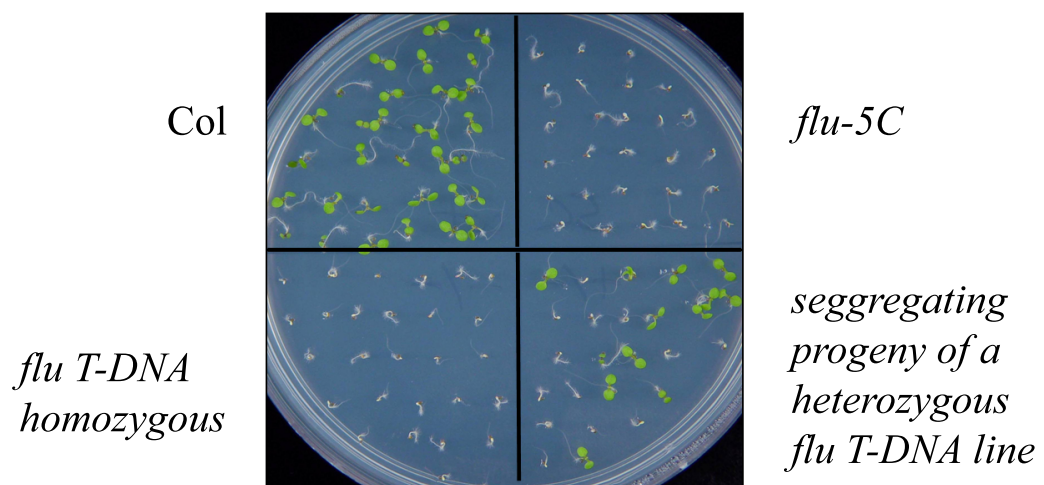


Figure 3.7: Phenotype of *flu*-KO

WT-Col, *flu-5C* (originally obtained from *flu-Ler*), homozygous *flu* T-DNA seedlings and progeny of heterozygous *flu* T-DNA line were grown from the beginning for 5 days under long day conditions. *flu* T-DNA has a similar phenotype as the original *flu-5C* mutant.

3.1.9. The complementation of *soldat30* with a BAC clone

To identify the *SOLDAT30* gene, a BAC (Bacterial Artificial Chromosome) complementation approach was undertaken. This involved investigating which fragment of DNA could complement the *soldat30* phenotype. *soldat30/flu* was transformed with DNA fragments and the transformed plants were checked for the *flu* phenotype.

BAC is a bacterial DNA vector able to carry an insert of DNA which has a typical size of 80 to 300 kb. It has additional replication origins and an antibiotic resistance gene which allows selection of the bacteria that carry the BAC. In the ABRC (Arabidopsis Biological Resource Center) collection clones F20H23 (~100kb) and T11I18 (~60kb) were found in the database to cover the region between the two closest markers. However, these BAC clones were too large to be integrated directly into Arabidopsis chromosomes. Therefore, BACs had to be cut by restriction enzymes into smaller fragments. These smaller fragments were cloned in a cosmid vector. A cosmid vector is a hybrid between a plasmid and a phage. It has a selection marker for bacterial culture (antibiotic resistance), a replication origin and *cos* sites from a lambda phage allowing integration into the lambda vector. The pBIC cosmid can integrate a fragment from 9 kb to 25 kb. Fragments from above 9 kb obtained by partial digestion of the original BAC were selected and ligated into the pBIC cosmid vector. The different cosmids were characterized using primers designed to anneal evenly along the 150kb region. The cosmid clones were selected in order to obtain a continuous contig covering the entire region (Figure 3.8). The *soldat30/flu* mutants were then transformed using the different cosmid constructs.

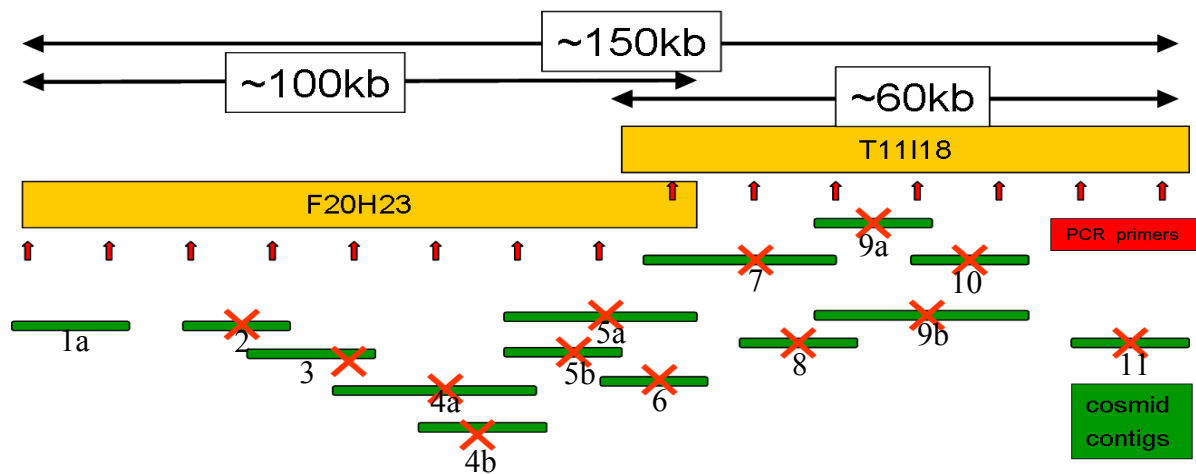


Figure 3.8: BAC complementation

2 BACs covered the 150 kb region. Primers were designed to anneal evenly along this region to characterize the different cosmids. The cosmid 1a gave a positive complementation.

3.1.10. Complementation of the *soldat30/flu* phenotype

soldat30/flu plants transformed with the different cosmids were selected on kanamycin medium. Their phenotypes were checked at the seedling stage under non-permissive light/dark conditions (Figure 3.9). *soldat30/flu* transformed with the construct 1a died after the dark/light shift, like the parental *flu* mutant and unlike *soldat30/flu* or WT plants.



Figure 3.9: Complementation of the *soldat30/flu* phenotype

The insertion of the *SOLDAT30* wild type copy into the *soldat30/flu* mutant restored the original *flu* phenotype.

3.1.11. Determination of the *soldat30* gene

The DNA fragment that could complement the *soldat30* mutation carried 3 genes (Figure 3.10). In order to determine which of these genes is responsible for the *soldat30* phenotype, the 3 genes were sequenced (Figure 3.10). The only gene that carried a mutation was the gene At3g03710, encoding a polyribonucleotide nucleotidyltransferase (PNPase), having a classical G to A EMS mutation. The G to A mutation was found to be localized at the end of the 12th exon (the position 1436 of the cDNA) and led to an amino acid exchange from Arg to His (Figure 3.11).

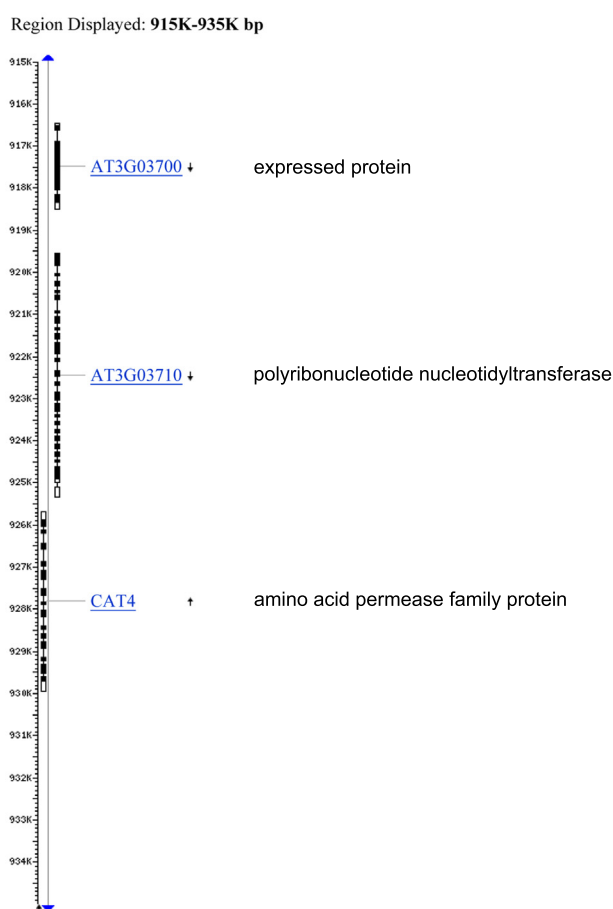


Figure 3.10: Genes localized within the interval between the two PCR markers (from TAIR).

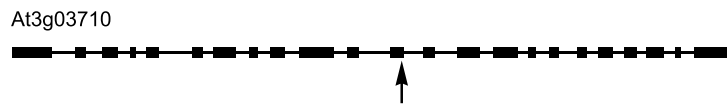


Figure 3.11: Localization of the mutation in the PNPase gene

A G to A mutation led to an amino exchange from Arg to His in the 12th exon

3.1.12. *In silico* analysis of the *soldat30* gene

3.1.12.1. Gene and protein sequence *soldat30*

The gene of the PNPase has 25 coding exons (Figure 3.11). The length of its cDNA from the ATG to the stop codon is 2769bp. The predicted protein sequence is shown in Figure 3.12. The amino acid exchange is underlined.

MIGSENIWE	IKTRFNLKPE	TRLATPHTES	QEKLPRLQGT	DKVSLFLTLSSLKKEED
VDESHSGGGG	KLCSLSLLSG	SGAGKFSVRA	LVRPDDTDDA	DSVGDGSLAFPNHVSVKIPF
GNREILVETG	LMGRQASSAV	TVTDTGETIVY	TSVCLADVPS	EPSDFLPLYVHYQERFSAVG
RTSGGFFKRE	GRTKDHEVLI	CRLIDRPLRP	TMPKGFYNET	QILSWVLSYDGLHAPDALAV
TSAGIAVALS	EVPNAKAIAG	VRVGLIGGEF	IVNPTVKEME	ESQLDLFLAGTDTAILTIEG
YSNFLPEEML	LQAVKVGQDA	VQATCIAIEV	LAKKYGKPKM	LDAIRLPPPELYKHVKELAG
EELTKALQIK	SKISRRKAIS	SLEEKVLTIL	TEKGYVIDEV	AFGTIEAQPDLEDEDEDEE
VVPEGEVDQG	DVHIRPIPRK	PIPLLFSEVD	VKLVFKEVSS	KLLRRRIVEGGKRS DGR TLD
EIRPINSRCG	LLPRAHGSTL	<u>FT</u>RGETQALA	VVTLGDKQMA	QRIDNLEGSDEYKRFYLQYT
FPPSSVGEVG	RIGAPSRREI	GHGTLAERAL	ETILPSDDDF	PYTIRVESTVIESNGSSSMA
SVCGGCLALQ	DAGVPVKCSV	AGIAMGMVWD	TEEFGGSGSP	LILSDITGAEDASGDMDFKV
AGNEDGV TAF	QMDIKVGGIT	LEIMEKALIQ	AKAGRRHILA	EMAKSPPTLSLSKYAPLI
LIMKVHPSKV	YSLIGSGGKK	VKSIIEESGV	EAIDMQDDGT	VKIM AIDVASLERAKAIISG
LTMVPSV GDI	YRNCEIKSMA	PYGAFVEIAP	GREG LCHISE	LSAEWLAKPEDAYKVGDRID
VKLIEVNEKG	QLRLSVRALL	PESETDKDSQ	KQQPAGDSTK	DKSSQRKYVNTSSKDRAAAG
ASKVSSGDEL	VLKKKDV RRA	TGGSSDKTMN	SNSSTNEESL	VNGEATIS*

Figure 3.12: The PNPase protein sequence

The Arg (**R** shown in bold and underlined) is replaced by His in the *soldat30* mutant

The protein consists of 922 amino acids and has a molecular weight of roughly 100 kDalton. Five domains can be found: a putative transit peptide which would allow the protein to be imported into the chloroplast, a 3' exoribonuclease domain, a S1 RNA-binding domain, a polyribonucleotide nucleotidyltransferase RNA binding domain and a KH domain which is also involved in RNA binding. The mutation affects the exoribonuclease domain (Figure 3.13).

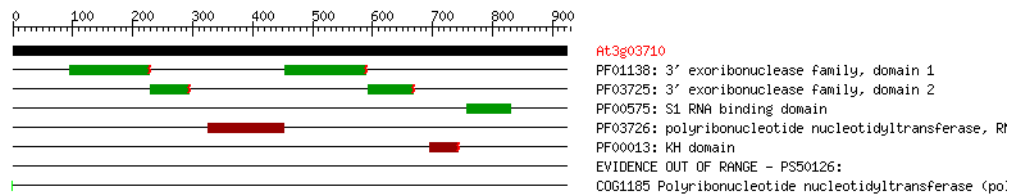


Figure 3.13: Domains of the PNPase predicted by the TIGR (The Institute for Genomic Research) program analysis

The PNPase has 4 domains, an exoribonuclease domain, a S1 RNA binding domain, a RH domain and a polyribonucleotide nucleotidyltransferase domain. The positions of the domains are indicated by the boxes.

3.1.12.2. The effect of the mutation on the maturation of 23S rRNA

The PNPase in chloroplasts has been found to be involved in the maturation of RNAs. One of them, the 23S RNA, has been shown to be 100 nt larger in PNPase knock-out plants when compared to the WT (Sauret-Gueto et al., 2006). To determine the effect of the *soldat30* mutation on the PNPase activity, the size of the 23S rRNA was determined. An agarose gel electrophoresis was run with total RNA extracted from *flu* and *soldat30/flu* grown under continuous light (Figure 3.14). The 23S RNA from *soldat30/flu* had, as expected, a higher molecular weight than the one extracted from *flu*. Furthermore, no correctly processed 23S rRNA could be observed, suggesting that the point mutation knocks out the function of the PNPase.

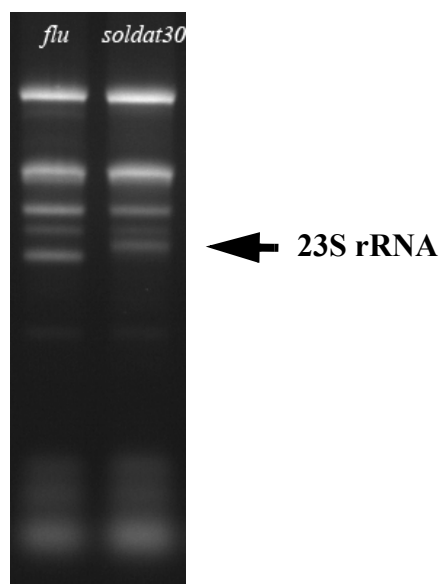


Figure 3.14: Agarose gel electrophoresis of total RNA

rRNA band pattern was compared between *flu* and *soldat30/flu*. The 23S rRNA is indicated by an arrow. The 23S rRNA is larger in *soldat30/flu* than in *flu*.

Recently, an allelic PNPase knock-out line *rif10* (Resistant to Inhibition by Fosmidomycin (FSM) 10) was isolated in a screen using a sublethal concentration of FSM, an inhibitor of the second step of the methylerythritol phosphate (MEP) pathway. This pathway leads to the formation of all isoprenoids derived from chloroplasts (Figure 3.15) (Sauret-Gueto et al., 2006). The resistance of the allelic mutant, *rif10*, was shown to correlate with the significant overaccumulation of the enzyme inhibited by FSM as well as other key enzymes of the pathway. However, the content of chlorophylls and carotenoids was reduced in the mutant, which can probably be explained by a reduced amount of light harvesting complexes, a parallel effect of the PNPase mutation. Yet, it is possible that other end products accumulate. Another possible end product would be tocopherols. Tocopherols originate from two pathways, the shikimate pathway and the isoprenoid pathway. They are well known singlet oxygen scavengers, mainly α -tocopherol. Therefore, the content of tocopherols was measured in *soldat30*.

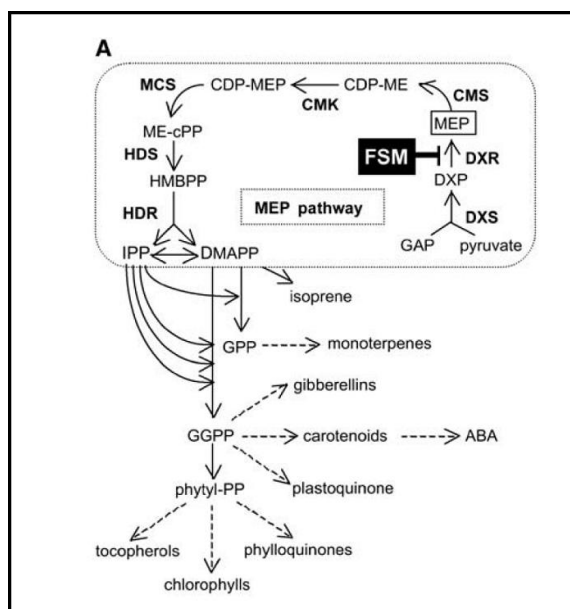


Figure 3.15: MEP pathway and its derivatives

Plastidial isoprenoids and FSM resistance. A, Schematic pathway for the biosynthesis of MEP-derived isoprenoids. Multiple steps are indicated by dashed arrows. The step inhibited by FSM is shown by a black box. GAP, glyceraldehyde 3-P; DXP, deoxyxylulose 5-P; MEP, methylerythritol 4-P; CDP-ME, 4-diphosphocytidyl-methylerythritol; CDP-MEP, CDP-ME 2-P; ME-cPP, methylerythritol 2,4-cyclodiphosphate; HMBPP, hydroxymethylbutenyl 4-diphosphate; IPP, isopentenyl diphosphate; DMAPP, dimethylallyl diphosphate; GPP, geranyl diphosphate; GGPP, geranylgeranyl diphosphate; ABA, abscisic acid. Enzymes are indicated in bold. DXS, DXP synthase; DXR, DXP reductoisomerase; CMS, CDP-ME synthase; CMK, CDP-ME kinase; MCS, ME-cPP synthase; HDS, HMBPP synthase; HDR, HMBPP reductase (From Sauret-Gueto et al., 2006).

3.1.13. Analysis of tocopherols in *soldat30/flu* and their role in the singlet oxygen signalling pathway

3.1.13.1. Measurement of the content of tocopherols in *soldat30/flu*

Tocopherols were extracted from 5 day-old *flu* and *soldat30/flu* seedlings. They were separated by HPLC and detected by a fluorescence detector. The corresponding chromatographs are shown in Figure 3.16.

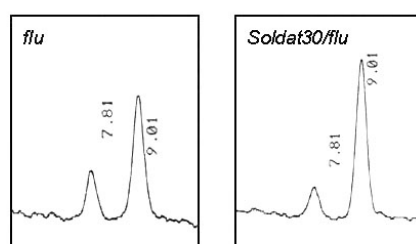


Figure 3.16: Tocopherol measurements in *soldat30/flu* seedlings

Tocopherols were detected by HPLC. HPLC of α - and γ -tocopherol showed that the peak with the retention time (RT) 7.81 corresponds to the γ -tocopherol, the one with a RT of 9.01 corresponds to α -tocopherol.

The mutation induces a 2-fold increase in α -tocopherol, the most efficient singlet oxygen scavenger (Figure 3.17).

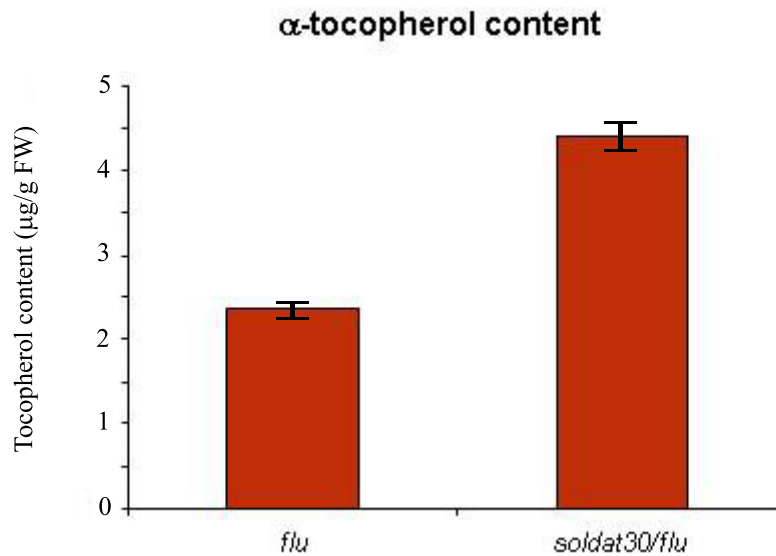


Figure 3.17: Content of α -tocopherol in *flu* and *soldat30/flu*

The α -tocopherol content of *soldat30/flu* was compared with that of *flu*. *soldat30/flu* contains roughly two times more α -tocopherol than the *flu* mutant.

Tocopherols may play a role as scavengers in *soldat30/flu* after the release of singlet oxygen and this would explain the reversion of the *flu* phenotype under non-permissive light/dark conditions, although the tocopherol overaccumulation may not be the only cause of this reversion. PNPase may have other effects which can lead to the inactivation of the singlet oxygen signaling pathway. To obtain more information about the role of tocopherols during the *flu* cell death response, a knock-out approach was used.

3.1.13.2. The *vte1* mutant

The *vte1* mutant is an EMS mutant that does not accumulate any tocopherols (Porfirova et al., 2002). The point mutation in the *vte1* mutant leads to complete inactivity of tocopherol cyclase (Figure 3.18). This mutant was crossed with the *flu* mutant in order to get a *flu* mutant devoid of tocopherols. *VTE1* is located on chromosome 4 and *FLU* on chromosome 3. Among the F2 generation of this cross, *flu* homozygous mutants containing or lacking the mutation of *vte1* were selected at the rosette stage. They were transferred to long day conditions for 2 days. The plants that developed necrotic spots on rosette leaves, showing them to be homozygous for *flu*, were selected to produce seeds. The F3 seedlings were grown and leaf samples were collected in order to determine whether or not the plants contained tocopherols (data not shown). *flu*

plants devoid of tocopherols (corresponding to the double mutant *flu/vte1*) were selected and seeds were collected. The F4 generation from one of the double mutants was used for the experiments

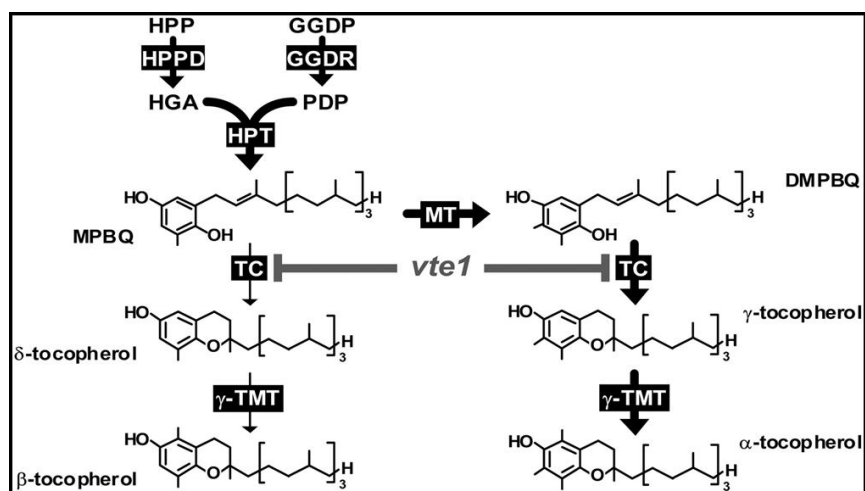


Figure 3.18: Tocopherol pathway showing *vte1*

The synthesis of tocopherols starts from DMPBQ and HGA. The tocopherol cyclase (TC) function is impaired in *vte1*. Abbreviations: DMPBQ, dimethylphytylbenzoquinone; DXP, 1-deoxy-D-xylulose-5-phosphate synthase; GGDP, geranylgeranyl diphosphate; HGA, homogentisic acid; HGGT, homogentisate geranylgeranyl transferase; HPPD, p-hydroxyphenylpyruvate dioxygenase; HPT, homogentisate phytyltransferase; MPBQ, methylphytylbenzoquinone; MT, methyltransferase; PDP, phytyl-diphosphate; T, tocopherol; g-TMT, g-tocopherol methyltransferase

3.1.13.3. The induction of cell death in the double mutant *vte1/flu*

The role of tocopherols in the *flu* mutant was investigated by comparing the phenotype of the *vte1/flu* double mutant with the *flu* single mutant under non permissive conditions (Figure 3.19). However, the strength of these conditions was reduced by decreasing the length of the dark period to 2 hours. Under these conditions, 5-day old *flu* seedlings were able to grow whereas the *flu/vte1* seedlings stopped to grow.

The effect of the release of $^1\text{O}_2$ on cell death was monitored after a 2 hour dark/light shift using trypan blue which stains specifically dead cells (Figure 3.20). A positive trypan blue staining was observed already after 2 hours of reillumination in the *flu/vte1* double mutant, while 12 to 24 hours were needed to obtain the same intensity of cell death in the *flu* single mutant.



Figure 3.19: Phenotype of *vte1/flu* and *flu* 12h after dark/light shift

flu and *flu/vte1* seedlings were grown for 5 days under continuous light on MS-agar plates before being transferred to long day conditions (2 h dark, 22 h light) for one week.

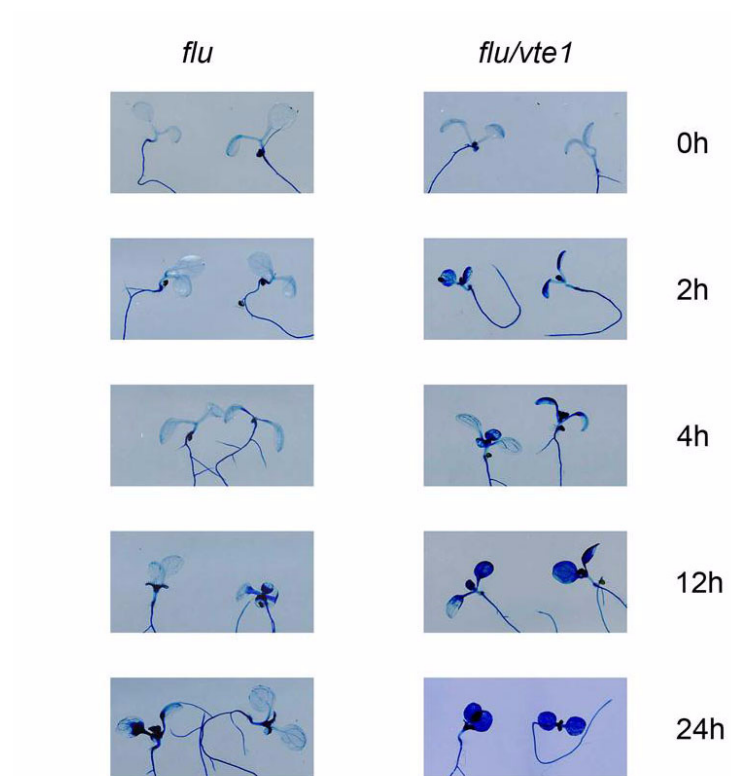


Figure 3.20: Cell death in *flu* and *flu/vte1*

Trypan blue staining was used to visualize cell death in 5 day-old *flu* and *flu/vte1* seedlings induced after the indicated time of reillumination. The dark period was reduced to 2 h so as not to be under saturation conditions.

3.1.13.4. Tocopherols can attenuate cell death in *flu* protoplast

An attempt was made to increase the tocopherol content of *flu* by overexpressing *VTE1*. The *VTE1* cDNA was fused to the 35S promoter. Tocopherol was extracted from transformed plants. In contrast to what was expected, no tocopherol was detected in these plants probably due to cosuppression of *VTE1*. Hence, another approach was undertaken to test the effect of elevated tocopherol levels on $^1\text{O}_2$ -mediated cell death. Five day-old *flu* seedlings were sprayed with an α -tocopherol solution (10 μM α -tocopherol, water, Tween20 0.1%(v/v)) and they were kept in the dark for 15 hours. Subsequently, protoplasts were prepared from these seedlings, and the beginning of cell death was monitored by counting protoplasts with positive Evans blue staining (Figure 3.21). Protoplasts prepared from *flu* plants sprayed with α -tocopherol showed a significant reduction of the cell death rate response by about 60% compared to protoplasts of mock-sprayed control seedlings. These results support a protective role of tocopherols in the *flu* seedlings during singlet oxygen mediated stress response.

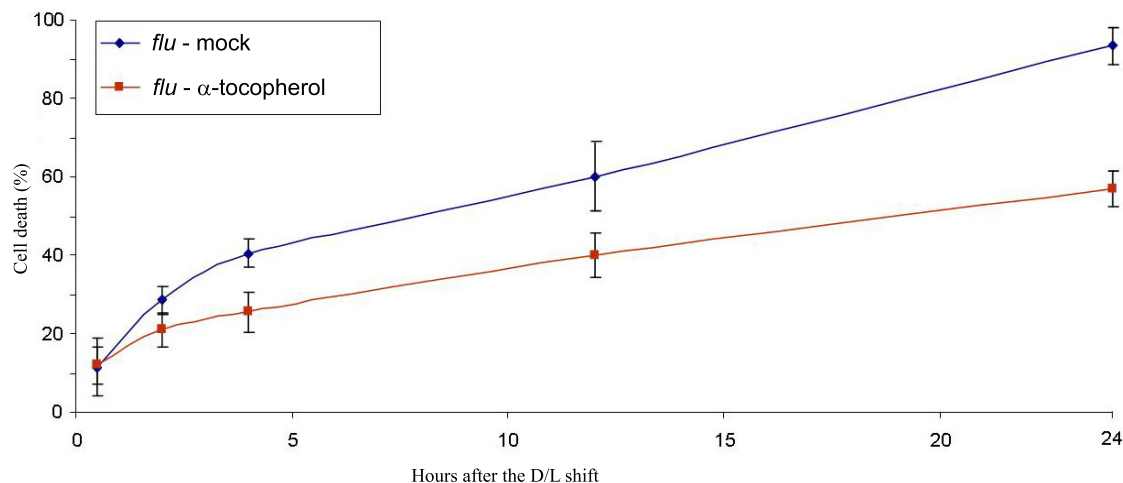


Figure 3.21: The scavenging effect of tocopherol on the cell death of the *flu* mutant

flu seedlings were grown for 5 days under continuous light and sprayed with α -tocopherol or with a mock solution. They were subsequently placed under dark conditions for 15 h. The protoplasts were prepared after the dark period and transferred to continuous light. Cell death was monitored by staining the seedlings with Evans blue.

3.1.14. *soldat30* has also an increased resistance to superoxide

The major ROS which are produced during the stress reaction are superoxide ($O_2^{\cdot-}$) and H_2O_2 . H_2O_2 is generally derived from $O_2^{\cdot-}$ by dismutation, either by a spontaneous chemical reaction with H_2O , or by the superoxide dismutase enzyme (see section 1.3.2). The *soldat30* mutant was tested to determine whether or not the mutation confers a higher resistance to $O_2^{\cdot-}$. In order to induce production of $O_2^{\cdot-}$ in chloroplasts, paraquat (1,1'-dimethyl-4,4'-bipyridinium) was used. Paraquat also affects all respiratory chain complexes in mitochondria. Paraquat is univalently reduced by PS I to its cation radical, which rapidly donates electrons to oxygen thereby producing superoxide radicals ($O_2^{\cdot-}$) (Babbs et al. 1989; Hiyama *et al.* 1993). Such superoxide production by PS I exceeds the antioxidant ability of the superoxide dismutase-ascorbate-peroxidase system (for a review see Asada (1994)).

The experiment was carried out with the *soldat30* line without the *flu* mutation. The *soldat30/flu* was backcrossed with Ler. Among the segregating F2 progeny, *soldat30* seedlings showing a pale green phenotype were selected and transferred to soil under long day conditions. Sequencing and RNA gel analysis confirmed the *soldat30* homozygous state of selected plants (see Figure 3.13). To test the homozygous state of the WT allele of the *FLU* gene, the segregation of the progeny of selected F2 plants were tested for the presence of the *flu* phenotype under non-permissive conditions.

A protoplast system was used to precisely quantify cell death. The protoplasts prepared from 5 day-old WT-Ler and *soldat30* seedlings were treated with different concentrations of paraquat (Figure 3.22). After 4, 8 and 24 h, the extent of cell death in the protoplasts was measured using Evans blue staining. The *soldat30* mutation attenuated the frequency of paraquat-induced cell death by 40% after 24 hours (Figure 3.22).

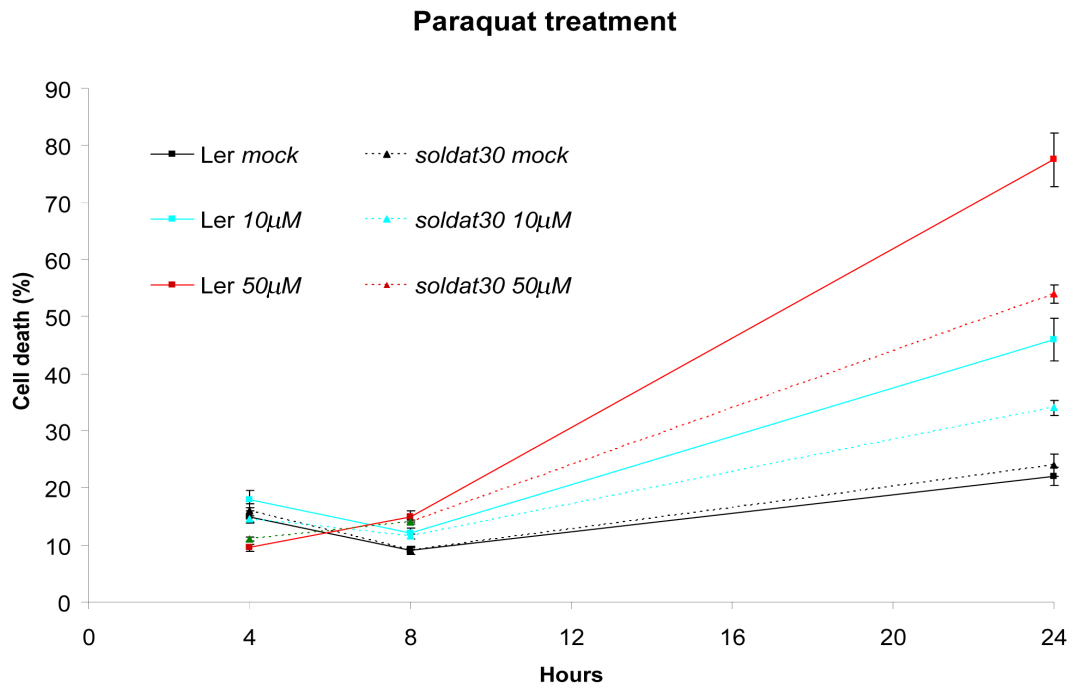


Figure 3.22: Effect of paraquat on protoplasts of the *soldat30* mutant

Cell death was measured in protoplasts prepared from 5 day-old seedlings of WT-Ler and *soldat30* grown in continuous light ($100 \text{ mmol.m}^{-2}.\text{s}^{-1}$) treated with paraquat or a mock solution. Cell death was monitored by Evans blue staining.

3.1.15. The effect of *soldat30* in seedlings exposed to natural stress conditions

Under severe stress conditions photoinhibition occurs, usually leading to a higher rate of ROS production. These stress conditions are known to induce cell death in a way similar to $^1\text{O}_2$ in the *flu* mutant. The effect of the *soldat30* mutation on seedlings was tested under high light and cold stress.

The conditions were optimized to induce a genetically controlled cell death and to avoid cytotoxic effects. The experimental setup is shown in Figure 3.23. *soldat30* seedlings or WT seedlings were grown under low light and room temperature ($10 \mu\text{mol}\cdot\text{m}^{-2}\cdot\text{s}^{-1}$, 21°C) for 6 days. The seedlings were then transferred to the dark for 4 h while the temperature was lowered to 10°C . The light stress consisted of irradiating the seedlings at $250 \mu\text{mol}\cdot\text{m}^{-2}\cdot\text{s}^{-1}$ at 10°C . The photosynthetic activity (Fv/Fm) was measured at different time points after reillumination (Figure 3.24). The Fv/Fm values of non-prestressed seedlings (np) were compared with those of prestressed (p) seedlings (Figure 3.23 and 3.24). The Fv/Fm values of the non-prestressed seedlings (np) were compared with those of prestressed (p) seedlings at the same time points (Figure 3.23 and 3.24). We can distinguish between two stages of stress response. During the first stage, np and p WT and np and p *soldat30* lost their photosynthetic activity similarly. The Fv/Fm values decreased from 0.8 to 0.6 after 4 days due to photoinhibition. During the second stage, in the subsequent time period, plants behaved differently. The p WT recovered (Fv/Fm increased again), whereas the np WT died (Fv/Fm continued to decrease). The Fv/Fm value of the np *soldat30*, like that of the p *soldat30*, remained constant. Interestingly, no difference between the p *soldat30* and np *soldat30* was observed during the experiment, hence, *soldat30* seemed to be already preacclimated to the high light/cold stress. After 9 days under these high light/cold stress conditions, the *soldat30*, either pretreated or not, looked phenotypically similar to the pretreated WT, whereas np WT died.

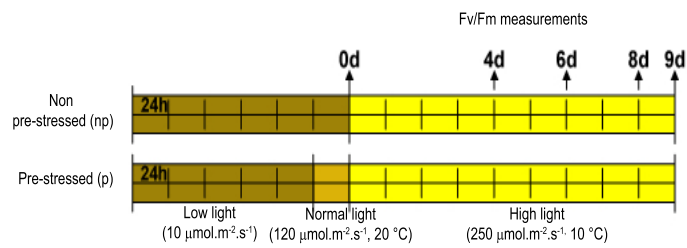


Figure 3.23: The experimental design for the analysis of acclimation to high light stress

The non-prestressed seedlings had initially been grown for 6 days under low light before they were shifted to the high light/cold stress. The photosynthetic activity (F_v/F_m) was measured at 0, 4, 6, 8, and 9 days after the beginning of the stress treatment. The prestressed seedlings were kept at 120 $\mu\text{mol.m}^{-2}.\text{s}^{-1}$ and room temperature (RT) for one day before the stress treatment.

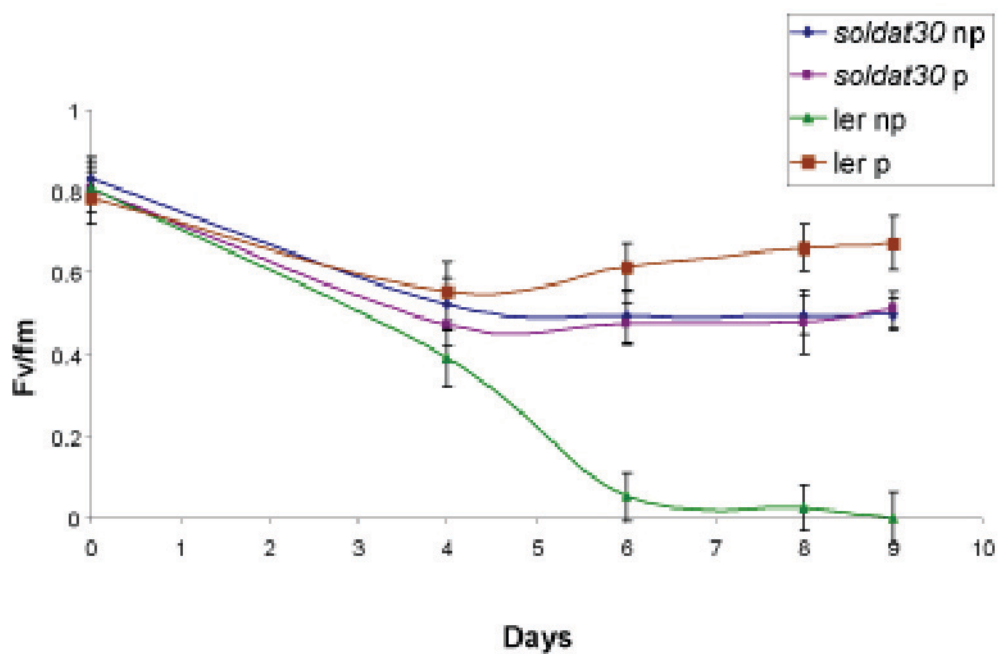


Figure 3.24: The effect of acclimation to high light / cold stress on WT and *soldat30*

WT seedlings that had been subjected to high light prior to the high light / cold stress were more stress resistant than np WT seedlings, whereas both np and p *soldat30* were equally resistant to the stress program, suggesting that *soldat30* could have been constitutively preacclimated. The data are the results of 3 independent experiments in which 50 seedlings were used per condition and per time point.

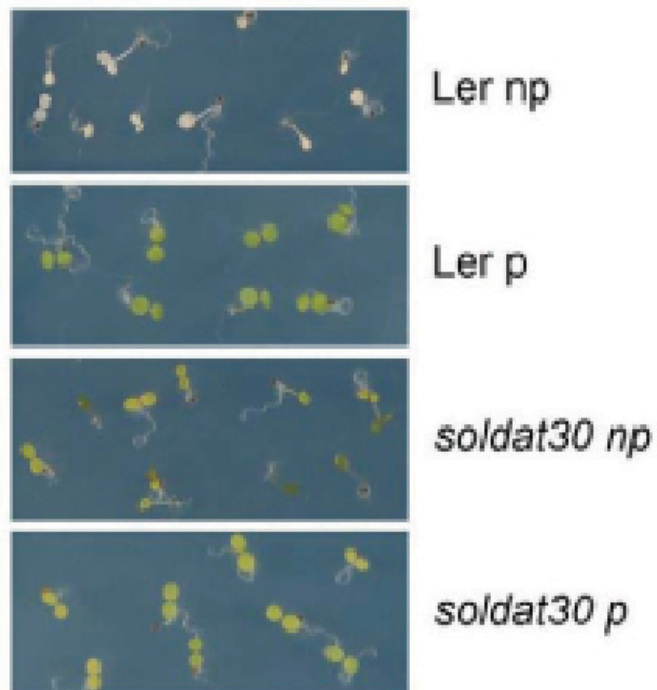


Figure 3.25: The phenotypic differences between 9 day-old pretreated and non pretreated WT and *soldat30* seedlings

The pretreatment of the seedlings with high light conferred an acclimation state that allowed the WT to resist the stress program. np *soldat30* and p *soldat30* looked phenotypically similar.

3.1.16. The effect of acclimation on the tocopherol content of *soldat30* and WT seedlings

The role of tocopherols during acclimation to stress was first addressed by using the *vte1* mutant, which has an impaired tocopherol biosynthesis. The *vte1* mutant was compared with WT-Col during the light/cold stress program. The tocopherol content of WT and *soldat30* was measured after the acclimation period and was compared with the tocopherol content of non-preacclimated seedlings (Figure 3.23 and 3.26). It was observed that the pretreatment by high light stress allowed the WT to recover from the high light/cold stress conditions whereas np WT died like np *vte1*. Interestingly, the p *vte1* mutant was not able to survive the high light/cold stress showing that tocopherols may play an important role during the acclimation period.

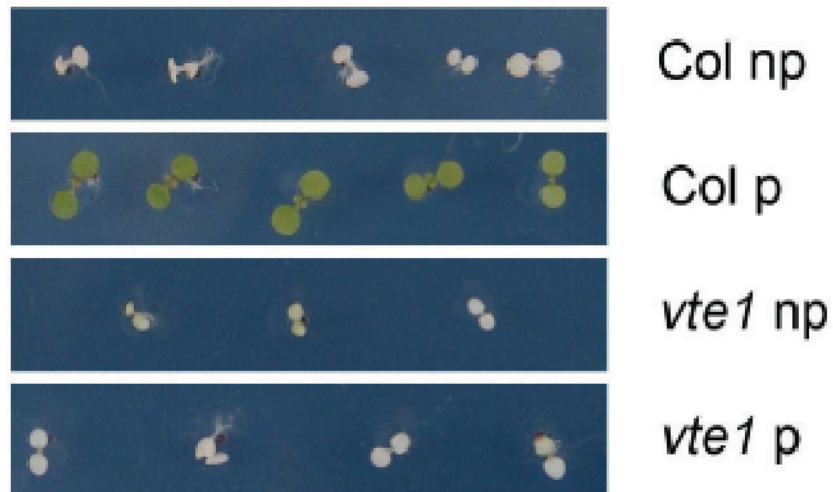


Figure 3.26: Phenotype of WT and *vte1* after 5 days of the stress treatment of high light and cold

While the pretreatment conferred a higher resistance of the WT to high light/cold stress, *vte1* was not able to acquire the acclimation state required to tolerate the stress program, showing that tocopherols play an important role during the acclimation process.

The higher accumulation of tocopherols in *soldat30* could be one of the reasons why the *soldat30* mutation conferred a higher resistance against the light/cold stress. The levels of tocopherol were measured in WT and *soldat30* before and after the pretreatment (Figure 3.27). The level of tocopherol in *soldat30* was higher than in the WT in particular α -tocopherol which reached three times the value of WT. During the pretreatment (24 h, $120 \mu\text{mol.m}^{-2}.\text{s}^{-1}$) the synthesis of tocopherol was upregulated by more than 10 times in both WT and in the *soldat30* mutant. This supports further the notion that the accumulation of tocopherols during acclimation may be a key process for establishing resistance to the subsequent stress program. The higher amounts of tocopherol in *soldat30* may be sufficient to detoxify the ROS induced by the stress treatment.

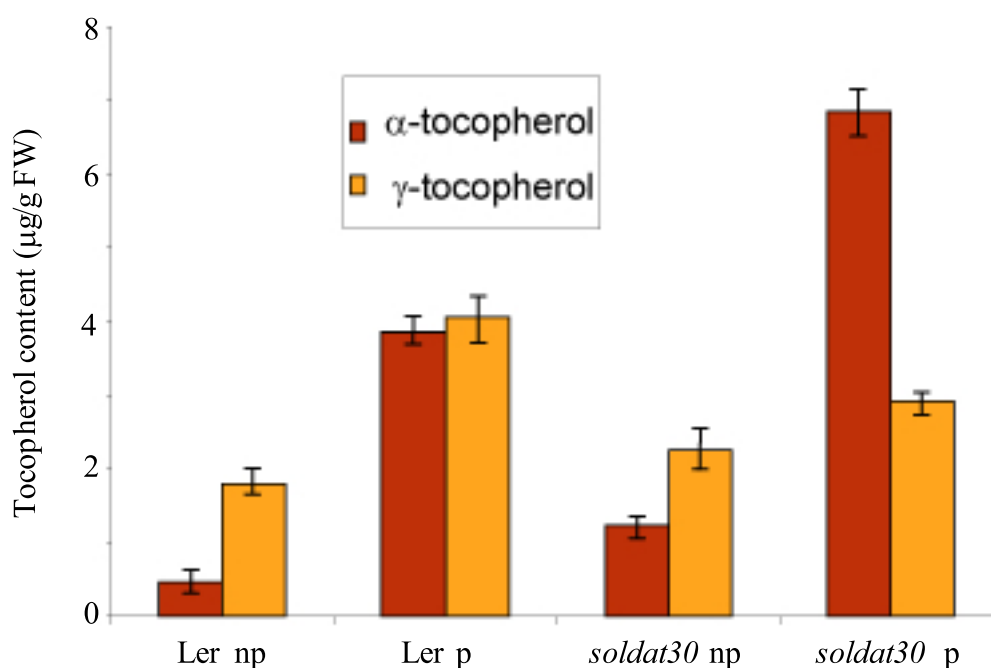


Figure 3.27: Tocopherol content in Ler and in the *soldat30* mutant after preacclimation

α - and γ -tocopherol contents were determined in Ler and in *soldat30* seedlings prestressed or not prestressed.

3.2. The biochemical characterization of the effect of singlet oxygen in the *flu* mutant

3.2.1. Pigment accumulation in *flu* after a dark-light shift

In addition to the genetic analysis, the *flu* cell death was also characterized biochemically. Since the singlet oxygen is known to have various effects on a variety of molecules, the effect of singlet oxygen on the amount and composition of the carotenoids and chlorophylls in the *flu* mutant was investigated after a dark/light shift. The *flu* seedlings were grown for 5 days in LL, and incubated in the dark for 15 hours. During the subsequent reillumination, samples were collected at 0, 0.5, 1, 2, 4, and 12 h of light exposition. The pigment contents were measured and expressed relative to the pigment content after the dark period (Figure 3.28).

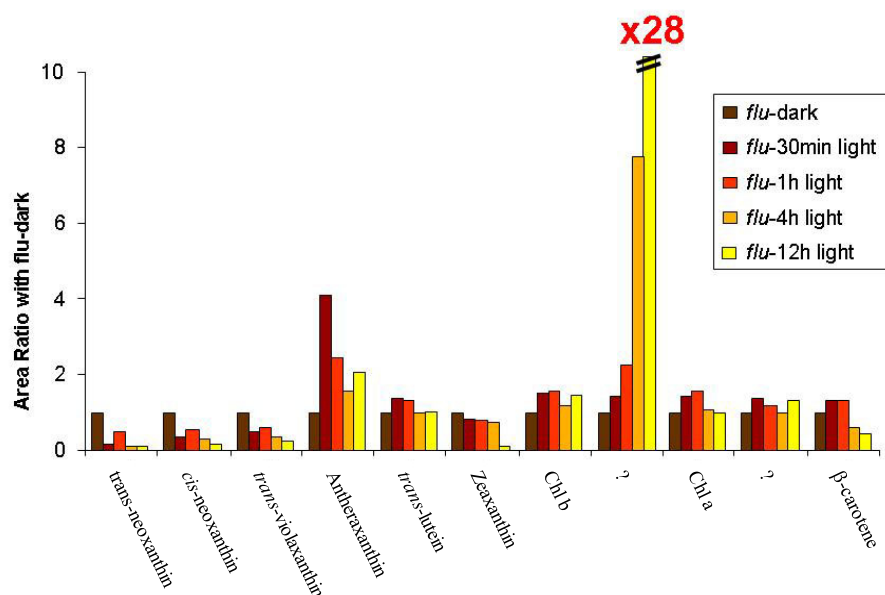


Figure 3.28: Accumulation of pigments of the *flu* mutant after a dark-light shift

The carotenoid content was analysed at different time points of reillumination by HPLC using a detection wavelength of 440nm. The content was expressed relative to the content at time 0 after the dark period.

Although the chlorophyll levels remained quite constant, the majority of carotenoids decreased with time, particularly epoxycarotenoids which are responsible for photoprotection during an excess of light. However, another compound increased dramatically under these conditions (Figure 3.28 and 3.29). Because of its striking upregulation in response to $^1\text{O}_2$, this compound was analyzed in more detail.

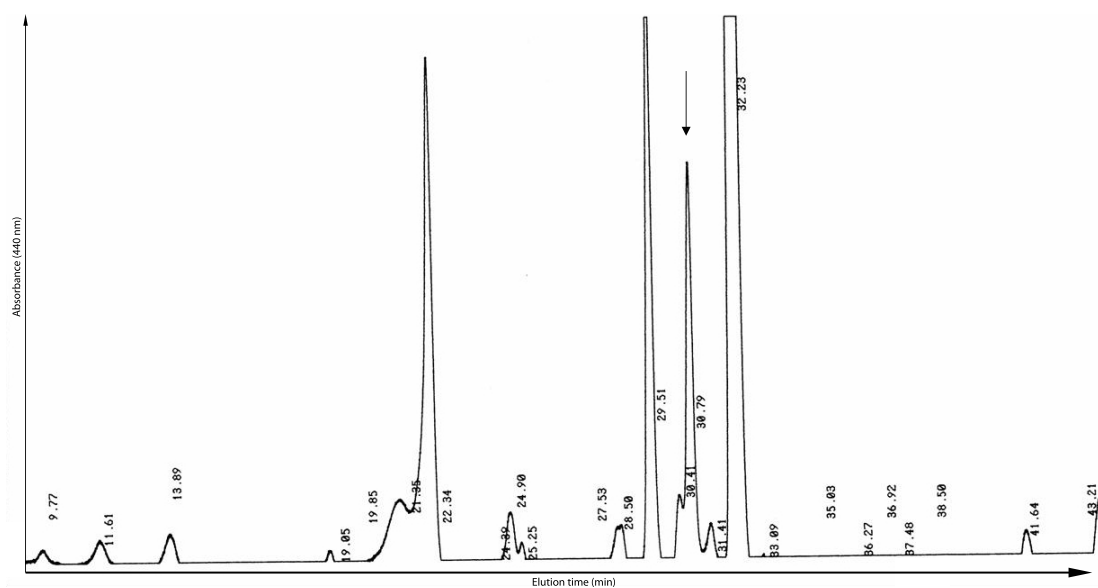


Figure 3.29: HPLC chromatogram of extracted pigments of *flu* 12 hours of reillumination

The arrow indicates the peak corresponding to the unknown pigment (Rt=30.79). The other peaks correspond to *trans*-neoxanthin (Rt=9.77), *cis*-neoxanthine (Rt=11.61), *trans*-violaxanthin (Rt=13.89), antheraxanthin (Rt=19.05), zeaxanthin (Rt=21.35), *trans*-lutein (Rt=22.34), Chl b (Rt=29.51), Chl a (Rt=32.28), and β -carotene (Rt=43.21).

3.2.2. Spectrum of the unknown pigment in *flu*

At 440 nm, both chlorophylls and carotenoids absorb light. For the first crude characterization of the pigment, its absorption spectrum was recorded (Fig 3.30).

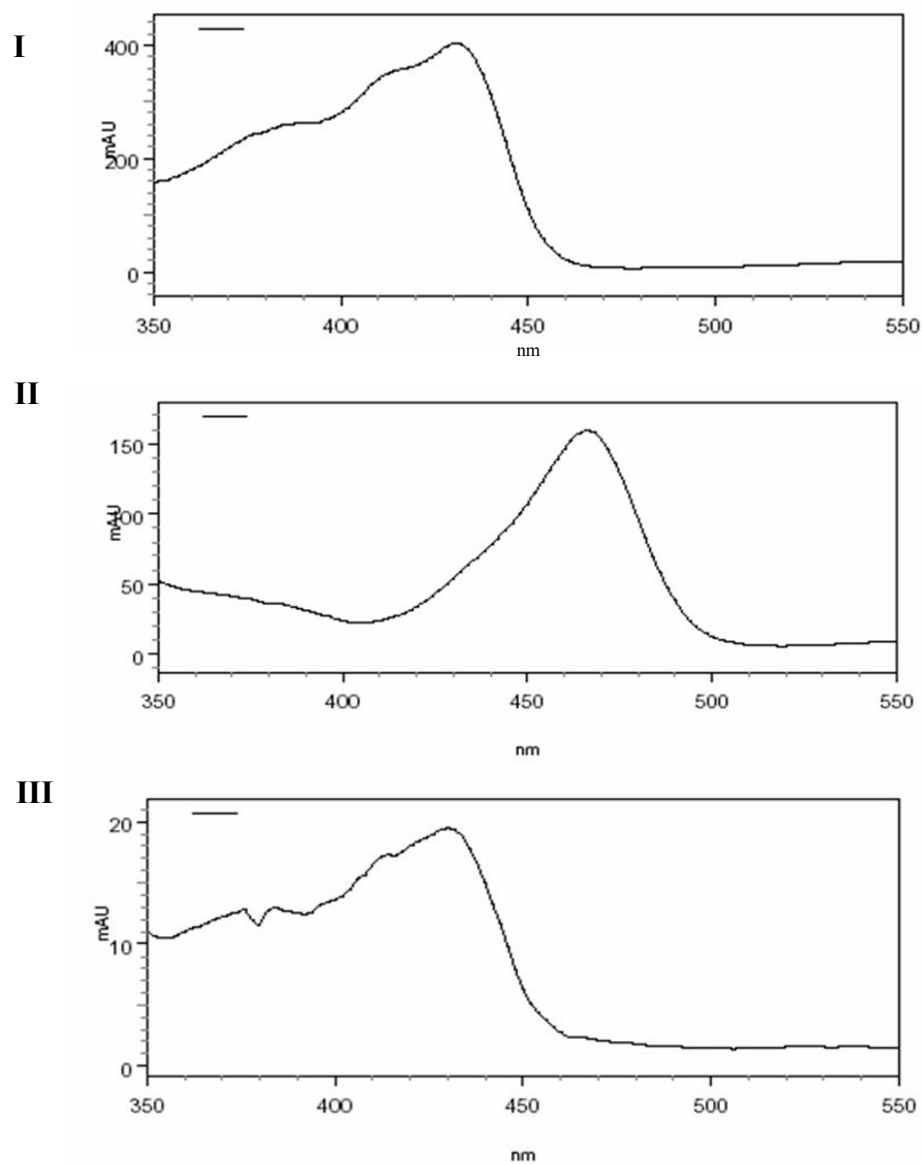


Figure 3.30: Absorbance spectrum of the unknown pigment. The spectrum was compared to those of chlorophyll a and b

The spectra were obtained using a diode array detector. I: Spectrum of chlorophyll a, II: Spectrum of chlorophyll b, III: Spectrum of the unknown pigment.

The spectrum of the unknown pigment looked like that of chlorophyll a, so it was concluded that this unknown pigment must be a derivative of chlorophyll a. Because this compound eluted earlier in the HPLC system, it was assumed that this derivative is more polar than chlorophyll a. It was speculated that this derivative of chlorophyll a might be an oxidation product after reaction of $^1\text{O}_2$ with chlorophyll a.

3.2.3. The localization of the pigment in different photosystem sub-complexes

Chlorophyll a is known to be involved in the transfer of light energy in the antennae and in the reaction centers of PS II and PS I. PS II is known to be more sensitive to oxidative stresses than PS I. Thus, the localization of this putative oxidation product of chlorophyll a may be enhanced in PS II. Subcomplexes of photosynthetic membranes of *flu* and WT grown 5 days under continuous light with a subsequent dark(8h)-light(12h) shift were separated on a semi denaturing diphosphate-polyacrylamide gel (green gel, Fig 3.31). The pigments were then eluted from the gel and the contents of Chl a, Chl b and the derivative of chlorophyll a (dubbed Chl a') were analyzed by HPLC (Fig 3.32). The content of the derivative of Chl a and b was reduced in all photosystem subcomplexes in the *flu* mutant compared to the wild type. Moreover, the content of Chl a' increased in all photosystem subcomplexes.

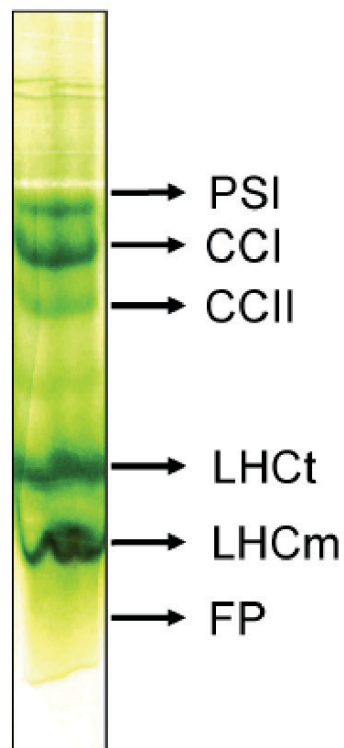


Figure 3.31: Electrophoretic separation of Chl-subcomplexes on a semi-denaturing SDS-PAGE

Abbreviations: PSI: photosystem I; CCI core complex I; CCII corecomplex II; LHCt: light harvesting complex II trimeric form; LHCm: light harvesting complex monomeric form; FP: free pigments. Based on the literature (Scioli and Zilinskas (1988))

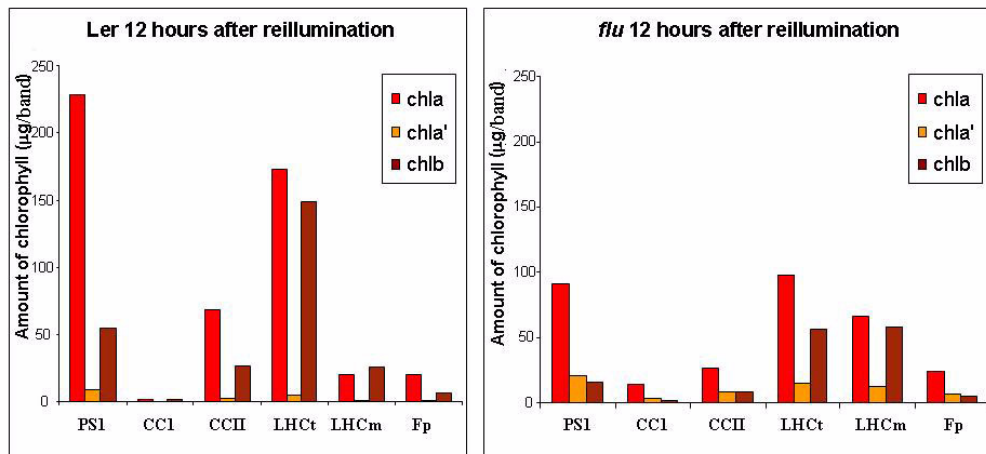


Figure 3.32: Presence of the chlorophyll derivative (chl a') in different photosynthetic subcomplexes

Abbreviations: PSI: photosystem I; CCI core complex I; CCII corecomplex II; LHCt: light harvesting complex II trimeric form; LHCm: light harvesting complex monomeric form; FP: free pigments. The data are given in the amount of Chl extracted from the corresponding band cut in the green gel.

3.2.4. Accumulation of the Chl derivative under different stress conditions

So far, the formation of the Chl derivative has been attributed to $^1\text{O}_2$ production. However, it is conceivable that its production may also be triggered by other oxidants. Hence, WT seedlings were exposed to other oxidative stress conditions, and an HPLC analysis was used to determine the relative amounts of the Chl derivative.

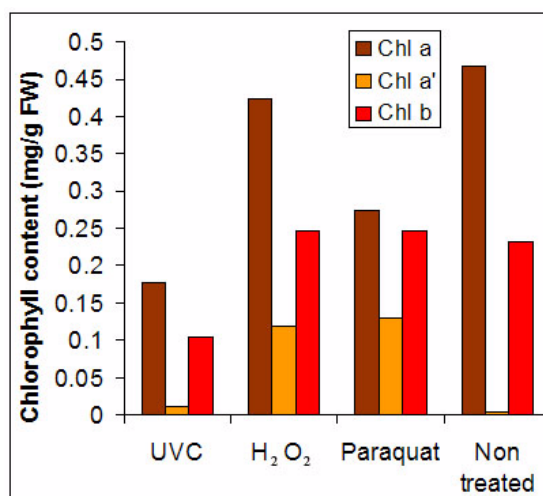


Figure 3.33: Accumulation of the Chl a derivative *in planta* after treatment with H₂O₂, paraquat and UVC

Five day-old seedlings grown under continuous light (100 $\mu\text{mole.m}^{-2}.\text{s}^{-1}$) were treated with UV-C (50 kJ.m^{-2}), H₂O₂ (100 μM , Tween20 0.1%(v/v)), Paraquat (50 μM , Tween20 0.1%(v/v)) or treated with mock solution(Tween20 0.1%(v/v)). After 12 hours, the pigments were extracted and the concentration of Chlorophylls were determined by HPLC.

The Chl a derivative also accumulated *in vivo* in seedlings treated with H₂O₂ and paraquat. Almost no accumulation was observed in seedlings treated with UV C.

3.2.5. *In vitro* oxidation of Chl a by Rose Bengal

The *in vitro* accumulation of different oxidation products of chlorophyll a was tested by incubating Chl a with different ROS. Chlorophyll a was solubilized in acetone and irradiated with 100 $\mu\text{mol.m}^{-2}.\text{s}^{-1}$ in the presence of Rose bengal (100 μM). Rose bengal is a potent photosensitizer similar to Pchlde and reacts with molecular oxygen to produce ¹O₂ in the light. After 1h of illumination, the sample was analyzed by HPLC (Figure 3.34). In addition to the main peak of chlorophyll a (Rt=22.83), another compound had been formed (Rt=21.14). This peak may correspond to the Chl a derivative formed *in vivo* in the *flu* mutant after the dark/light shift. When a similar *in vitro* experiment was performed with H₂O₂, this additional peak was not formed (data not shown).

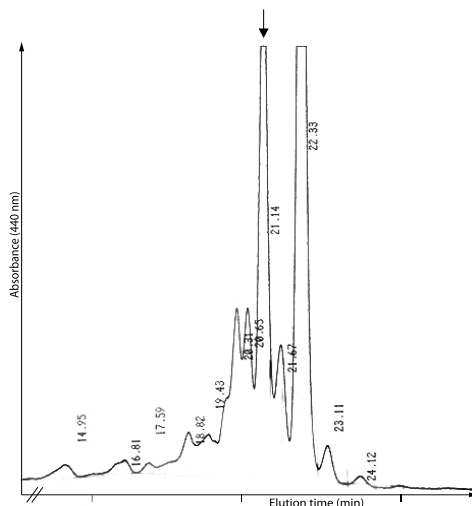


Figure 3.34: *In vitro* accumulation of the Chl a derivative after Rose bengal treatment

Chlorophyll a was incubated in acetone in the presence of Rose bengal (100 μM) under light (100 $\mu\text{mole.m}^{-2}.\text{s}^{-1}$). After one hour, 50 μl were injected in the HPLC. The chromatogram shows that in addition to the main peak of chlorophyll a ($R_t=22.83$), another compound (indicated by an arrow) had been formed ($R_t=21.14$). This peak may correspond to the Chl a derivative formed *in vivo* in the *flu* mutant after the dark/light shift. When a similar *in vitro* experiment was performed with H_2O_2 , this additional peak was not formed (data not shown).

3.2.6. Accumulation of the Chl a derivative in *soldat30/flu* double mutant

The impact of the *soldat30* mutation on the accumulation of the Chl a derivative was investigated in the *flu* background. The pigments were extracted from *soldat30/flu* and compared with the pigments of *flu* in 5 day-old seedlings placed in the dark for 15 hours and transferred back to light for 12 hours (Figure 3.35). While *flu* accumulates the Chl a derivative, the Chl a derivative was hardly detectable in *soldat30/flu*.

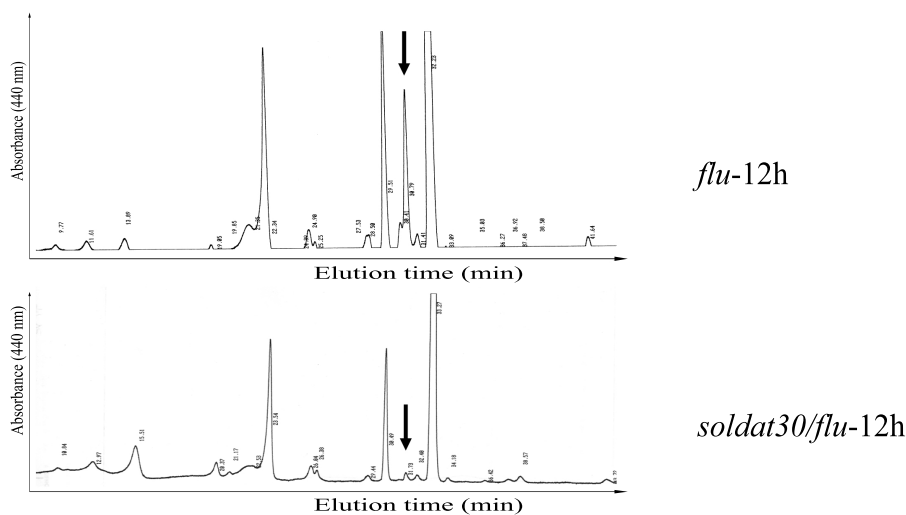


Figure 3.35: The HPLC chromatogram of pigments extracted from 5 day-old *flu* and *soldat30/flu* seedlings 12 hours after reillumination

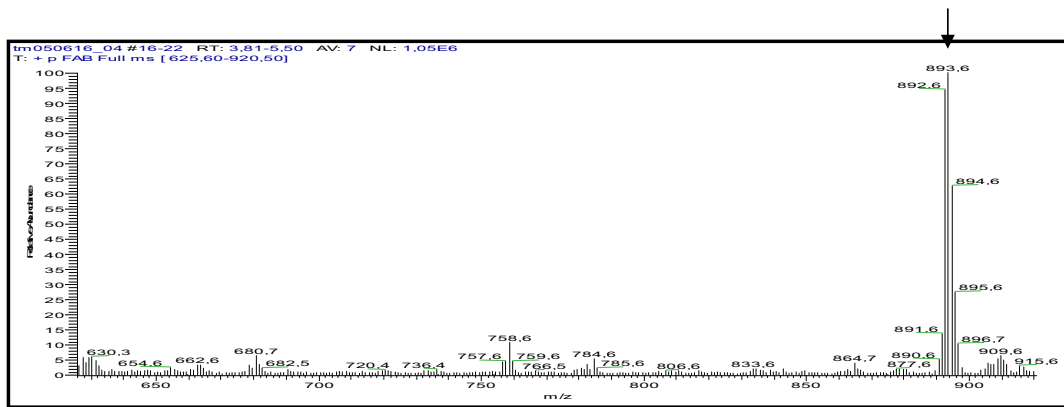
flu or *soldat30/flu* seedlings were grown for 5 days under continuous light. After 8 hours dark and 12 hours light, the pigments were analysed by HPLC. The chromatogram was recorded at 440 nm.

3.2.7. Structural analysis of the pigment

3.2.7.1. MS analysis

To define the structure of the Chl a derivative, a MS analysis was performed. Mass spectrometric (MS) analysis allows to determine the molecular weight of a molecule. The mass-to-charge ratio of the main ionized product was 893, which corresponds to the molecular weight of chlorophyll a. The corresponding peak of the chlorophyll a derivative is 909, 16 higher than the Chl a peak, which would correspond precisely to the MW of Chl a plus an additional oxygen atom. This itself strongly suggests that the chlorophyll a derivative contains an additional oxygen (Figure 3.36).

Chl a



Chl a'

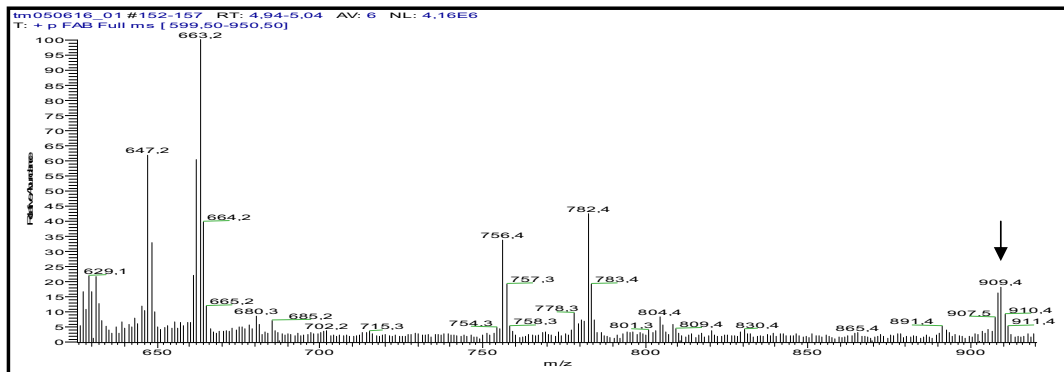


Figure 3.36: The MS spectra of the Chl a derivative extracted from *flu* after 12 h reillumination

The MS analysis was done by Dr. Thomas Müller in the laboratory of Prof. Bernard Kräutler (Innsbruck, Austria). The arrows indicate the molecular weight of the chlorophyll molecule, which is 16 mass units higher for the chlorophyll derivative (MW of Chl a'=909.4) compared to the Chl a (MW=893.6).

3.2.7.2. NMR analysis of the Chl a derivative

To precisely localize the additional oxygen, we performed a NMR (Nuclear Magnetic Resonance) analysis. The analysis of different spectra of the NMR indicated that the additional oxygen is localized on the C13² of Chl a, on the tetrapyrrole ring (Figure 3.37).

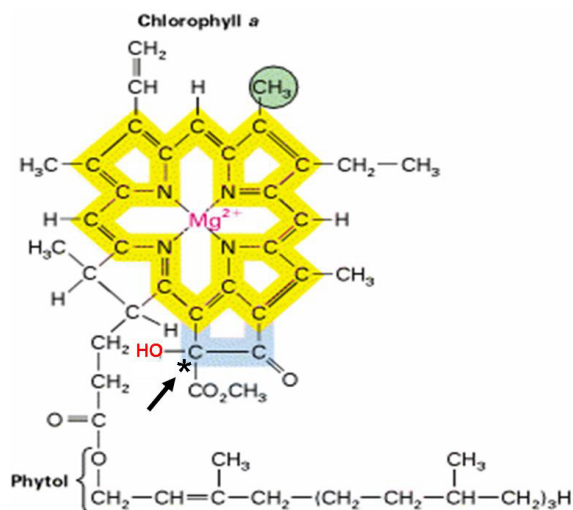


Figure 3.37: Structure of the derivative according to NMR analysis

The NMR analysis was done by Dr. Thomas Müller in the laboratory of Prof. Bernard Kräutler (Innsbruck, Austria)

4. Discussion

4.1. Oxidative stress and mode of action of ROS

Reactive oxygen species (ROS) are produced in animals and plants because of their aerobic life. In animals, the main sites of ROS production are the mitochondrion and the peroxisome. In plants, under light conditions, the main site of ROS production is the chloroplast. Under steady state conditions, plants have developed systems (see section 1.3.4 and 1.3.5) to counteract the deleterious effects of ROS and have found a way to keep an equilibrium between ROS production and detoxification. During stress, this balance is lost and the accumulation of ROS causes photooxidative damage. The reduction of growth and productivity (Long et al., 1994) observed under stress could be a consequence of photooxidative damage because ROS are known to induce the same effects as biotic and abiotic stresses (Apel and Hirt, 2004).

Originally, cytotoxic effects of ROS were considered to be responsible for stress responses such as cell death and growth inhibition. ROS modify or degrade biological molecules such as proteins, lipids and nucleic acids into molecules which may have an even stronger effect than the ROS. This random modification of molecules could lead to cytotoxic damage and cell death.

Recent studies, however, suggest that ROS may also be involved in strictly controlled processes. H_2O_2 is, up to now, the best studied ROS molecule. H_2O_2 has been shown to be a key signalling component during several processes such as stomatal closure, root growth, gravitropism, and responses to pathogens (Neill et al., 2002; Laloi et al., 2004).

All ROS might have specific biological roles, including development and stress reactions. ROS are a family of chemically distinct molecules that differ in their half life and their reactivity. Their target molecules might be different, as well as their modification process. Depending on the type of stress, ROS might be produced in different compartments of the cell, such as plasma membranes, chloroplasts, mitochondria and peroxisomes. One kind of stress might thus induce ROS patterns in a particular cellular compartment which may lead to a specific response by the plant. It is possible to detect and visualize the presence of most of the ROS by using colorimetric techniques. Alternatively, the amount of ROS may also be determined more indirectly by measuring the accumulation of oxidation products (*e.g.*

malondialdehyde after singlet oxygen stress) or by the induction of marker genes (Laloi et al., 2006) that are specifically induced under one particular oxidative stress. However, because different ROS are generated simultaneously, it is difficult to determine the biological activity and mode of action for each of these ROS separately.

4.2. The *flu* system to study the singlet oxygen effects

In order to determine the biological activity and mode of action for each ROS separately, one would need to find conditions under which only one specific ROS is generated at a given time, within a well-defined subcellular compartment, and which also triggers a visible stress response that is easy to score. The conditional *flu* mutant of *Arabidopsis thaliana* fulfills these requirements. The mutant generates singlet oxygen in plastids in a controlled and noninvasive manner. Immediately after the release of singlet oxygen, mature *flu* plants stop growing, whereas seedlings bleach and die (Wagner et al., 2004).

The *flu* mutant accumulates an excess of free pchl_a in the thylakoid membranes of chloroplasts under dark conditions (Przybyla et al., 2008). Upon reillumination, this pchl_a acts as a photosensitizer and reacts with triplet oxygen to produce singlet oxygen. It is possible to manipulate the amount of singlet oxygen produced by varying the length of the dark period. Thus, it is possible to induce the release of ¹O₂ at a given stage of plant development by individually growing plants under continuous light until they reach a stage we are interested in, shifting them into the dark and then placing them back into light.

After the release of singlet oxygen, two stress reactions of *flu* can be observed. One is the cell death reaction observed mainly at the seedling stage, and the other is the growth inhibition of mature plants. The growth inhibition and the cell death were shown to be hormone dependent. After the release of ¹O₂, an upregulation of jasmonic acid (JA) was measured in the *flu* mutant. Analysis of mutants impaired in the synthesis or the signalling pathway of oxylipins showed that JA acts as a stimulator of cell death. Not only oxylipins play a role in the *flu* cell death, but also salicylic acid (SA) and ethylene (Danon et al., 2005). Studies by Danon et al. (2005) showed that protoplasts prepared from *flu* seedlings grown on a medium supplemented with aminoethylvinylglycine, an inhibitor of ethylene biosynthesis, that overexpressed NahG, a SA degradation enzyme, were almost fully protected against the cell death induced in the original

flu mutant.

On the other hand, it was shown that the two stress reactions induced by $^1\text{O}_2$ in Arabidopsis can be abrogated by the mutation of a single gene, *executer1* (Wagner et al., 2004). EXECUTER1 is a nuclear-encoded plastid protein which has an unknown function. The additional mutation of *executer2*, a gene homologous to *executer1*, reduces the $^1\text{O}_2$ -induced-gene expression pattern almost to the level of the wild type (Lee et al., 2007). However, *executer1* or *executer1/executer2* double mutants are not able to reverse the phenotype if the conditions are too harsh. In 5-day-old seedlings, when the dark period is increased from 8 to 15 hours, the *executer1* mutation is no longer able to revert the *flu* phenotype because of the higher content of pchl_{ide}. None of the isolated second-site mutants could revert the *flu* phenotype when etiolated mutant seedlings were transferred to light. This shows that cell death may be induced by the cytotoxic effect of singlet oxygen, or it may be genetically controlled. Similar effects have been reported in animals (Ryter et al., 2007).

All these results show that ROS can act as toxic molecules as well as signalling molecules. We can hypothesize that in the *flu* mutant the amount of singlet oxygen produced after a dark/light shift is very high compared to natural stress conditions. The average amount of pchl_{ide} present in the *flu* mutant following 8 hours of dark was roughly 8 times higher than in the wild type. Under these conditions, we could presume that plants would not be able to counteract the toxic effect of singlet oxygen. However, the introduction of the *executer1* mutation can revert the *flu* phenotype. Hence under these conditions, the $^1\text{O}_2$ does not seem to act as a toxic molecule, but rather as a signalling molecule.

4.3. Comparison between *soldat30*, *soldat8* and *soldat10* mutants

soldat mutants were isolated in the same screen that led to the discovery of *executer1*. The *soldat* mutants showed reversion of the *flu* phenotype at the seedling stage (cell death), but did not abolish the growth inhibition at the rosette leaf stage. Until now, three *soldat* mutants have been characterized. All three mutations affect nuclear-encoded chloroplast proteins and lead to a pale green phenotype in the seedlings. *SOLDAT8* has been found to be allelic to SIGMA FACTOR 6, *SOLDAT10* to a chloroplast protein synthesis termination factor and *SOLDAT30* to the chloroplastic PNPase. Sánchez-Coll (2006) and Würsch (2006) showed that *soldat8* and

soldat10 five day-old seedlings accumulate a reduced amount of pchlride compared to *flu* after the dark period (60% and 50%, respectively). Interestingly, *soldat30* accumulates about 90% of the Pchlride accumulated by *flu*. The reduced amount of pchlride in *soldat10* and *soldat8* could be the reason behind the *flu* phenotype reversion. However, these authors observed that the kinetics of the photosynthetic activities and the phenotype after 9 days of the *soldat8* and *soldat10* seedlings under the cold/high light stress program were similar to those of *soldat30* (figure 3.24). They thus proposed that the mutation of chloroplasts disturbs homeostasis and induces a preacclimation status of the plant. A preacclimated plant is more resistant to subsequent stress. All *soldat* mutants were able to overcome the high light-cold stress conditions, including *soldat30*, showing that *soldat30* could also be preacclimated.

4.4. The mutation of *SOLDAT30* suppresses the *flu* phenotype by increasing the tocopherol content

SOLDAT30 is allelic to the gene encoding polyribonucleotide nucleotidyltransferase (PNPase). This enzyme has an exoribonuclease activity as well as a polynucleotide transferase function on RNA. Two PNPase homologues are present in plants. One is targeted to the chloroplast, and the other one to the mitochondria (Yehudai-Resheff et al., 2001). Chloroplastic PNPase (cpPNPase) is a homologue of the *E. coli* PNPase, which is part of the degradosome.

The *E. coli* degradosome is involved in the degradation of mRNA. It affects mRNA stability and permits timely changes in gene expression by limiting the lifetime of a transcript. It is composed of RNase E, a PNPase and a DEAD-box helicase (Carpousis, 2002). RNase E is a single-strand-specific endonuclease involved in rRNA processing and degradation of mRNAs. It is also a 5' end-dependent endonuclease. The RNase E has a higher activity if the 5' end of the mRNA is terminated by a monophosphate rather than by a triphosphate. The *E. coli* PNPase has a 3' → 5' exoribonuclease and a phosphorylytic activity, respectively. The helicase supports RNA degradation or maturation by unwinding the secondary structure of RNA, which impedes the activity of other enzymes such as PNPase.

The chloroplastic PNPase lacks the *E. coli* C-terminal domain which is involved in the assembly of the PNPase with the other enzymes of the degradosome. In spite of a first report suggesting the presence of a degradosome-like complex in chloroplasts, an isolated chloroplastic PNPase from spinach was shown to be part of a 580-600 kDa homo-multimer

complex (Baginsky et al., 2001). Chloroplasts also lack the major poly-adenylation enzyme, the poly(A) polymerase from *E. coli* (Yehudai-Resheff et al., 2001). It was reported that PNPase may act as a poly(A)-polymerase, replacing this enzyme. These studies demonstrated that degradation and processing of RNA in chloroplasts differs from *E. coli*.

The PNPase in chloroplasts has several functions in different types of RNA, including rRNA, tRNA and mRNA (Sugiura, 1992; Monde et al., 2000; Walter et al., 2002).

Besides the 3' → 5' exoribonuclease activity involved in the maturation of rRNA, the PNPase also has a 3' → 5' exoribonuclease activity on mRNA. The polyadenylation of the *psbA* transcript was analyzed in WT, in a cosuppression line (PNPase⁻) and in an overexpressing line. In PNPase⁻ plants, polyadenylated transcripts accumulated to a much higher level than in the WT. In the PNPase overexpressing line, the transcript of *psbA* was hardly detectable. The same trend was also observed with other mRNAs, like the mRNA encoding *rbcL*, or the ribosomal protein *rps14*. These results suggest that there is another enzyme distinct from PNPase that acts as a poly (A) polymerase in higher plant chloroplasts (Sugiura, 1992).

The sensitivity of the mRNA to degradation increases with the length of the poly(A) extension (Kudla et al., 1996). Therefore, mRNAs in PNPase-deficient plants are less stable. Interestingly, in these PNPase⁻ plants, *psbA* and *rbcL* mRNAs are larger in size (200-300 nt) because of incorrect processing, but they are present at the same concentration as in the WT.

Collectively, these results suggest that PNPase interacts with different types of RNA. Recently the *rif10* mutant (Resistant to Inhibition by Fosmidomycin) was isolated from a mutant screen performed with the presence of sub-lethal concentrations of fosmidomycin, an inhibitor of deoxyxylulose 5-P reductoisomerase that catalyses one of the first steps of the methylerythritol phosphate (MEP) pathway (Sauret-Gueto et al., 2006). The *rif10* mutant had a T-DNA insertion within the PNPase gene which was shown to be a knock-out mutation of the PNPase gene. *rif10* is allelic to *soldat30*. In contrast to the PNPase⁻ line, *rif10* and *soldat30* have a similar visible phenotype which differs from that of the WT. They contain less chlorophyll and carotenoids than WT. It is particularly visible in cotyledons and in cauline leaf bases. This suggests that in the cosuppression line, the remaining PNPase is sufficient. Similarly, a reduction of the PNPase by antisense or RNAi in *Chlamydomonas reinhardtii* showed neither an alteration of cpRNA levels, nor a visible change of phenotype (Yehudai-Resheff et al., 2007).

PNPase is also involved in acclimation to phosphorus limitation in *Chlamydomonas reinhardtii* (Yehudai-Resheff et al., 2007). Under phosphorus stress, the PSR1 protein (Phosphorus Starvation Response 1) down-regulates the PNPase. The down regulation of PNPase leads to an accumulation of cpRNA providing evidence that PNPase is involved in cpRNA level adjustments.

In *E.coli*, PNPase is also induced by cold shock and PNPase is necessary for adaptive growth resumption of cold shock treated cells (Beran and Simons, 2001; Sarkar and Fisher, 2006). Cold shock proteins (CSP) are synthesized during cold shock stress. They block translation by binding to mRNAs and ribosomes, and inhibit the growth of *E.coli* during its acclimation phase. At the end of the acclimation phase, PNPase specifically degrades the CSP mRNA. The downregulation of CSP releases the translation inhibition and allows translation to resume. In the end, the growth of the bacteria is reactivated. This whole process allows bacteria to survive under unfavorable conditions.

Similarly, the human PNPase (hPNPase) plays an important role in the growth inhibition mediated by IFN- β , an apoptosis inducer that acts by specifically degrading the oncoprotein c-myc (Sarkar and Fisher, 2006). hPNPase is mainly targeted to the mitochondria, but it has also been found in small amounts in the cytoplasm. An overexpression of this PNPase induces a cell cycle arrest in the G1 phase and an inhibition of DNA synthesis followed by the induction of apoptosis.

It has been hypothesized that hPNPase plays a role during animal cell senescence. It serves to regulate the activity of inflammatory components of senescence by increasing ROS accumulation. Overexpressing hPNPase induces generation of ROS, which induce inflammation reactions (the release of proinflammatory cytokines) via the NF- κ B pathway. The antioxidant N-acetyl-L-cystein (NAC) could inhibit the responses induced in the hPNPase-overexpressing cell lines.

All these results demonstrate the importance of PNPase in various physiological processes in animals as well as in plants.

4.4.1. The mutation of the PNPase in *soldat30* reverts the *flu* phenotype

As mentioned above, PNPase is involved in several processes in bacteria, in animals and also in plants under normal conditions as well as under stress conditions. Expression of PNPase in *Arabidopsis* is highly regulated during plant development (Figure 4.1) and mainly occurs in young tissues (Figure 4.1 and 4.2).

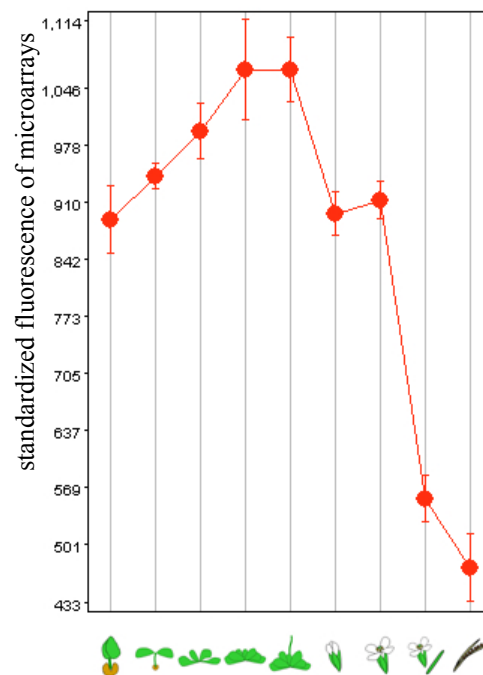


Figure 4.1: PNPase expression during development of *Arabidopsis thaliana*

The PNPase expression varies depending on the developmental stage of the plant. It is at its maximum during the growth and the vegetative stages, respectively. (From <https://www.genevestigator.ethz.ch/>).

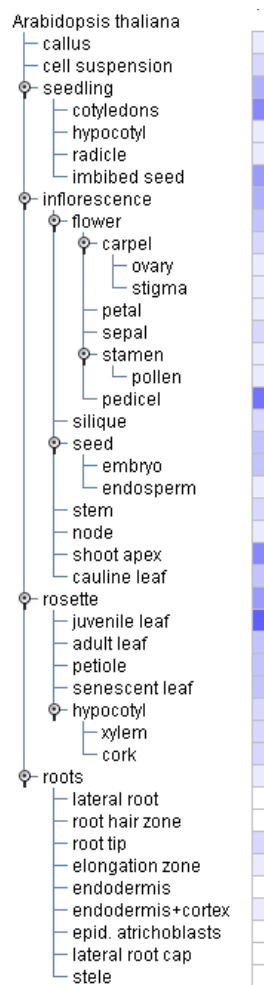


Figure 4.2: PNPase expression in different organs of *Arabidopsis thaliana*

The more intense the color, the higher the expression (From <https://www.geneinvestigator.ethz.ch/>).

The *soldat30* mutant shows a pale green phenotype and grows more slowly than the WT. The allelic line *rif10* shows the same phenotype as *soldat30*. Both mutant lines confirm that the loss of PNPase may induce a phenotypic change. These results are in contrast to earlier reports obtained with a cosuppression line (Walter et al., 2002). The *rif10* mutant was resistant to a sublethal concentration of fosmidomycin, an inhibitor of DXR. In *rif10*, the mutation led to an increased accumulation of key enzymes of the methylerythritolphosphate (MEP) pathway, which is involved in the synthesis of isoprenoids in chloroplasts. Mutations showing similar effects have been previously reported. An accumulation of key enzymes of the MEP pathway was also observed after chloramphenicol treatment, a specific inhibitor of chloroplast translation (Sauret-Gueto et al., 2006). However, a pale phenotype was not automatically associated with the accumulation of MEP pathway enzymes. Thus, Sauret-Gueto *et. al.* (2006)

suggested that the overaccumulation of MEP pathway enzymes requires specific cues from the chloroplast. These results agree with the recent findings about the functions of PNPase (see previous section). PNPase may target specific cpRNAs, and its mutation may induce specific cues that modify nuclear gene expression via a retrograde signalling pathway leading to the upregulation of MEP pathway enzymes. Although a down-regulation of carotenoids and chlorophyll was observed, an up-regulation of other end products, mainly α -tocopherol, a well known singlet oxygen scavenger, was observed.

4.5. Scavenging effect of tocopherol in singlet oxygen-induced cell death

4.5.1. Tocopherols

Tocochromanols and carotenoids are the two most abundant groups of lipid-soluble antioxidants in chloroplasts (DellaPenna and Pogson, 2006). Tocopherols form a group of 8 derivatives which can be divided into 2 groups: tocopherols and tocotrienols. They have in common a rather hydrophilic chromanol ring and a rather hydrophobic side chain. A saturated side chain characterizes the group of tocopherols, whereas an unsaturated lateral chain is typical for the group of tocotrienols. α , β , γ , and δ -tocochromanols differ by the number and the position of methyl groups on the aromatic ring. The polar head group derives from tyrosine, whereas the saturated tail derives from phytyl diphosphate. The tocochromanol content and their composition vary enormously in different plant tissues. The tocochromanol content in seeds is very high, whereas in leaves it is 10 times lower. In seeds, tocotrienols and γ -tocopherols are predominant, whereas in leaves the main compound is α -tocopherol.

Tocopherols interact preferentially with acyl groups, and protect lipid membranes, particularly the polyunsaturated fatty acids (PUFA), against oxidative damage by scavenging peroxide radicals and quenching or chemically reacting with singlet oxygen or other ROS (Schneider, 2005).

4.5.2. The mutant *flu/vte1* is more sensitive to singlet oxygen than *flu*

To address the role of tocopherols in *flu* cell death, a mutant impaired in tocopherol biosynthesis was used. The *vte1* mutant lacks functional tocopherol cyclase, an enzyme needed for the synthesis of all tocopherols. *vte1* was crossed with *flu* to obtain a *flu* mutant which does not accumulate any tocopherol. By comparing the cell death induced in these two lines at seedling stage under non permissive conditions, it was observed that the lack of tocopherol increased the response to stress induced by singlet oxygen. However, the phenotypic differences between *flu* and *flu/vte1* decreased when the intensity of stress was increased by increasing the length of darkness preceding the reillumination (data not shown). The same trend was observed at the cell death level using trypan blue staining. In contrast, protoplasts extracted from *flu* plants treated with α -tocopherol were more resistant to singlet oxygen compared to protoplasts extracted from *flu* plants given a mock treatment, even if it did not completely abolish singlet oxygen-induced cell death. Obviously, a *VTE1* over-expression line would have been a better approach to investigate the extent to which tocopherols can reduce the singlet oxygen effects, since we do not know exactly how α -tocopherols are integrated into the plastid during the plant treatment. In *soldat30/flu*, the excess tocopherol may be integrated at its natural locations, in thylakoids and in the envelope of chloroplasts where pchlide accumulates as well. Tocopherols may directly scavenge the $^1\text{O}_2$ produced after the dark/light shift. Knowing that one tocopherol molecule can deactivate up to 120 molecules of $^1\text{O}_2$, we can assume that a small increase of the tocopherol content in the plants can have a big effect on the survival of *flu* plants under non permissive conditions, or on WT plants under stress conditions when singlet oxygen is mainly produced (MunneBosch and Gerald, 2007).

Because one tocopherol molecule can deactivate up to 120 molecules of $^1\text{O}_2$, either by charge or energy transfer, we can assume that a small increase in tocopherol content can have an important effect on the survival of both *flu* plants under non permissive conditions and WT plants under stress conditions.

It is generally assumed that singlet oxygen induces direct oxidation of PUFA via a non-enzymatic pathway. This leads to the production of substrates for the synthesis of oxilipins, such as 12-oxo phytodienoic acid (OPDA) and jasmonic acid (JA), which are involved with the control of various metabolic and developmental processes in plants. In *flu* plants, Przybyla

et al. (2008) detected lipid peroxidation after a dark-light shift. Surprisingly, the oxidative products derived from PUFA came almost exclusively from an enzymatic reaction. It can be assumed that the singlet oxygen released after a dark-light shift induced a programmed cell death via a non cytotoxic pathway. The isolation of the second site mutant *ex1*, which can abolish the $^1\text{O}_2$ -induced cell death, further supports that statement (Wagner et al., 2004), along with the work of Lee *et al.* (2007) on the characterization of *ex2* and *ex1/ex2*, in which the changes in gene expression induced by $^1\text{O}_2$ are almost completely abolished .

4.5.3. The role of tocopherol in reversion of the *flu* phenotype in *soldat30/flu*

The mutation of PNPase induces an increase in the tocopherol content in *soldat30/flu*, mainly α -tocopherol. α -Tocopherol has the highest antioxidant capacity of all tocopherols in terms of preventing lipid peroxidation, although all tocopherols may act as direct singlet oxygen scavengers. In the *flu* mutant, Pchl a accumulates mainly in thylakoid membranes. It is reasonable to think that the increased accumulation of tocopherols in the *flu* mutant may act upstream of EX1 and EX2, directly at the location of the $^1\text{O}_2$ production after the dark-light shift, and prevent the initiation of the $^1\text{O}_2$ pathway. *Soldat30* was also more resistant to cell death induced by paraquat, which induces a release of superoxide and this can also be explained by the increased accumulation of tocopherol in the mutant. Indeed, tocopherols may also act as scavengers against oxidation induced by other ROS (Schneider, 2005).

The resistance of *soldat30* against more natural stresses, during which ROS are known to be produced, was also tested. *Soldat30* was more resistant to high light/cold stress than the WT, whereas the *vte1* mutant was much more sensitive to this stress. This showed that tocopherols play a crucial role in photoprotection under these stresses. When the WT was prestressed for one day by an intermediate light stress, the WT became resistant to the high light/cold stress. During this acclimation process, WT accumulated 10 times more tocopherols, mainly α -tocopherol, than under normal conditions, which can confer resistance to the subsequent oxidative stress. This supported previous work when tocopherol was shown to be a key component during cold acclimation (Maeda et al., 2006).

The fact that the *ex1* mutant was not able to overcome a treatment by paraquat (data not published), or the high light/cold stress, showed that *ex1* is not involved in the acclimation

process. The *soldat30* mutant must prevent the $^1\text{O}_2$ -induced cell death by a process different from that of *ex1*, which is less specific for singlet oxygen. Thus, tocopherols and mainly α -tocopherol may quench the effect of any ROS in the thylakoids by preventing the initial reaction of cell death via the activity of the PNPase enzyme.

4.6. Biochemical characterization of singlet oxygen-induced cell death

4.6.1. The carotenoid content decreased after the release of singlet oxygen

Carotenoids have two important roles in photosynthetic organisms. Firstly, they act as accessory light-harvesting pigments, effectively extending the range of light absorbed by the photosynthetic apparatus. Secondly, they perform an essential photoprotective role by quenching triplet state chlorophyll molecules and scavenging singlet oxygen and other toxic oxygen species formed within the chloroplast and, in addition, by dissipating the excess of energy by the xanthophyll cycle (Young, 1991). Over-expression of β -hydroxylase, which leads to an up-regulation of carotenoid production, conferred an increased resistance to high temperature and high-light stress (Davison et al., 2002)}. In parallel, it has been described that singlet oxygen increased the content of some carotenoids (Schroeder and Johnson, 1995). However, the direct effect of singlet oxygen released within chloroplasts on carotenoids has never been reported. The release of singlet oxygen in the *flu* mutant induced a rapid decrease in carotenoid content, particularly the xanthophylls neoxanthin and violaxanthin. This shows that they might be involved in the cell death induced by singlet oxygen. Interestingly, the content of neoxanthin and violaxanthin levels rapidly decreased after the dark-light shift. Although these xanthophylls decreased rapidly, the content of chlorophylls remained relatively stable. Both neoxanthin and violaxanthin can be cleaved by epoxy-carotenoid dioxygenase (NCED), and these cleavage products are further modified to produce abscisic acid (ABA) (Schwartz et al. 1997; Seo and Koshiba, 2002). Further analysis of the ABA content after the release of singlet oxygen is required to gain more insight into the role of ABA in *flu* cell death.

4.6.2. A chlorophyll a derivative is produced after the dark-light shift in the *flu* mutant

Interestingly, another unknown compound increased dramatically following the dark-light shift. This pigment reached a concentration about 30 times higher than that of the control. During Reverse-Phase HPLC, the pigment eluted after chlorophyll a and before chlorophyll b. The spectrum of this pigment revealed that it probably had a structure closer to chlorophyll a than chlorophyll b. However, the difference in retention time suggested that it was more polar than chlorophyll a. A published chromatogram of plant leaf pigments described a derivative of chlorophyll a which elutes between Chl a and Chl b, and was shown to be an artifact during extraction by a process called allomerization (Hynninen and Hyvarinen, 2002). MS and NMR analysis undertaken on this derivative demonstrated that an additional oxygen atom was present at the carbon C13² of the tetrapyrrole ring of Chl a, forming a hydroxyl function, corresponding to what was already described (Hynninen and Hyvarinen, 2002). However, we can see for the first time that accumulation of the 13²-HO-Chl a might be a natural phenomenon, since this pigment accumulation increased with time.

4.6.3. The chlorophyll a derivative accumulates in all photosystem subcomplexes

Photosystem II is known to be more sensitive to photooxidation than photosystem I, since photosystem II is the main site of singlet oxygen production and photosystem I is associated with an effective ROS detoxification system. 13²-HO-Chl a was found in photosystem II and a significant amount was also found in photosystem I. Przybyla et al. (2008) showed that Pchl_{id} accumulates mainly in thylakoid membranes (> 90%). However, the Pchl_{id} might be distributed evenly within the thylakoid membranes. Hence, after reillumination, the singlet oxygen might be produced in all thylakoids membranes, not only in PS II. This would explain the even distribution of the 13²-HO-Chl a.

4.6.4. The accumulation of the chlorophyll a derivative is induced by other ROS

The 13²-OH-Chl a accumulation was observed after the release of singlet oxygen, but also after H₂O₂ or paraquat treatment. The treatment with UV-C, which is known to induce a ROS independent-programmed cell death, did not increase the amount of 13²-HO-Chl a. Thus, it seems

to be induced only under oxidative stresses and to not be strictly dependent on cell death. The accumulation of the 13²-OH-Chl a was then tested under more natural conditions. Under high light, cold stress, or under combined stresses no significant accumulation was observed (Data not shown). Two possibilities can be envisaged. Either the site of ROS production is different in WT under natural stress conditions from that in the *flu* mutant, or the amounts of ROS produced under natural stress conditions are much lower than the artificial conditions during which a large amount of one particular ROS is produced. However, even in the WT the pigment could be detected, although at a very low concentration.

4.6.5. *In vivo* significance of the 13²-HO-Chl a

The derivative of Chl a has been mainly characterized *in vitro*. The presence of the 13²-HO-Chl a *in vivo* has already been mentioned, however, it has always been recorded as an extraction artifact. With the *flu* system, a gradual accumulation of the Chl a derivative after the dark-light shift in 5-day-old seedlings was observed. However, the stable bilin product derivative was not detected, nor the derivatives of chlorophyll a which normally appear during senescence (personal communication, S. Hörtensteiner). The 13²-HO-Chl a accumulation *in vivo* upon singlet oxygen production can be explained either by its formation by a chemical process other than published until now (Hynninen and Hyvarinen, 2002) or by the formation of H₂O₂ in the *flu* mutant after the release of the singlet oxygen. Indeed, the accumulation of the pigment remains significant 4 hours after reillumination, even though its accumulation was detected at 30 min. A number of studies showed that singlet oxygen inhibits enzymes involved in the ROS detoxification pathway, such as SOD or catalase. Thus, it is possible that the H₂O₂ concentration or other radical ROS may favor a so called free radical allomerization pathway (Hynninen and Hyvarinen, 2002) which yields 13²-HO-Chl a. On the other hand, the 13²-HO-Chl a accumulation was very much induced by paraquat or H₂O₂. This observation further supports the hypothesis that H₂O₂ may be induced upon singlet oxygen release in the *flu* mutant. The accumulation of this molecule was reported recently (Wang et al., 2000) in tobacco cells treated with 2-(2-chloro-5-propoxycarbonylphenyl)aminomethylidene-5,5-dimethyl-cyclohexane-1,3-dione (RWH-21), a cyclohexanedione derivative herbicide. The chemical reaction within the cells is not known. 13²-HO-Chl a appeared under dark conditions and under light conditions, however, the

accumulation was faster under light conditions. The 13²-HO-Chl a possibly acts as a photosynthesizer itself, like the Pchl_a, leading to the production of singlet oxygen under light conditions. The oxidation of PUFA by singlet oxygen in tobacco cells was tested by measuring the MDA (malondialdehyde) content (Wang et al., 2000). MDA accumulated only under light conditions, supporting the hypothesis that the derivative may act as photosynthesizer. This theory is further supported by the absence of the derivative of Chl a in the *soldat30/flu* mutant (Figure 3.35), which can be explained by a higher scavenging capacity conferred by a higher content of tocopherols, and not by the absence of cell death. Indeed, cell death induced by UV-C is not accompanied by a significant accumulation of 13²-HO-Chl a (Figure 3.33). Hence, we can assume that the 13²-HO-Chl a may accelerate singlet oxygen induced cell death.

4.7. Conclusion and future prospects

In the present work, first, a forward genetic approach and second, a biochemical approach was undertaken to characterize the singlet oxygen stress response in *flu* after a dark light shift.

The genetic approach led to the characterization of SOLDAT30, a gene allelic to PNPase. It has been previously shown that a T-DNA insertion leading to the loss of function of that gene (*rif*) induced a significant upregulation of the enzyme involved in the MEP pathway. It is reasonable to think that the point mutation of the *soldat30* characterized in the present work led to a loss of function of that gene as well, since *soldat30* and *rif* have a similar dwarf phenotype and have a similar molecular phenotype (chloroplastic 23S rRNA is not processed correctly). The upregulation of the genes involved in the MEP pathway might induce an overaccumulation of an end product of that pathway, *i.e.* tocopherols, well known as singlet oxygen scavenger. We cannot exclude that the mutation of the PNPase in *soldat30/flu* acts at a different level, for example as a level more downstream of the signaling by the singlet oxygen. To address this question, a triple *rif/flu/vte1* mutant has been created to investigate the preponderance of the scavenging by tocopherols over other targets of PNPase. The analysis of the cell death after dark-light shift in the triple mutant will be compared to the cell death in the double mutants *rif/flu* and *flu/vte1*. The triple mutant could also be tested against the double mutants to investigate further the role of the PNPase in the acclimatory response.

The biochemical approach revealed that the singlet oxygen release induced a downregulation of all carotenoids, and more particularly the xanthophylls. Interestingly, one component was observed to strongly overaccumulate after the dark-light shift in the *flu* mutant. This study

showed that it is a derivative of chlorophyll a, which could also be observed *in planta* under other ROS treatment. It is tempting to speculate that the chlorophyll derivative plays a role in the cell death induced by ROS. It would be interesting to test whether or not the mutation of *exl* can abrogate the cell death induced by cyclohexanedione, knowing that cyclohexanedione induces an overaccumulation of that pigment. It would also be interesting to know whether this pigment is enzymatically produced or if the process is purely chemical, by testing the accumulation of the pigment in *flu* at 4°C for example, since only enzymatic reactions are temperature-dependent.

5. References

- Agarwal, P., Agarwal, P., Reddy, M., and Sopory, S.** (2006). Role of DREB transcription factors in abiotic and biotic stress tolerance in plants. *Plant Cell Reports* **25**, 1263-1274.
- Apel, K., and Hirt, H.** (2004). Reactive oxygen species: metabolism, oxidative stress, and signal transduction. *Annual Review of Plant Biology* **55**, 373-399.
- Asada, K.** (1994). Production and action of active oxygen species in photosynthetic tissues. In CH Foyer, PM Mullineaux, eds, *Causes of Photooxidative Stress and Amelioration of Defenses Systems in Plants*. CRC Press, Boca Raton, FL, 77-104.
- Babbs, C.F., Pham, J.A., and Coolbaugh, R.C.** (1989). Lethal hydroxyl radical production in paraquat-treated plants. *Plant Physiology* **90**, 1267-1270.
- Baginsky, S., Shteiman-Kotler, A., Liveanu, V., Yehudai-Resheff, S., Bellaoui, M., Settlage, R.E., Shabanowitz, J., Hunt, D.F., Schuster, G., and Gruissem, W.** (2001). Chloroplast PNPase exists as a homo-multimer enzyme complex that is distinct from the *Escherichia coli* degradosome. *RNA* **7**, 1464-1475.
- Beran, R.K., and Simons, R.W.** (2001). Cold-temperature induction of *Escherichia coli* polynucleotide phosphorylase occurs by reversal of its autoregulation. *Molecular Microbiology* **39**, 112-125.
- Berman-Frank, I., Lundgren, P., and Falkowski, P.** (2003). Nitrogen fixation and photosynthetic oxygen evolution in cyanobacteria. *Research in Microbiology* **154**, 157-164.
- Bird, A.** (2007). Perceptions of epigenetics. *Nature* **447**, 396-398.
- Boyer, J.S.** (1982). Plant productivity and environment. *Science* **218**, 443-448.
- Bray, E.A., Bailey-Serres, J., and Weretilnyk, E.** (2000). Responses to abiotic stresses. *Biochemistry and Molecular Biology of Plants*, American Society of Plant Biologists, Rockville, MD, 158-1249.
- Cadet, J., Ravanat, J.-L., Martinez, G.R., Medeiros, M.H.G., and Mascio, P.D.** (2006). Singlet oxygen oxidation of isolated and cellular DNA: Product formation and mechanistic insights. *Photochemistry and Photobiology* **82**, 1219-1225.
- Carpousis, A.J.** (2002). The *Escherichia coli* RNA degradosome: structure, function and relationship in other ribonucleolytic multienzyme complexes. *Biochemical Society Transactions* **30**, 150-155.

- Dall'Osto, L., Lico, C., Alric, J., Giuliano, G., Havaux, M., and Bassi, R.** (2006). Lutein is needed for efficient chlorophyll triplet quenching in the major LHCII antenna complex of higher plants and effective photoprotection *in vivo* under strong light. *BMC Plant Biology* **6**, 32.
- Danon, A., Miersch, O., Felix, G., Camp, R.G.L., and Apel, K.** (2005). Concurrent activation of cell death-regulating signaling pathways by singlet oxygen in *Arabidopsis thaliana*. *The Plant Journal* **41**, 68-80.
- Davies, M.J.** (2004). Reactive species formed on proteins exposed to singlet oxygen. *Photochemical & Photobiological Sciences* **3**, 17-25.
- Davison, P.A., Hunter, C.N., and Horton, P.** (2002). Overexpression of beta-carotene hydroxylase enhances stress tolerance in *Arabidopsis*. *Nature* **418**, 203 - 206.
- DellaPenna, D., and Pogson, B.J.** (2006). Vitamin synthesis in plants: tocopherols and carotenoids. *Annual Review of Plant Biology* **57**, 711-738.
- Esterbauer, H., Schaur, R.J., and Zollner, H.** (1991). Chemistry and biochemistry of 4-hydroxynonenal, malonaldehyde and related aldehydes. *Free Radical Biology and Medicine* **11**, 81-128.
- Fujita, M., Fujita, Y., Noutoshi, Y., Takahashi, F., Narusaka, Y., Yamaguchi-Shinozaki, K., and Shinozaki, K.** (2006). Crosstalk between abiotic and biotic stress responses: a current view from the points of convergence in the stress signaling networks. *Current Opinion in Plant Biology* **9**, 436-442.
- Hanahan, D.** (1983). Studies on transformation of *Escherichia coli* with plasmids. *Journal of Molecular Biology* **166**, 557-580.
- Hiyama, T., Ohinata, A., and Kobayashi, S.** (1993). Paraquat (methylviologen): its interference with primary photochemical reactions. *Z. Naturforsch* **48c**, 374-378.
- Holt, N.E., Zigmantas, D., Valkunas, L., Li, X.-P., Niyogi, K.K., and Fleming, G.R.** (2005). Carotenoid cation formation and the regulation of photosynthetic light harvesting. *Science* **307**, 433-436.
- Hynninen, P.H., and Hyvarinen, K.** (2002). Tracing the allomerization pathways of chlorophylls by ¹⁸O-labeling and mass spectrometry. *The Journal of Organic Chemistry* **67**, 4055-4061.
- Jander, G., Norris, S.R., Rounsley, S.D., Bush, D.F., Levin, I.M., and Last, R.L.** (2002). *Arabidopsis* map-based cloning in the post-genome era. *Plant Physiology*. **129**, 440-450.

- Jarillo, J.A., Gabrys, H., Capel, J., Alonso, J.M., Ecker, J.R., and Cashmore, A.R.** (2001). Phototropin-related NPL1 controls chloroplast relocation induced by blue light. *Nature* **410**, 952-954.
- Kamal-Eldin, A., and Appelqvist, L.-Å.** (1996). The chemistry and antioxidant properties of tocopherols and tocotrienols *Lipids* **7**, 671-701.
- Kochevar, I.E.** (2004). Singlet oxygen signaling: From intimate to global. *Science's STKE* **2004**.
- Koller, D.** (1990). Light-driven leaf movements. *Plant, Cell & Environment* **13**, 615-632.
- Krieger-Liszkay, A., and Trebst, A.** (2006). Tocopherol is the scavenger of singlet oxygen produced by the triplet states of chlorophyll in the PSII reaction centre. *Journal of Experimental Botany* **57**, 1677-1684.
- Kudla, J., Hayes, R., and Gruissem, W.** (1996). Polyadenylation accelerates degradation of chloroplast mRNA. *The EMBO Journal* **15**, 7137-7146.
- Laloi, C., Apel, K., and Danon, A.** (2004). Reactive oxygen signalling: the latest news. *Current Opinion in Plant Biology* **7**, 323-328.
- Laloi, C., Przybyla, D., and Apel, K.** (2006). A genetic approach towards elucidating the biological activity of different reactive oxygen species in *Arabidopsis thaliana*. *Journal of Experimental Botany* **57**, 1719-1724.
- Lee, K.P., Kim, C., Landgraf, F., and Apel, K.** (2007). EXECUTER1- and EXECUTER2-dependent transfer of stress-related signals from the plastid to the nucleus of *Arabidopsis thaliana*. *Proceedings of the National Academy of Sciences of the USA* **104**, 10270-10275.
- Li, X.-P., Bjorkman, O., Shih, C., Grossman, A.R., Rosenquist, M., Jansson, S., and Niyogi, K.K.** (2000). A pigment-binding protein essential for regulation of photosynthetic light harvesting. *Nature* **403**, 391-395.
- Long, S.P., Humphries, S., and Falkowski, P.G.** (1994). Photoinhibition of Photosynthesis in Nature. *Annual Review of Plant Physiology and Plant Molecular Biology* **45**, 633-662.
- Maeda, H., Song, W., Sage, T.L., and DellaPenna, D.** (2006). Tocopherols play a crucial role in low-temperature adaptation and phloem loading in *Arabidopsis*. *The Plant Cell* **18**, 2710-2732.

- Matsufuji, H., Ochi, H., and Shibamoto, T.** (2006). Formation and inhibition of genotoxic malonaldehyde from DNA oxidation controlled with EDTA. *Food and Chemical Toxicology* **44**, 236-241.
- Meskauskiene, R., Nater, M., Goslings, D., Kessler, F., op den Camp, R., and Apel, K.** (2001). FLU: A negative regulator of chlorophyll biosynthesis in *Arabidopsis thaliana*. *Proceedings of the National Academy of Sciences of the USA* **98**, 12826-12831.
- Meskauskiene, R., and Apel, K.** (2002). Interaction of FLU, a negative regulator of tetrapyrrole biosynthesis, with the glutamyl-tRNA reductase requires the tetratricopeptide repeat domain of FLU. *FEBS Letters* **532**, 27-30.
- Meyer, K., Leube, M.P., and Grill, E.** (1994). A protein phosphatase 2C involved in ABA signal transduction in *Arabidopsis thaliana*. *Science* **264**, 1452-1455.
- Mittler, R.** (2006). Abiotic stress, the field environment and stress combination. *Trends in Plant Science* **11**, 15-19.
- Moller, I.M.** (2001). Plant mitochondria and oxidative stress: electron transport, NADPH turnover, and metabolism of reactive oxygen species. *Annual Review of Plant Physiology and Plant Molecular Biology* **52**, 561-591.
- Monde, R.A., Schuster, G., and Stern, D.B.** (2000). Processing and degradation of chloroplast mRNA. *Biochimie* **82**, 573-582.
- MunneBosch, S., and Gerald, L.** (2007). -Tocopherol: A multifaceted molecule in plants. In *Vitamins & Hormones* (Academic Press), pp. 375-392.
- Murashige, T., and Skoog, F.** (1962). A revised medium for rapid growth and bioassays with tobacco tissue cultures. *Physiologia Plantarum* **15**, 473-497.
- Neill, S., Desikan, R., and Hancock, J.** (2002). Hydrogen peroxide signalling. *Current Opinion in Plant Biology* **5**, 388-395.
- Niyogi, K.K.** (2000). Safety valves for photosynthesis. *Current Opinion in Plant Biology* **3**, 455-460.
- Ohloff, G.** (1975). Singlet oxygen: a reagent in organic synthesis. *Pure and Applied Chemistry* **43**, 481-502.
- Oleinick, N., and Evans, H.** (1998). The photobiology of photodynamic therapy: cellular targets and mechanisms. *Radiation Research* **150**, S146-156.
- Penuelas, J., and Munne-Bosch, S.** (2005). Isoprenoids: an evolutionary pool for photoprotection. *Trends in Plant Science* **10**, 166-169.

- Peter, G.F., Takeuchi, T., and Philip Thornber, J.** (1991). Solubilization and two-dimensional electrophoretic procedures for studying the organization and composition of photosynthetic membrane polypeptides. *Methods* **3**, 115-124.
- Porfirova, S., Bergmüller, E., Tropf, S., Lemke, R., and Dörmann, P.** (2002). Isolation of an Arabidopsis mutant lacking vitamin E and identification of a cyclase essential for all tocopherol biosynthesis. *Proceedings of the National Academy of Sciences of the USA* **99**, 12495-12500.
- Przybyla, D., Gobel, C., Imboden, A., Hamberg, M., Feussner, I., and Apel, K.** (2008). Enzymatic, but not non-enzymatic, $^1\text{O}_2$ -mediated peroxidation of polyunsaturated fatty acids forms part of the EXECUTER1-dependent stress response program in the flu mutant of *Arabidopsis thaliana*. *The Plant Journal* **54**, 236-248.
- Ravanat, J.-L., Di Mascio, P., Martinez, G.R., Medeiros, M.H.G., and Cadet, J.** (2000). Singlet oxygen induces oxidation of cellular DNA. *Journal of Biological Chemistry* **275**, 40601-40604.
- Ravanat, J.L., Martinez, G.R., Medeiros, M.H., Di Mascio, P., and Cadet, J.** (2004). Mechanistic aspects of the oxidation of DNA constituents mediated by singlet molecular oxygen. *Archives of Biochemistry and Biophysics* **423**, 23-30.
- Reumann, S., and Weber, A.P.M.** (2006). Plant peroxisomes respire in the light: Some gaps of the photorespiratory C2 cycle have become filled--Others remain. *Biochimica et Biophysica Acta (BBA) - Molecular Cell Research* **1763**, 1496-1510.
- Rizhsky, L., Liang, H., and Mittler, R.** (2003). The water-water cycle is essential for chloroplast protection in the absence of stress. *Journal of Biological Chemistry* **278**, 38921-38925.
- Ryter, S.W., Kim, H.P., Hoetzel, A., Park, J.W., Nakahira, K., Wang, X., and Choi, A.M.K.** (2007). Mechanisms of cell death in oxidative stress. *Antioxidants & Redox Signaling* **9**, 49-89.
- Sambrook, J., Fritsch, E.F., and Maniatis, T.** (1989). *Molecular cloning: a laboratory manual*. 2nd ed. N.Y., Cold Spring Harbor Laboratory, Cold Spring Harbor Laboratory Press **ISBN 0-87969-309-6**.
- Sánchez-Coll, N.** (2006). Identification and characterization of *soldat8*, a suppressor of the cell death program activated by singlet oxygen in Arabidopsis seedlings. Diss., Eidgenössische Technische Hochschule ETH Zürich, Nr. 16511, 2006

- Sarkar, D., and Fisher, P.B.** (2006). Polynucleotide phosphorylase: An evolutionary conserved gene with an expanding repertoire of functions. *Pharmacology & Therapeutics* **112**, 243-263.
- Sauret-Gueto, S., Botella-Pavia, P., Flores-Perez, U., Martinez-Garcia, J.F., San Roman, C., Leon, P., Boronat, A., and Rodriguez-Concepcion, M.** (2006). Plastid cues posttranscriptionally regulate the accumulation of key enzymes of the methylerythritol phosphate pathway in *Arabidopsis*. *Plant Physiology* **141**, 75-84.
- Schneider, C.** (2005). Chemistry and biology of vitamin E. *Molecular Nutrition & Food Research* **49**, 7-30.
- Schrader, M., and Fahimi, H.D.** (2004). Mammalian peroxisomes and reactive oxygen species. *Histochemistry and Cell Biology* **122**, 383-393.
- Schroeder, W.A., and Johnson, E.A.** (1995). Singlet oxygen and peroxy radicals regulate carotenoid biosynthesis in *Phaffia rhodozyma*. *Journal of Biological Chemistry* **270**, 18374-18379.
- Schwartz, S.H., Tan, B.C., Gage, D.A., Zeevaert, J.A., and McCarty, D.R.** (1997). Specific oxidative cleavage of carotenoids by VP14 of maize. *Science* **276**, 1872-1874.
- Scioli, J.R., and Zilinskas, B.A.** (1988). Cloning and characterization of a cDNA encoding the chloroplastic copper/zinc-superoxide dismutase from pea. *Proceedings of the National Academy of Sciences of the USA* **85**, 7661-7665.
- Seo, M., and Koshiba, T.** (2002). Complex regulation of ABA biosynthesis in plants. *Trends in Plant Science* **7**, 41-48.
- Shikanai, T.** (2007). Cyclic Electron Transport Around Photosystem I: Genetic Approaches. *Annual Review of Plant Biology* **58**, 199-217.
- Sugiura, M.** (1992). The chloroplast genome. *Plant Molecular Biology* **19**, 149-168.
- Wagner, D., Przybyla, D., op den Camp, R., Kim, C., Landgraf, F., Lee, K.P., Wursch, M., Laloi, C., Nater, M., Hideg, E., and Apel, K.** (2004). The genetic basis of singlet oxygen-induced stress responses of *Arabidopsis thaliana*. *Science* **306**, 1183-1185.
- Walter, M., Kilian, J., and Kudla, J.** (2002). PNPase activity determines the efficiency of mRNA 3'-end processing, the degradation of tRNA and the extent of polyadenylation in chloroplasts. *The EMBO Journal* **21**, 6905-6914.

- Wang, J.M., Asami, T., Murofushi, N., and Yoshida, S.** (2000). Isolation and initial characterization of 13(2)-hydroxychlorophyll a induced by cyclohexanedione derivatives in tobacco cell suspension cultures. *Photochem Photobiol* **71**, 84-89.
- Wilkinson, F., Helman, W.P., and B. Ross, A.** (1995). Rate constants for the decay and reactions of the lowest electronically excited singlet state of molecular oxygen in solution. An expanded and revised compilation. *Journal of Physical and Chemical Reference Data* **24**, 663-1021.
- Würsch, M.** (2006). Identifizierung und Charakterisierung von *soldat10*, einem Unterdrücker des durch Singulett Sauerstoff induzierten Zelltodprogramms in Arabidopsis Keimlingen Diss., Eidgenössische Technische Hochschule ETH Zürich, Nr. 16894, 2006
- Yehudai-Resheff, S., Hirsh, M., and Schuster, G.** (2001). Polynucleotide phosphorylase functions as both an exonuclease and a poly(A) polymerase in spinach chloroplasts. *Molecular and Cellular Biology* **21**, 5408-5416.
- Yehudai-Resheff, S., Zimmer, S.L., Komine, Y., and Stern, D.B.** (2007). Integration of chloroplast nucleic acid metabolism into the phosphate deprivation response in *Chlamydomonas reinhardtii*. *The Plant Cell* **19**, 1023-1038.
- Young, A.J.** (1991). The photoprotective role of carotenoids in higher plants. *Physiologia Plantarum* **83**, 702-708.
- Zambryski, P., Joos, H., Genetello, C., Leemans, J., Montagu, M.V., and Schell, J.** (1983). Ti plasmid vector for the introduction of DNA into plant cells without alteration of their normal regeneration capacity. *The EMBO Journal* **2**, 2143-2150.

Acknowledgements

This thesis would not have been written without help from a lot of people.

I would like to thank my supervisors, Prof. Apel, who gave me the initial opportunity to come to Zurich to carry out my PhD research, and Dr. Antoine Danon. I greatly appreciated the approachability of Prof. Apel and Antoine, although Antoine probably received the greater share of everyday problems and worries, especially during the first two years of my PhD. A special thank you also to Prof. Apel for his guidance with the writing of this thesis and the time that he spent on corrections.

Thanks also to Prof. Amrhein for being my co-referee.

I would like to acknowledge all my colleagues who contributed directly or indirectly to this work. Special thanks to: Chanhong for his great help concerning the day to day technical problems and also for helpful discussions and sharing of ideas; Ais for our interesting evening discussions, for giving much valued insight into Asian cooking and culture and for his friendship; Nuria for critical discussion and sharing ideas on our *soldat* mutants, but also for making life in the lab fun; Christophe for the time he spent with me to discuss my project, how to increase the quality of the experiments and my presentations; Mena for showing me how to handle Arabidopsis plants and especially André who took care of the thousands of plants that were necessary for this work; and finally all of my colleagues and everyone else not mentioned by name.

Obviously, this work would not have been possible without the collaboration with the group of Prof. Bernhard Kräutler. I would like to especially acknowledge Thomas Müller, who did the MS and NMR analysis of the chlorophyll a derivative and Bilal and Florence for making the first analysis of the spectrum of the chlorophyll a derivative, but also for their precious advice and encouragement during the worse periods.

Since I am not an English native speaker and my English writing still needs to be improved, I would also like to thank Emma for the hours she spent correcting my thesis to be readable.

Finally, special thanks to my family, especially my mother for her continued support and encouragements and special thank you to Wiola for her help and her patience.

Thank you.

List of publications

Florence Bouvier, Jean Charles Isner, Mialoundama Samba Alexis, Odette Dogbo and Bilal Camara (2006). Plastid isoprenoids: biogenesis and molecular regulation. In: Floriculture, Ornamental and Plant Biotechnology, J.A. Teixeira da Silva (ed) vol 1, pp 339-358. Global Science Books

Bouvier, F., Linka, N., Isner, J.C., Mutterer, J., Weber, A.P., and Camara, B. (2006). Arabidopsis SAMT1 Defines a Plastid Transporter Regulating Plastid Biogenesis and Plant Development. Plant Cell 18, 3088-3105.

Bouvier, F., Isner, J.C., Dogbo, O., and Camara, B. (2005). Oxidative tailoring of carotenoids: a prospect towards novel functions in plants. Trends Plant Sci 10, 187-194.

Curriculum vitae

Name Jean-Charles Isner
E-mail: charlie068@gmail.com
Date of Birth: 10th January 1976
Place of Birth Mulhouse
Nationality: French

Education:

2002 - Present PhD at the Swiss Federal Institute of Technology (ETH), Zürich,
Switzerland

2000- 2001 Master of Biochemistry, option physiologie végétale in Institut de Biologie
Moléculaire des Plantes (IBMP), Strasbourg, France, with honours

1995-1998 Diploma of Biochemistry, Faculté des Sciences de la Vie, Strasbourg,
France obtained with honours (top 10)

1994 Secondary School Leaving Exam (Maturity Exam), Lycée Alfred Kastler,
Guebwiller, France